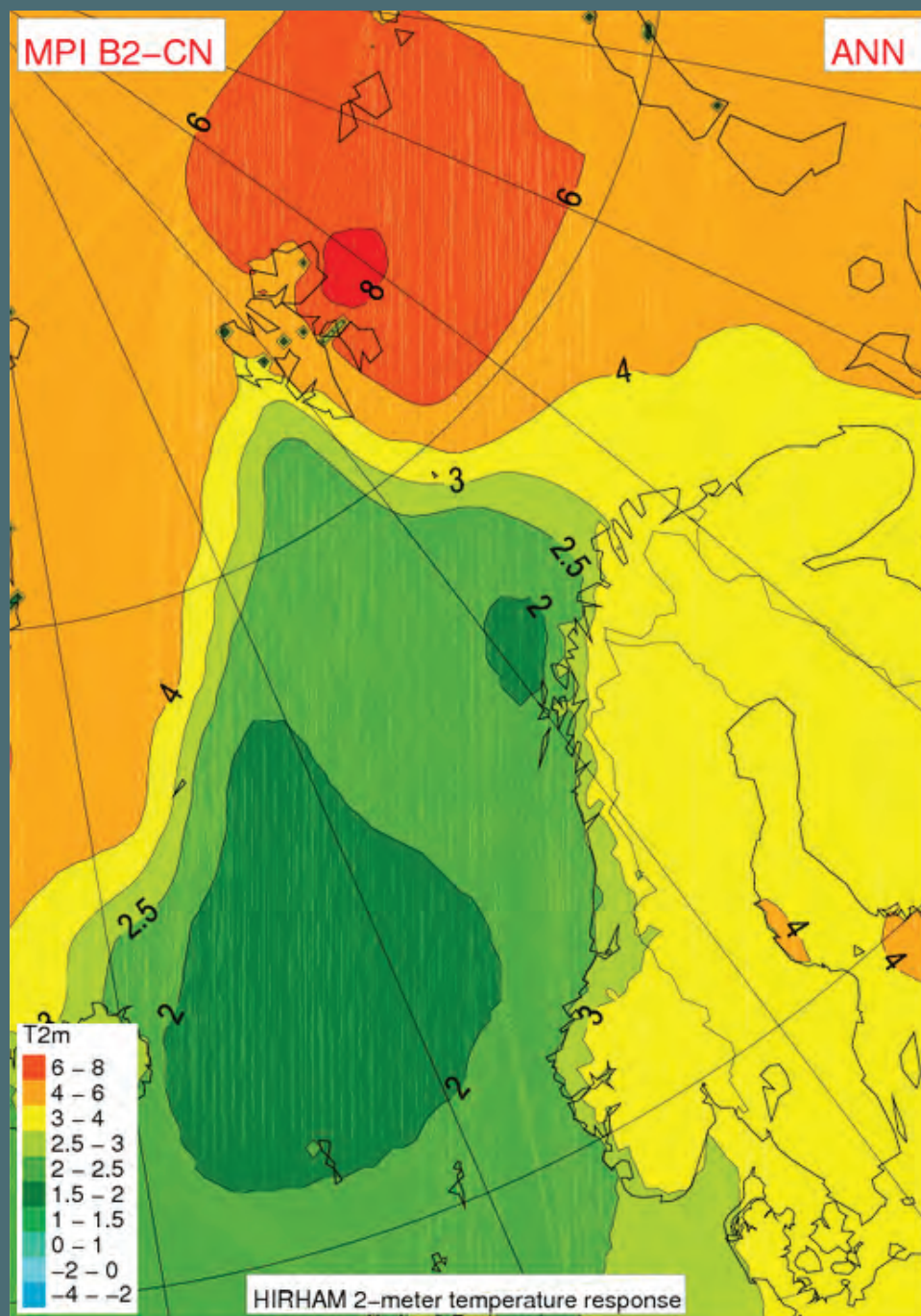


Climate development in North Norway and the Svalbard region during 1900–2100

E. J. Førland (ed), R. E. Benestad, F. Flatøy, I. Hanssen-Bauer, J. E. Haugen, K. Isaksen, A. Sorteberg, B. Ådlandsvik





Report series no. 128

Rapportserie nr. 128

Climate development in North Norway and the Svalbard region during 1900–2100

E. J. Førland (ed), R. E. Benestad, F. Flatøy, I. Hanssen-Bauer,
J. E. Haugen, K. Isaksen, A. Sorteberg, B. Ådlandsvik

The Norwegian Polar Institute is Norway's main institution for research, monitoring and topographic mapping in Norwegian polar regions. The Institute also advises Norwegian authorities on matters concerning polar environmental management.

Norsk Polarinstitutt er Norges sentralinstitusjon for kartlegging, miljøovervåking og forvaltningsrettet forskning i Arktis og Antarktis. Instituttet er faglig og strategisk rådgiver i miljøvernaker i disse områdene og har forvaltningsmyndighet i norsk del av Antarktis.

Adresse/Address

E. J. Førland (ed) ----- Norwegian Meteorological Institute, Oslo
R. E. Benestad ----- Norwegian Meteorological Institute, Oslo
F. Flatøy ----- Bjerknes Centre for Climate Research, Bergen
I. Hanssen-Bauer ----- Norwegian Meteorological Institute, Oslo
J. E. Haugen ----- Norwegian Meteorological Institute, Oslo
K. Isaksen ----- Norwegian Meteorological Institute, Oslo
A. Sorteberg ----- Bjerknes Centre for Climate Research, Bergen
B. Ådlandsvik ----- Institute of Marine Research, Bergen

Techn. editor: Gunn Sissel Jaklin, Norsk Polarinstitutt
Design/layout: Audun Igesund, Norsk Polarinstitutt
Printed: April 2009
ISBN: 13 978-82-7666-256-6
ISSN: 0803-0421

Preface

NorACIA is an initiative taken by the Norwegian government in order to follow up on the findings of the project "Arctic Climate Impact Assessment" (ACIA) which was undertaken by the Arctic Council. NorACIA will contribute to the development, consolidation and dissemination of the current understanding of climate change, impacts of climate change and adaptation to climate change in the Norwegian Arctic, i.e. Northern Norway, Svalbard and the Barents Sea.

NorACIA is organized with a steering committee with representatives from the Ministry of Environment (chair), the Norwegian Directorate for Nature Management, the Norwegian Polar Institute and the Norwegian Pollution Control Authority, and has a secretariat coordinated by the Norwegian Polar Institute.

Within the framework of NorACIA focus is on communication, providing advice and conducting assessment studies related to climate change in the Norwegian Arctic. The main goal for NorACIA is to consolidate updated and known knowledge about climate change in the Norwegian Arctic as a basis for further consideration of actions related to climate change and consequences of climate change in this region.

The assessment studies in NorACIA will be concluded with the production of five scientific reports, as well as one easy accessible synthesis report. The scientific reports will cover the following topics:

- Climate scenarios for the Norwegian Arctic
- Physical and biogeochemical processes
- Impacts on ecosystems and biodiversity
- Consequences for people and society
- Adaptation and mitigation measures

A large number of research and management institutions in Norway contribute to the work. The scientific reports and the final synthesis report will be finalized in the course of 2009.

The present report is the first of the five scientific reports and covers climate scenarios for the Norwegian Arctic. The Norwegian Meteorological Institute has been responsible for coordinating the work on this report.

Tromsø, 27 April 2009

Birgit Njåstad

The NorACIA Secretariat

Extended summary

Introduction

The Arctic land areas have over the latest 2–3 decades experienced more warming than any other region on earth, and the sea-ice cover has decreased in the order of 10% in the same period (ACIA, 2005; IPCC, 2007). The Arctic climate conditions show large variability, both from year-to-year, but also on a decadal scale. A warm period, almost as warm as the present, was observed in the Arctic from 1925 to 1945, but its geographical distribution appears to have been different from the recent warming since the extent was not global (IPCC, 2007).

IPCC (2007) states that most of the observed increase in globally-averaged temperatures since the mid-20th century is very likely due to the observed increase in anthropogenic greenhouse gas concentrations, and that it is likely that there has been significant anthropogenic warming over the past 50 years averaged over each continent except Antarctica.

Climate models furthermore indicate that anthropogenic global warming will be enhanced in the northern high latitudes due to complex feedback mechanisms in the atmosphere – ocean – ice system. The climate changes seen in the Arctic have already led to major impacts on the environment and on economic activities. If the present climate warming continues as projected, these impacts are likely to increase, greatly affecting ecosystems, cultures, lifestyles and economies across the Arctic. The Arctic climate is a complex system and has multiple interactions with the global climate system. Changes in the Arctic climate are thus very likely to have significant impacts on the global climate system.

In any regional attribution study for the Arctic, the importance of natural variability must be recognized. In climate model simulations, the Arctic signal resulting from human-induced warming is large but the variability (noise) is also large. Hence, the signal-to-noise-ratio may be

lower in the Arctic than at lower latitudes. For Arctic climate studies, data scarcity and measuring problems are other important issues.

Present climate in the Norwegian Arctic

The Norwegian and Barents Seas are exceptionally warm for their latitude. The Norwegian Sea is ice-free except for the northernmost part in the Fram Strait. The Atlantic water mass in the Barents Sea is also ice free, while most of the Arctic water has seasonal ice cover. The Barents Sea is now essentially ice free in summer, with ice typically covering only a small area in the north-eastern part. The ice coverage is, however, highly variable between years.

The coastal regions in North Norway usually experience rather mild winter climate and cool summers, while the interior parts are dominated by continental climate, with low winter temperatures and high summer temperatures. For the Svalbard stations the climate will be "maritime" (relatively mild and humid) in years (or periods) when the sea around the stations is ice-free. When the stations are surrounded by sea-ice, the climate will be "continental" (cold and dry) because the sea-ice isolates from the latent and sensible heat sources of the sea, and further reflects much of the solar radiation. Thus the high-Arctic temperatures show great inter-annual fluctuations, considering the high latitude.

In North Norway there are large gradients in annual precipitation: The highest average annual station values are close to 3000 mm/year in southern parts of Nordland, while at some stations in interior parts of North Norway the annual precipitation is below 300 mm/year. In the Svalbard region, the annual precipitation is low because air masses usually are stable stratified and contain small amounts of water. On Spitsbergen there is a gradient from higher values in the southwest to lower values in the northeast.

Climate variability and trends in the 20th century

The recent global warming is widespread over the globe, with a maximum at higher northern latitudes. The average surface temperature in the Arctic (ACIA, 2005) increased by approximately 0.09°C per decade over the past century, and the pattern of change is similar to the global trend (i.e. an increase up to the mid-1940s, a decrease from then until the mid-1960s and a steep increase thereafter with a warming rate of 0.4°C per decade). It should be stressed that in the Arctic, a warm period, almost as warm as the present, was observed from the late 1920s to the early 1950s.

The annual temperature in North Norway has increased significantly during the latest 100 years, with a linear trend of ca. 0.1°C per decade. The warm period in the 1930s is very evident. For all parts of North Norway except for Finnmarksvidda, there are significant positive temperature trends for the spring, summer and autumn seasons. For the high-Arctic stations there is variability on a multi-decadal scale, leading to mainly positive temperature trends before the 1930s, a rather warm period the next couple of decades, a temperature fall from the 1950s to the 1960s, and thereafter a general temperature increase.

In the Longyearbyen area the annual mean temperature has increased significantly from 1912 to present. The linear seasonal temperature trends at Svalbard Airport/Longyearbyen from 1912 to 2007 are +0.22°C per decade (annual), +0.21°C per decade (winter), +0.45 (spring), +0.10 (summer) and +0.16 (autumn). Except for the winter season all seasonal trends are statistically significant at least at the 5%-level.

Observations suggest (ACIA, 2005; IPCC, 2007) that it is probable that total annual precipitation has increased in the Arctic north of 60°N over the past century. For North Norway,

except for the Varanger Peninsula, the annual precipitation has increased with approximately 2% per decade during the latest 100 years. All Norwegian high-Arctic series show a positive trend in annual precipitation throughout the period of observations. At Svalbard Airport the annual precipitation has in average increased by 2% per decade, while the increase on Bjørnøya is 3% per decade.

The temperature at the top of the permafrost layer (-2 m depth) at Janssonhaugen close to Longyearbyen has during the latest 2–3 decades been increasing by an average of 0.7 °C per decade. The average temperature increase at 30 m deep is about 0.35 °C per decade and at 60 m 0.05 °C per decade. The analyses also show that the temperature increase in the permafrost is accelerating, particularly during the latest decade. With an Arctic undergoing rapid change, including an increased frequency of temperature extremes, the future warming of the permafrost can to a greater degree be more irregular than regular.

With around 140 individual cyclones and a mean residence time of 2.6 days, cyclones entering the Arctic are a common feature. For cyclones entering the Arctic from the Greenland/Norwegian Seas, positive trends are seen in both the mean intensity of the cyclones and in the intensity of the most intense cyclones. The cyclone activity index has increased in all seasons, with an annual increase of 27% over the 1950–2006 period.

Sea ice coverage data back to the 1970s show a decline for the whole Arctic and for the Barents Sea in particular. ACIA (2005) stated that it is very probable that there have been decreases in average Arctic sea-ice extent over at least the past 40 years. The time series of ice coverage for April show a strong reduction. For the summer ice, the reduction is even more pronounced. After year 2000 there have been four years with essentially no summer ice. Less data is available on ice thickness, but a time series from Hopen shows a reduction in ice thickness over a 40 year period.

Climate projections for the 21st century

The most sophisticated tools available for projecting global climate development are comprehensive Atmosphere Ocean General Circulation Models (AOGCMs) which include dynamical descriptions of atmospheric, oceanic and sea ice processes and often land surface processes. The resolution in the AOGCMs is presently sufficient for modelling most of the large-scale features, but in general too coarse to enable these models to reproduce the climate on regional or local scale. When more detailed climate data are needed, output from AOGCMs have to be “downscaled” by either dynamical (Regional Climate Model, RCM) or Empirical-Statistical (ESD) methods. Both these approaches were used within NorACIA.

Global climate model simulations (ACIA, 2005) indicate that up to the end of the 21st century, Arctic temperature is projected to increase by 7°C and 5°C for the A2 and B2 emission scenarios, respectively. The strongest warming will occur during autumn and winter. The Multi-Model Dataset used in the regional climate projections for IPCC (2007) projected an annual warming of the Arctic of 5°C at the end of the 21st century.

There are large discrepancies in how different global and regional climate models describe both present and future ice conditions in the Norwegian Arctic, and the uncertainties in the Arctic climate projections are thus considerable. The dedicated NorACIA-RCM seems to give a realistic description of the present climate conditions in North Norway and the Svalbard region. Assuming that the input data are reasonable, the model probably also give an adequate description of future climate conditions. However, just a few global climate models are currently downscaled by the NorACIA-RCM. To provide a more robust description of future climate in the Norwegian Arctic, a summary of projections of temperature and precipitation from various analyses are summarized in Table 1.

Results from the NorACIA-RCM simulations up to year 2050 (Figure 1a) indicate an increase in annual temperature of approximately 1°C in the coastal areas in Nordland and Troms, and between 1.5–2.0°C in eastern parts of Finnmark and southwest of Spitsbergen. A large gradient in the magnitude of the increase is present from south-western to north-eastern parts of the Svalbard region. This pattern is found in many scenarios (e.g. Haugen and Iversen, 2008). The projected decrease in sea-ice coverage will largely influence the temperature in the lower atmosphere.

A stronger annual warming is projected from 1961–90 to 2071–2100 than up to year 2050 (Figure 1 and Table 1). In large parts of North Norway the temperature is projected to increase by 2.5–3.5°C, with smallest increase in western coastal areas and greatest in the Varanger area and interior parts of Finnmark. For Svalbard the increase in annual temperature is ca 3°C in the southwest and ca. 8°C in the northeast. The projected warming is smallest for the summer season and greatest for autumn and winter. This is particularly valid for inland areas. A substantial increase in air temperature is also projected for the ocean areas between Svalbard and Novaja Zemlja – particularly in the period September – May. The increase is greatest in areas where sea-ice is replaced by open water.

The ACIA (2005) climate scenarios projected that over the Arctic (60 – 90°N), annual total precipitation will increase by roughly 12% from 1981–2000 to 2071–2090. IPCC (2007) states that increase in the amount of precipitation are very likely at high-latitudes. The percentage precipitation increase is largest in winter and smallest in summer, consistent with the projected warming.

For large parts of North Norway the projected increase in annual precipitation from 1981–2010 to 2021–2050 is 20–30%, while for north-eastern parts of Spitsbergen the increase is up to 40% (Figure 2 and Table 1). The seasonal precipitation is projected to increase over the whole region during all seasons – with the largest increase during winter and spring. It should however be stressed that precipitation is quite scarce in this region during the winter season, implying that despite the large percentage increase the absolute increase in precipitation may be just a few millimetres.

The ACIA (2005) climate scenarios project that the Arctic snow cover will continue to decrease with the greatest decreases projected for spring and autumn. Snow cover extent over higher northern latitudes has declined by about 10% over the past 30 years, and model projections suggest that it will decrease an additional 10 – 20% before the end of this century (ACIA, 2005). Projections for North Norway indicate that the season with snow cover will be reduced substantially up to the end of the 21st century. The strongest decrease (more than two months) is projected for the coastal areas in North Norway, while in interior parts of Finnmarksvidda the decrease is less than one month. On the other hand, over interior parts of Finnmark and in mountainous regions as well as for large parts of the Svalbard region, the maximum snow water equivalent may increase. The reason is that although the snow season will be shorter in a warmer climate in these areas; this will be compensated by the strong increase in winter precipitation as snow.

The downscaled projections of changes in wind conditions, are not giving robust signals, and large uncertainties are connected to the projections. The NorACIA-RCM simulations of average daily maximum wind speed for the period 1980–2050 indicate small changes during summer, but an increase north and east of Svalbard during the other seasons. Also up to the end of the 21st century rather small changes are projected over North Norway. However, a larger than 10% increase in average maximum daily wind speed during winter is indicated for the area north and east of Svalbard. This feature is linked to the extensive shrinking of sea ice modelled for this area. The NorACIA RCM simulations for changes in maximum wind speed indicate that the values exceeding the 95 percentile will occur more frequent in the future. The largest increase (1.5 – 2 times more frequent than present level) is indicated in an area between Spitsbergen and Novaja Zemlja.

For heavy 1-day rainfall the 5-percent exceedance value (“95-percentile”) was used as one indicator. The results indicate that this 95%-value at the end of this century over most of the area will be exceeded 1 – 1.5 times more frequently than in present day climate. Also for number of days with precipitation >20 mm an increase was projected for the whole region. However, except for parts of Nordland County, the number of days with heavy rainfall will still be quite modest over large parts of the region.

Projections of number of days with heavy snowfall (>10 cm per day) indicate a decrease in coastal regions of North Norway and south-western parts of the Svalbard region, and increasing values in interior parts of North Norway and northern parts of Svalbard.

From pilot studies with the NorACIA-RCM it was concluded that the potential for Polar Lows outside the coast of Norway will decrease.

An oceanic simulation for the Arctic Ocean and the Barents Sea has been performed with a regional ocean model system. The control run for the present climate covers the period 1986–2000, while the scenario is taken from the period 2051–2065 from the A1B simulation. The control run shows good results in the western Barents Sea. In the east, however, the model suffers extensive heat loss to the atmosphere. The mean temperatures at 50 m depth in Sep-

tember increased by 0.9°C in the studied area. The ice problem in the control run shows up as an unrealistic warming in the eastern part of the Barents Sea. In the western part the warming is less than 1°C. The downscaling shows a slight weakening of the Atlantic inflow to the Barents Sea with approximately the same heat transport.

The sea level is expected to increase during the 21st century. The main causes are melting of glaciers and thermal expansion of sea water. Changes in circulation in atmosphere and ocean influence the mean sea level regionally. Recent estimates indicate a sea level increase along the coast of Troms and Finnmark of 18 – 20 cm towards 2050 and 45 – 65 cm towards 2100. These numbers are corrected for land rise.

Downscalings have been performed to assess changes in future wave climate. Areas that are presently ice-covered in winter and ice-free

in the future will experience a rougher wave climate. Otherwise the changes are not significant. The storm surge climate does not show a significant change on a yearly basis, but there is a significant increase in the autumn surge activity. However, combined with the mean sea level increase, the impact of the surges may become more severe.

It is important to keep in mind that the projections of local and regional climate changes are affected by a range of uncertainties and shortcomings:

- Unpredictable internal natural variability (particularly large in Nordic Arctic region)
- Uncertainty in climate forcings
- Imperfect climate models
- Weaknesses in downscaling techniques

Table 1. Projections of changes in annual and seasonal temperature and precipitation
The figures indicate intervals for geographic gradients, and do not give an estimate of the uncertainty

		Svalbard			Northern-Norway				
		A*	B*	ESD**	A*	B*	RegClim***	Comb****	ESD**
	Annual	1.5 - 4	3 - 8	-	1 - 2	2.5 - 3.5	2.8	2 - 3	-
Temp	Spring	1.5 - 4	2 - 6	6 - 7	1 - 1.5	2.5 - 3.5	2.9	2 - 3	4 - 7
(degC)	Summer	1 - 1.5	2 - 4	2 - 3	1	1 - 2	2.4	1.5 - 2.5	3 - 4
	Autumn	2 - 6	4 - 8	4 - 6	1 - 2	2.5 - 4	3.3	2.5 - 4	3 - 7
	Winter	2.5 - 8	4 - 8	6 - 10	1 - 2.5	2.5 - 4.5	2.8	2.5 - 4	4 - 11
	Annual	10 - 20	10 - 40	-	0 - 10	20 - 30	13	10 - 20	-
Precip	Spring	5 - 20	10 - 40	0 - 30	0 - 10	20 - 30	11	5 - 20	5 - 20
(%)	Summer	0	10 - 30	10 - 15	0	10	12	10 - 20	10 - 15
	Autumn	10 - 20	10 - 40	5 - 20	0	10 - 20	23	10 - 20	5 - 20
	Winter	10 - 40	0 - 40	20 - 50	10 - 20	20 - 40	7	10 - 20	10 - 30

* NorACIA-RCM: Change (A) from 1981–2010 to 2021–2050 and (B) from 1961–1990 to 2071–2100

** ESD: Empirical-Statistical Downscaling from 1961–90 to 2071–2100

*** RegClim (2005): Change from 1961–1990 to 2071–2100 from combined analysis of RCM simulations for two global climate models

**** From Haugen & Iversen (2008): Change during 70 years from combined analysis of RCM simulations for eight global climate models

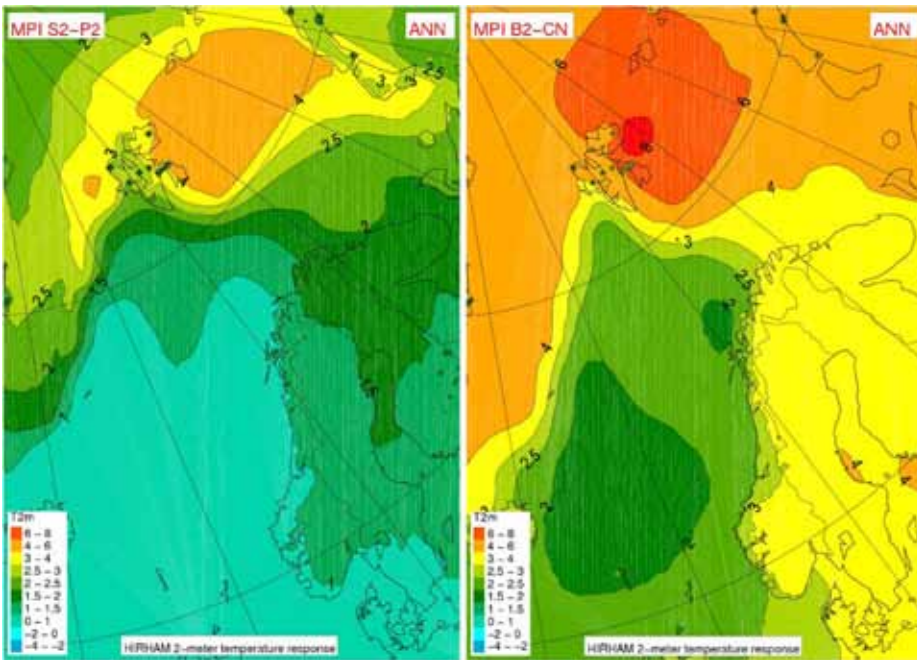


Figure 1. Projected change (°C) in mean annual temperatures from a). 1981-2010 to 2021-2050
b). 1961-90 to 2071-2100.

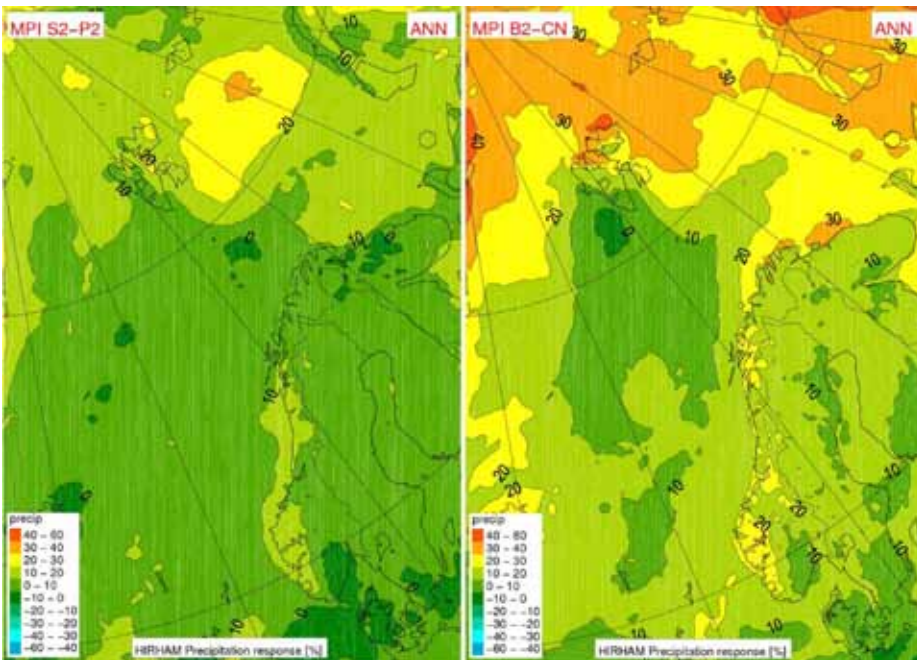


Figure 2. Projected change (%) in mean annual precipitation from a). 1981-2010 to 2021-2050, b). 1961-1990 to 2071-2100

References

- ACIA, 2005: Arctic Climate Impact Assessment, Cambridge University Press, 1042 p. (www.acia.uaf.edu)
- Haugen, J.E. & T.Iversen, 2008: Response in extremes of daily precipitation and wind from a downscaled multi-model ensemble of anthropogenic global climate change scenarios. *Tellus A*, Vol. 60A, No. 3, May 2008, 411-426.
- IPCC, 2007: Climate Change 2007: The Physical Science Basis. Contribution of Working Group I to the Fourth Assessment Report of the Intergovernmental Panel on Climate Change [Solomon, S., D. Qin, M. Manning, Z. Chen, M. Marquis, K. B. Averyt, M. Tignor and H. L. Miller (eds)]. Cambridge University Press, United Kingdom and New York, NY, USA, 996p
- RegClim, 2005: Norges klima om 100 år. Usikkerheter og risiko. <http://regclim.met.no>

Contents

Extended summary	3
Introduction	3
Present climate in the Norwegian Arctic	3
Climate variability and trends in the 20th century	3
Climate projections for the 21st century	3
1. Introduction	8
2. Climate in the “NorACIA-region”	9
2.1 Factors governing the climate in the Norwegian Arctic	9
2.2 Temperature	10
2.3 Precipitation	11
2.4 Wind and pressure distribution	12
2.5 Arctic and North Atlantic Oscillation	13
2.6 Ocean currents and water masses	13
2.7 Available climate and scenario data from the Norwegian Arctic	14
3. Climate variability and trends in the 20th century	15
3.1 Introduction	15
3.2 Land surface air temperature	15
3.3 Precipitation	18
3.4 Snow	20
3.5 Permafrost	20
3.6 Cyclones entering the Arctic	21
3.7 Marine indices	22
4 Climate projections for the 21st century	22
4.1 Climate modelling and downscaling	22
4.2 The NorACIA Regional Climate Model	24
4.3 Mean temperature	25
4.4 Precipitation	28
4.5 Snow	32
4.6 Wind	34
4.7 Climatic extremes	35
4.8 Polar Lows	36
4.9 Oceanic simulations	36
4.10 Sea level and storm surges	38
5. Uncertainties and shortcomings in climate projections	38
6. Knowledge gaps and suggested scientific actions	38
6.3. Spatial and temporal resolution of Arctic climate projections	38
6.4. Marine downscaling	39
6.5. Uncertainties	39
6.6. Dissemination and tailoring of climate projections for impact and adaptation studies	39
7. Summary	39
References	40
Acronyms	43

1. Introduction

The Arctic land areas have over the last 2 – 3 decades experienced more warming than any other region of the earth, and the sea-ice cover has decreased in the order of 10% in the same period (ACIA, 2005; IPCC, 2007). Climate models furthermore indicate that anthropogenic global warming will be enhanced in the northern high latitudes due to complex feedback mechanisms in the atmosphere – ocean – ice system. The climate changes seen in the Arctic have already led to major impacts on the environment and on economic activities (ACIA, 2005). If the present climate warming continues as projected, these impacts are likely to increase, greatly affecting ecosystems, cultures, lifestyles and economies across the Arctic. The Arctic climate is a complex system and has multiple interactions with the global climate system (ACIA, 2005). Changes in the Arctic climate are thus very likely to have significant impacts on the global climate system.

IPCC (2007) states that most of the observed increase in globally-averaged temperatures since the mid-20th century is very likely due to the observed increase in anthropogenic greenhouse gas concentrations, and that it is likely that there has been significant anthropogenic warming over the past 50 years averaged over each continent except Antarctica. The observed global warming trend agrees well with predictions (Rahmstorf et al., 2007). However, the observed temperature trend in western Europe over the last decades appears much stronger than simulated by state-of-the-art global climate models (Oldenborgh et al., 2008). This implies that climate predictions for western Europe probably underestimate the effects of anthropogenic climate change.

The drifting sea-ice in the Arctic is an indicator of climate variability. According to IPCC (2007) the annual average Arctic sea-ice extent has shrunk by about $2.7 \pm 0.6\%$ per decade since 1978 based on satellite observations. In September 2007 there was a record minimum ice area of less than 4 mill km² compared to the average value of 6 million km² over the 1979–2007 period. In September 2008 the extent was almost as low as in 2007 (www.nersc.no). The ACIA climate scenarios (ACIA, 2005) project that summer sea-ice will decrease by more than 50% over the 21st century. The projected reduction in sea-ice extent in winter is less than in summer; however, the models indicate that the March sea-ice edge will retreat substantially in the sub polar seas.

In any regional attribution study for the Arctic, the importance of natural variability must be recognized. In climate model simulations, the arctic signal resulting from human-induced warming is large but the variability (noise) is also large. Hence, the signal-to-noise-ratio may be lower in the Arctic than at lower latitudes. In the Arctic, data scarcity and measuring problems are other important issues. It is therefore crucial to make optimal use of observational series from the Arctic in monitoring the long-term variations of various climatic elements.

The ACIA report (ACIA, 2005) stated that there still is a substantial need for increased knowledge about the climate system and regional climate development in the northern polar areas. One fundamental limitation in the present understanding and simulation of the coupled ocean – atmosphere – terrestrial system in a regional perspective, involves the large differences between the spatial resolution of the global climate models and the scale of regional processes.

However, downscaling of global climate model results can provide information on substantially smaller spatial scales. Different techniques for “downscaling” the global models to regional and local scales include dynamical (i.e. Regional Climate Model, RCM) and empirical – statistical (ESD) downscaling.

When the ACIA-report was concluded in 2005, the available regional climate models were to a very limited degree focussing on the “Norwegian Arctic” and the optimal spatial resolution was approx. 50 km. The domain for the Norwegian regional climate model (<http://regclim.met.no>) did cover Spitsbergen, but the representativity of the climate simulations for the Svalbard region was dubious because this region was too close to the border of the model domain.

For most studies of impacts of climate change, detailed scenarios are needed for specific locations, i.e. with a much more detailed spatial resolution than the present RCM-simulations are able to provide. To get more site-specific climate projections, empirical downscaling is therefore used to adapt temperature and precipitation from large scale patterns in global or regional climate model. A large variety of national and international global climate model results (incl. all simulations used in the latest IPCC (2007) report) are downscaled for the weather stations

in the Norwegian Arctic (Benestad, 2008). Results from the empirical downscaling also may give a measure for the differences between scenarios from various global models and different emission scenarios. ESD may also illustrate the representativity for the global models used in the RCM-simulations compared to all IPCC 4AR projections.

To improve the description of the regional climate development and to provide more tailored information for impact and adaptation studies, it was decided to include the following tasks in a Norwegian follow-up to the ACIA-process (NorACIA, see www.noracia.npolar.no):

- Establish a regional climate model with high resolution for the region Svalbard – Barents Sea – Northern Scandinavia
- Apply empirical methods to “tailor” climate projections for impact studies at selected localities
- Demonstrate the spread in climate projections for this region, and illustrate the representativity of the selected simulations compared to the IPCC 4AR scenarios
- Consider potential surprises in the climate system; i.e. events that presently are unlikely but might have severe consequences. This includes e.g. unexpected disturbances in the weather system or in the thermohaline circulation

This report gives an assessment of current knowledge of climate conditions and climate development (1900–2100) within the Norwegian Arctic, with special emphasis on results from the climate scenario activities in the NorACIA-programme (reported in Førland et al., 2008). The main focus area is the Svalbard region, Jan Mayen and North Norway (Finnmark, Troms and Nordland counties); cf. Figure 2.1.



Figure 2.1. Map of the “Norwegian Arctic” including weather stations mentioned in the text

2. Climate in the "NorACIA-region"

2.1 Factors governing the climate in the Norwegian Arctic

The Norwegian high-Arctic weather stations (on Spitsbergen, Hopen, Bjørnøya and Jan Mayen, Figure 2.1) are all coastal stations situated in the northern part of the North Atlantic, where the major ocean heat transport between the northern mid and high latitudes takes place. In the eastern part of the area and along the coast of North Norway, the Norwegian Current (a branch of the North Atlantic Current) transports warm water masses, originating from the Gulf Stream, into the Barents Sea and along the western coast of Spitsbergen (Figure 2.8). In the western part of the Fram Strait, the East Greenland Current transports cold water (and sea ice) from the Polar basin to the North Atlantic.

Also the atmosphere contributes considerably to the south – north heat transport in this area. A key feature is the polar front, where cold polar air masses from the northeast meet warm maritime air masses from the southwest. Average sea level pressure patterns show that an area of low air pressure extends from Iceland towards the Barents Sea. This low pressure area is especially pronounced during winter, but also evident in autumn and spring (cf. chapter 2.4). South of this area, humid and mild air is transported northeast-ward, along the coast of North Norway. The islands Jan Mayen and Bjørnøya are situated rather close to this low pressure area. Hopen and Spitsbergen are situated in the pressure gradient zone north of the minimum pressure, where easterly and north-easterly winds are prevailing. The polar front is not static though, and variability in its position makes the Norwegian Arctic stations exposed for air masses of very different origin. This is one of the reasons why these stations, in spite of their coastal environments, show rather large climate variability.

Another reason for the large climate variability at the Norwegian high-Arctic stations, especially during the winter half of the year, is the variable sea-ice conditions. In summer, there is usually no sea-ice around the stations, except for Hopen where some ice may occur (Figure 2.2). The sea ice extent in winter and spring, however, varies widely (Figure 2.3) in response to the variations in ocean and atmosphere circulation and heat transfer. In years (or periods) when the sea around the stations is ice-free, the climate will be "maritime" (relatively mild and humid). When the stations are surrounded by sea-ice, the climate will be "continental" (cold and dry) because the sea-ice isolates from the latent and sensible heat sources of the sea, and further reflects much of the solar radiation.

The closer one comes to the North Pole, the more pronounced is the annual variation and the less accentuated is the diurnal variation in light conditions. All the Norwegian high-Arctic stations experience continuous daylight 3–4 months in summer with a net radiative heat gain, and 3–4 months continuous darkness during winter with a net radiative heat loss. As minimum cloudiness occurs in winter, there is a considerable radiation heat loss from the ground during this season. Maximum cloudiness occurs in summer, resulting in few hours of bright sunshine. Hanssen-Bauer et al (1990) studied the influence of cloudiness on temperature throughout the year. In January – March, the daily temperature was more than 10 °C higher on overcast than on clear days at Svalbard Airport, Ny-Ålesund and Sveagrøva. During June – August however, the temperature on clear days was found to be a few degrees centigrade higher than on overcast days.

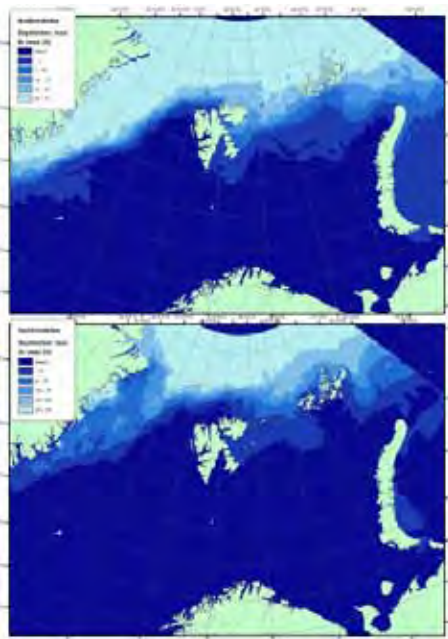


Figure 2.2 Maximum (upper) and minimum (lower) annual sea ice extent in September in the period 1971–2000. Number of years with max/min sea-ice extent between different limits is given with colour shadings (From Hygen, 2009)

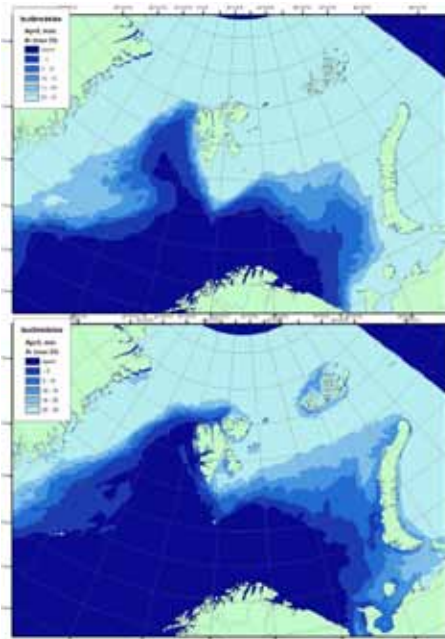


Figure 2.3 Maximum (upper) and minimum (lower) annual sea ice extent in April in the period 1971–2000. Number of years with max/min sea-ice extent between different limits is given with colour shadings (From Hygen, 2009)

2.2 Temperature

The average air temperature conditions in the area are illustrated by Figures 2.4 and 2.5. The maps in Figure 2.4, which are based upon the ERA40 (Källberg et al., 2004) downscaled by HIRHAM25 (Haugen and Haakenstad, 2006), give somewhat smoothed temperature gradients. Nevertheless, they demonstrate the rather mild winter climate along the coast of North Norway. Over Spitsbergen there is a strong temperature gradient from southwest to northeast. In winter, the average temperatures vary from around -10 °C along the west coast to below -20 °C in the north-east. In summer the contrasts are considerably smaller.

The interior parts of North Norway experience continental climate, with low winter temperatures and high summer temperatures (Figure 2.5). At e.g. Karasjok the average (1961–90) monthly temperature for July is 13.1°C and in February -15.4°C; i.e. a difference close to 30°C. For the coastal sites in the region the difference between July and February mean temperature is substantially lower: Bodø and Vardø 15°C, Tromsø and Hammerfest 16°C. For Jan Mayen the July – February difference is 10°C, for Bjørnøya 12, For Ny-Ålesund 20 and for Svalbard Airport 22°C.

One remarkable feature concerning winter air temperature is the relatively high mean values and great fluctuations which take place, considering the high latitude. Thus there are large inter-annual deviations from the mean temperature conditions outlined in figure 2.4 and 2.5. For e.g. Longyearbyen, Ny-Ålesund and interior parts of Finnmarksvidda, the difference between the highest and lowest recorded monthly mean in January is about 20°C. On Bjørnøya and Jan Mayen the similar difference is about 13 °C, and in Vardø, Tromsø and Bodø 8°C.

Among the stations on Spitsbergen, Sveagruba and Longyearbyen/ Svalbard Airport have the most continental climate. At these stations the winter temperatures are 2–5°C lower, and summer temperatures 1–2°C higher than at the coastal station at Isfjord Radio. Sveagruba usually has the lowest winter temperatures, while the two southernmost stations Bjørnøya and Jan Mayen have the highest. The mean winter temperature at Ny-Ålesund and Longyearbyen are quite similar; cf. Figure 2.5. During summer, Longyearbyen has the highest temperatures, while the mean temperatures at Ny-Ålesund and Isfjord Radio are similar. This tendency for a more “continental” climate during winter than during summer is, to some extent, also found at other stations. It may be explained by the stations proximity to fjords that are frozen during winter.

January – March is normally the coldest part of the year. Even during these months, above-zero temperatures have been recorded at all stations, both in the high-Arctic and at the Norwegian mainland. On Jan Mayen even temperatures up to 10°C may occur during this time of the year. The lowest recorded temperature on Spitsbergen is -49.4°C (Green Harbour, Spitsbergen, March,

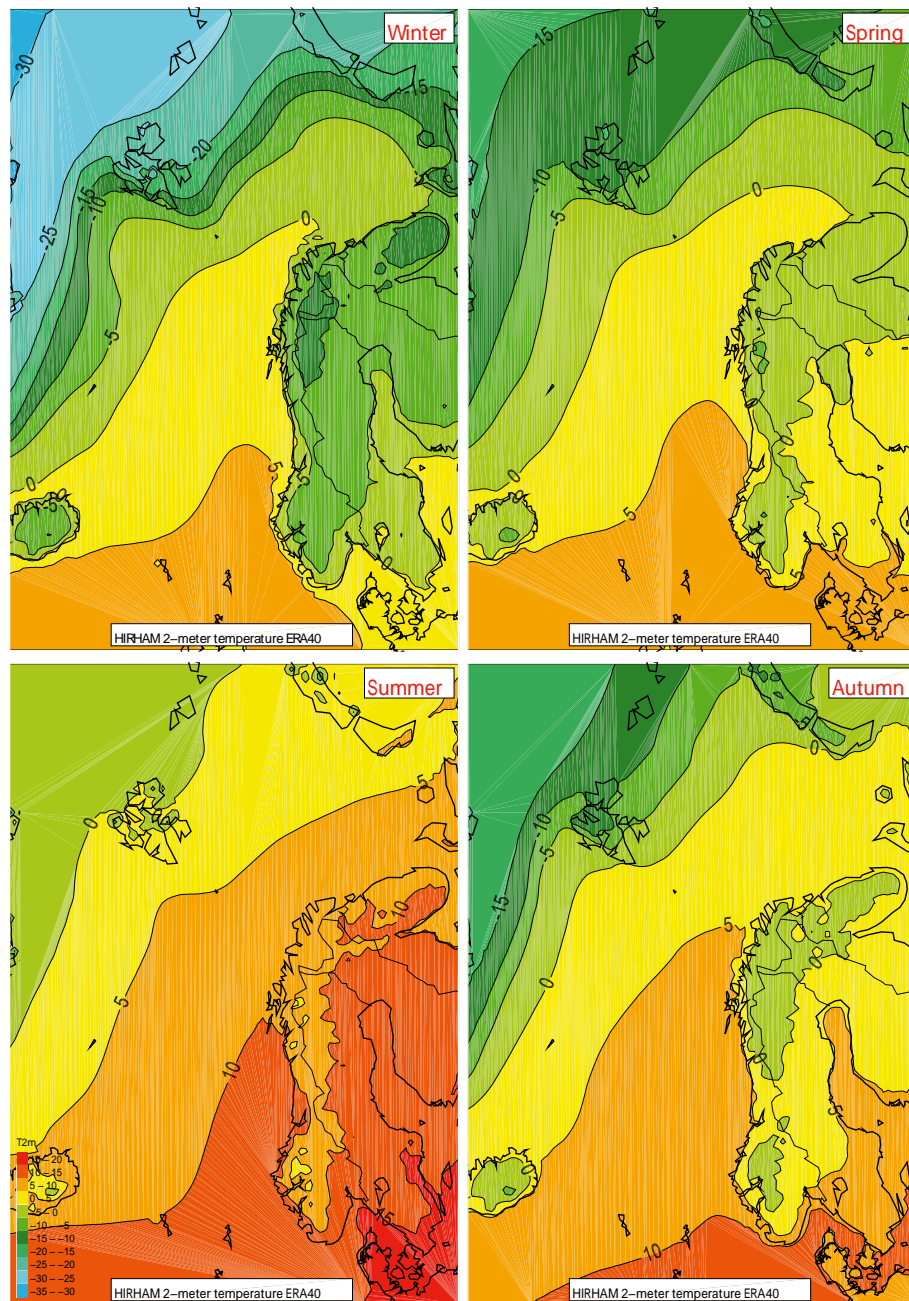


Figure 2.4 Mean temperature (°C) over the area for winter (upper left), spring (upper right), summer (lower left) and autumn (lower right) from 1961–2000 based upon a HIRHAM25 downscaling of ERA40

1917). Also in Longyearbyen, Svea and Ny-Ålesund, temperatures below -40°C have been recorded. On Bjørnøya the lowest minimum temperature is -31.6°C, and on Jan Mayen -28.4°C. At the coastal stations in North Norway minimum temperatures of approx. -20°C have occurred. The lowest winter temperatures in the Norwegian Arctic are, however, found in interior parts of Finnmarksvidda. Both Karasjok and Kautokeino have recorded winter temperatures well below -50°C.

The average (1961–90) summer temperatures show a marked uniformity in the high-Arctic; cf. Figure 2.5. The normal temperatures during the two warmest months are around 2°C at Hopen, compared to 4–6°C for the other stations. Minimum temperatures of several degrees below zero occur throughout summer. Only rarely do maximum temperatures exceed +15°C, but temperatures above 20°C have occasionally been

recorded on Bjørnøya and at Svalbard Airport. At the coastal stations in North Norway, summer temperatures above 25°C are not uncommon. Tromsø, Alta, Karasjok and Kautokeino have recorded maximum temperatures above 30°C. Thus the difference between highest and lowest recorded temperatures in interior parts of Finnmarksvidda is more than 80°C!

During the winter season, minimum temperatures at the high-Arctic stations are below 0°C for most days even at the southernmost stations Bjørnøya and Jan Mayen. During July and August the maximum temperatures usually exceed 0°C. At the coastal stations in North Norway the minimum temperatures usually stay above zero during July and August, but in the interior parts of Finnmarksvidda temperatures below zero have been recorded also in June, July and August.

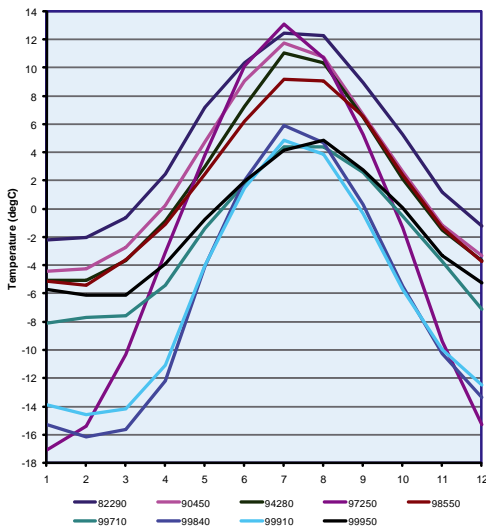


Figure 2.5 Average (1961-1990) monthly temperatures (°C) at selected stations (82290=Bodø, 90450=Tromsø, 94280=Hammerfest, 97250=Karasjok, 98550=Vardø, 99710=Bjørnøya, 99840=Svalbard Airport/Longyearbyen, 99910=Ny-Ålesund and 99950=Jan Mayen)

2.3 Precipitation

The precipitation values based on downscaling of ERA40 for the period 1961–2000 (Figure 2.6) are known to be somewhat too high in this area (Haugen & Haakenstad, 2006). Still Figure 2.6 indicates that the precipitation is at maximum during autumn and winter, that the precipitation is largest in the southernmost area, and that there is a gradient over Spitsbergen from high values in the southwest to lower values in the northeast in all seasons except during summer.

In North Norway there are large gradients in annual precipitation: The highest average annual station values (1961–2000) are close to 3000 mm/year in southern parts of Nordland (Lurøy), while at some stations in interior parts of North Norway the annual precipitation is below 300 mm/year (Dividalen).

Precipitation is normally low in the high-Arctic because air masses usually are stable stratified and contain small amounts of water vapour. Most of the precipitation in the Svalbard region occurs in connection with cyclones coming in from the Southwest – Northwest sector. On Spitsbergen, the mountain regions receive the greatest amounts of precipitation and the inner fjord districts the least; but the topography causes great local differences. Maps of distribution of annual precipitation on Spitsbergen have been based mainly on snow depth measurements, glacier accumulation studies and scattered streamflow measurements. Investigations of the distribution of glacial ice and the height of the snow line indicate large differences in annual snow accumulation on Spitsbergen (Hagen & Liestøl, 1990). The highest accumulation is found along the coast, especially in southeast, while the lowest accumulation occurs in the inner fjord areas, especially in northeast.

The normal (1961–1990) annual measured precipitation in the Svalbard region is 190–440

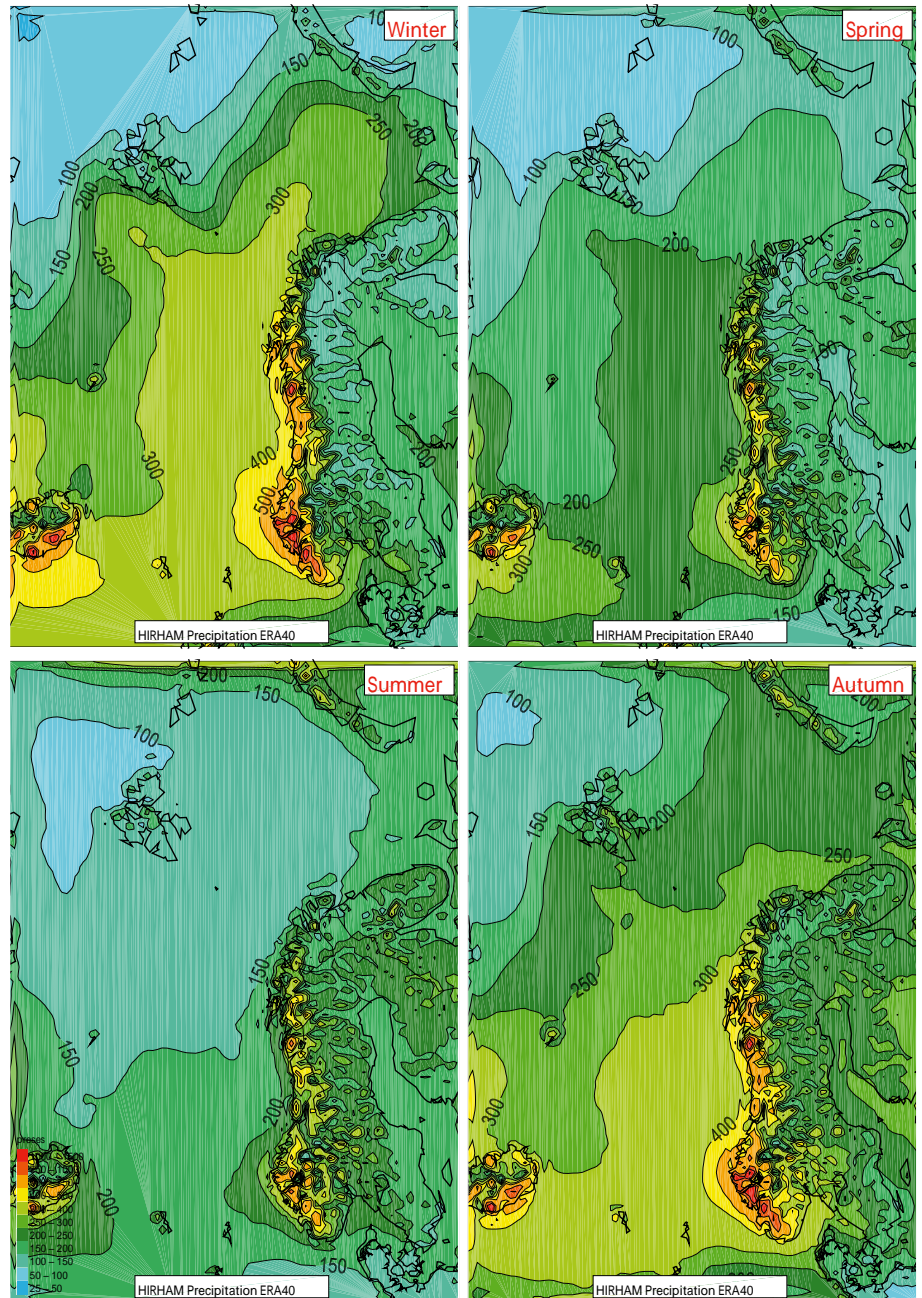


Figure 2.6 Mean precipitation (mm) over the area for winter (upper left), spring (upper right), summer (lower left) and autumn (lower right) for the period 1961–2000 based upon a HIRHAM25 downscaling of ERA40

mm, and at Jan Mayen 687 mm/yr (cf. Table 4.3). The annual value at Svalbard Airport (190 mm/yr) is the lowest normal value at any Norwegian station. Mean monthly precipitation is at a minimum during the period April – June. Most of the stations have maxima both in August and February – March. The highest annual precipitation amount recorded on Spitsbergen is 750 mm (Isfjord Radio, 1972), the highest monthly is 230 mm (Ny-Ålesund, November 1993), and highest daily 57 mm (Ny-Ålesund 1.Dec 1993).

One peculiar feature is that both rain and snow may occur at any time of the year at all Norwegian high-Arctic stations. It should be stressed that reliable measurements of precipitation are difficult to obtain under certain weather conditions. At the Arctic stations blowing or drifting snow may cause substantial problems. «Precipitation» just caused by blowing snow is excluded

through the quality control at the Norwegian Meteorological Institute, but in several occasions there is a combination of precipitation and blowing snow. In such cases it is difficult to distinguish the proportions of real precipitation and blowing snow.

On the other hand, the harsh weather conditions in the Arctic increase dramatically the catch deficiency of the precipitation gauges. A large proportion of the precipitation falls as snow during high wind speeds, and under such conditions the conventional gauges just catch a small fraction of the “ground true” precipitation (Førland et.al. 1996). Based on field measurements in Ny-Ålesund, Hanssen-Bauer et al. (1996) deduced correction factors for the aerodynamic catch deficiency in the Norwegian precipitation gauge. The correction factor was found to increase exponentially with increas-

ing wind speed. For solid precipitation, the correction factor was increasing with decreasing air temperatures, and for liquid precipitation it was decreasing with decreasing rain intensities. Hanssen-Bauer et al. (1996) concluded that for solid precipitation, a typical aerodynamic correction factor in Ny-Ålesund would be 1.65–1.75, for liquid precipitation it would be 1.05–1.10 and for sleet and mixed precipitation it would be around 1.40. A rough estimate is that for a «normal» year in Ny-Ålesund, the true climatological precipitation would be about 50% higher than the measured.

Førland & Hanssen-Bauer (2000) stated that in a warmer Arctic climate a larger fraction of the annual precipitation will be liquid, resulting in a fictive positive trend in measured precipitation. Accordingly, precipitation corrected for undercatch should be used in trend studies for the Arctic.

Scattered measurements confirm that the annual precipitation in the mountain areas of Spitsbergen is substantially larger than the measured amounts at the regular weather stations at the coast (see e.g. Steffensen, 1982; Jania & Pulina, 1994; Osokin et al., 1994). Even after subtracting contribution from glacier ablation, the streamflow measurements from e.g. the river Bayelva near Ny-Ålesund are indicating substantially higher river discharge than can be explained by the precipitation measured at the weather station in Ny-Ålesund (Killingtveit et al., 1994; Pettersson, 1994). Hagen & Lefauconnier (1995) found that the mean winter snow accumulation on Brøggerbreen during the period 1967–1991 was 720 ± 160 mm in water equivalent. On the other hand the mean annual precipitation (1961–90) measured at the weather station in Ny-Ålesund is just 370 mm/year (Førland, 1993).

Because of lifting and consequent cooling of airmasses over hills and mountains, precipitation is usually increasing with increasing altitude. Analyses of precipitation distribution on Spitsbergen based on an extended network of gauges, indicated a 5–10% increase in measured summer precipitation for each 100 m (Killingtveit et al., 1994). Based on snow surveys in two catchments, a probable vertical gradient of 14% per 100 m was assumed (Tveit & Killingtveit, 1994). In the Ny-Ålesund/Brøggerbreen area, Hagen & Lefauconnier (1995) found that the altitudinal increase of snow accumulation had a fairly constant gradient of 100 mm per 100m – equivalent to a 25% increase per 100 m altitude.

In a profile study across the glacier Austre Brøggerbreen, Førland et al. (1997a) found that the total precipitation amount at the glacier during the summer seasons 1994–95 was about 45% higher than recorded at the weather station in Ny-Ålesund. It was also found that the precipitation distribution in the Ny-Ålesund area was strongly dependent on the wind direction. For large-scale winds from south and southwest, the precipitation at the glacier was about 60% higher than in Ny-Ålesund, while for winds from northwest, Ny-Ålesund got more precipitation

than the stations at the glacier. The high precipitation amounts recorded at the central areas of the glacier are probably caused by a combination of spillover and seeder/feeder effects. A rough altitude-precipitation increase in the Ny-Ålesund area was estimated to be 20% per 100 m, at least up to 300 m a.s.l.

Førland et al. (1997a) concluded that the apparent discrepancy between precipitation measured in Ny-Ålesund and runoff/mass balance estimates for the Bayelva catchment could be fully explained by aerodynamic catch deficiency in the precipitation gauge in Ny-Ålesund and orographic precipitation enhancement in the glacier area.

2.4 Wind and pressure distribution

The climatology of mean sea level pressure (MSLP) and 10m windspeed is displayed in Figure 2.7a and b respectively. The distribution is computed from the HIRHAM25km downscaling forced by ERA40 data for the periode 1961–2000. The spatial structure of MSLP for autumn, winter and spring is very similar (Figure 2.7a). The area of low pressure from Iceland towards the Barent Sea reflects the major low pressure systems approaching Scandinavia, with lowest values in winter and autumn and strongest gradients during winter. The structure of wind speed (Figure 2.7b) is similar, with strongest values in the Norwegian Sea during winter.

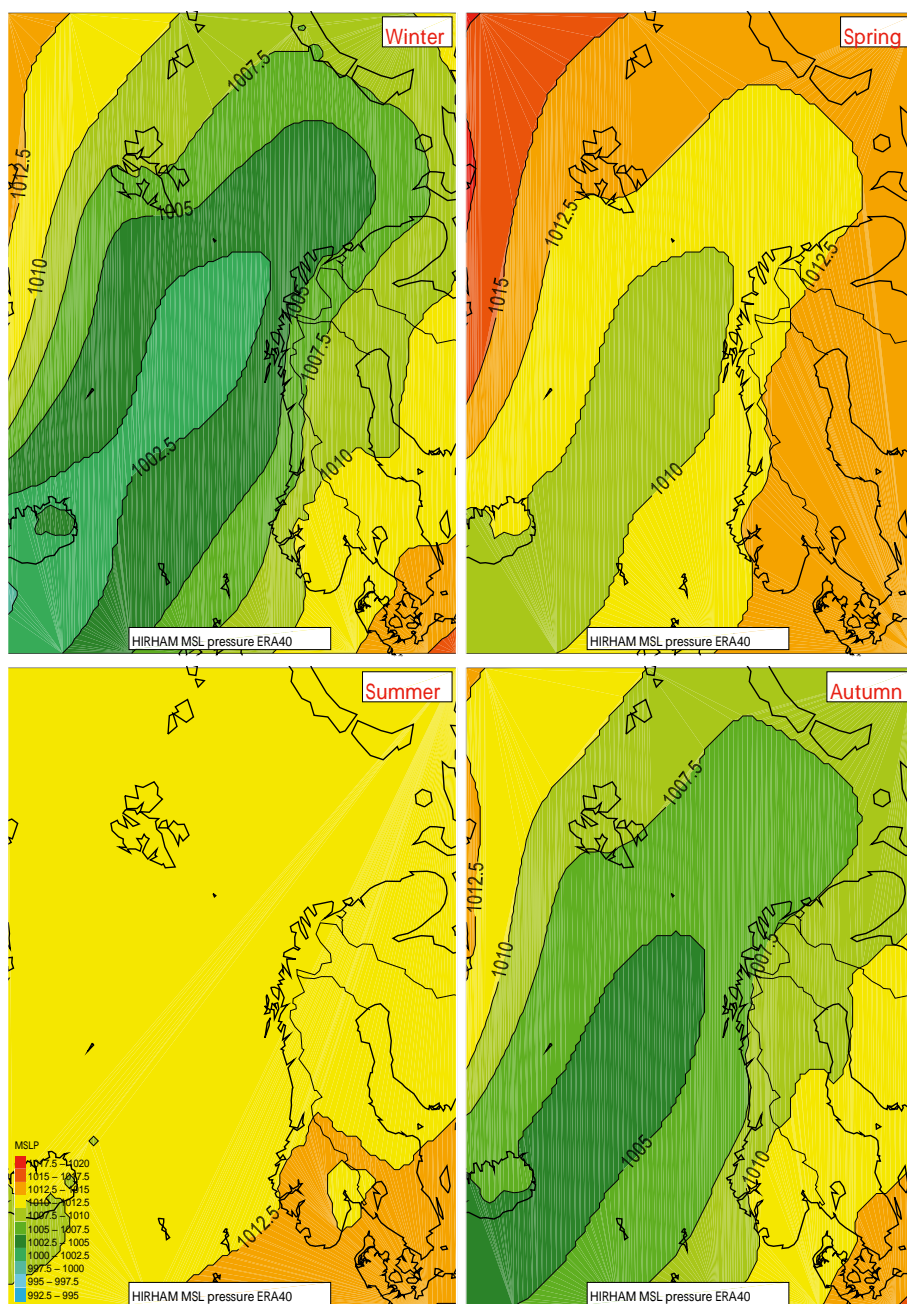


Figure 2.7a Seasonal mean sea level pressure (hPa) for the period 1961-2000 based upon HIRHAM25 downscaling with forcing from ERA40 data. Upper left: Winter (DJF), upper right: Spring (MAM), lower left: Summer (JJA) and lower right: Autumn (SON).

Observed seasonal frequencies of different wind directions demonstrate that the prevailing winds are from the northeast-southeast sector on Spitsbergen, except during summer (Hanssen-Bauer et al., 1990, Førland et al., 1997b). At each measuring station the most common wind direction is along valleys or fjords from the inland to the coast. This is partly caused by the topography's channelling effect on the large-scale wind field, which often has an easterly component, and partly by drainage winds transporting cold «heavy» air from the inland glaciers to the warmer sea. This is also the case at the inland stations in North Norway. At Finnmarksvidda, southerly «drainage» winds prevail during autumn, winter and spring. Along the fjords in Nordland, the wind pattern during these seasons

is dominated by easterly winds. However, at the coastal stations in Nordland, Troms and Finnmark the strongest wind forces usually occur in winds from sector SW-NW.

As the Norwegian Arctic lies in the border zone between cold Arctic air from the north and mild maritime air from the south, the cyclonic activity is great. Unstable and stormy weather is therefore common in winter. During November – March, Isfjord Radio and Jan Mayen in average experience more than 15–20 days/month with maximum wind force > 6 Beaufort. The wind at Isfjord Radio is strengthened locally by Isfjorden, which is narrower at the mouth than further in. At the other Spitsbergen stations, the frequencies of strong winds are substantially lower.

2.5 Arctic and North Atlantic Oscillation

The general large scale air currents over the northern Atlantic Ocean are determined by the low pressure area near Iceland and an area with relatively high pressure over Greenland and the Arctic Ocean (cf. Figure 2.7a). A common used index for the strength in the atmospheric westerlies in the North Atlantic is the North Atlantic Oscillation (NAO) (e.g. Hurrell 1995). The NAO has long been recognized as a major mode of atmospheric variability over the extra tropical ocean between North America and Europe. The NAO describes the difference in sea level pressure between the Icelandic Low and the Azores High. When both are strong (higher than normal pressure in the Azores High and/or lower than normal pressure in the Icelandic Low), the NAO index is positive. When both pressure systems are weak, the index is negative. The NAO is most obvious during winter, but can be identified at any time of the year. In winters with positive NAO index, enhanced westerly flow moves mild moist air over much of northern Europe and more intense and frequent storms occurs in the Norwegian Sea (Serreze et al., 1997).

As pointed out in the ACIA-report (2005) several authors argue that the NAO should be considered as a regional manifestation of a more basic annular mode sea-level pressure variability, which has come to be known as the Arctic Oscillation (AO). The AO is defined as the leading mode of variability from a linear principal component analysis of Northern Hemisphere sea-level pressure. It emerges as a robust pattern dominating both the month-to-month and year-to-year variability in sea-level pressure. The AO and NAO time series are highly correlated. The AO/NAO index was at its most negative in the 1960s. From about 1970 to the early 1990s there was a general positive trend (e.g. Hanssen-Bauer 2007). During the latest decade the NAO/AO index has been more positive than negative.

2.6 Ocean currents and water masses

The Norwegian and Barents Seas are exceptionally warm for their latitude. This is caused by the warm and salty Norwegian Atlantic Current flowing along the shelf edge. At the entrance to the Barents Sea the Atlantic Current splits in two branches (cf. Figure 2.8). The Spitsbergen branch continues northwards along the shelf edge in the Fram Strait and finally turns eastwards into the Arctic Ocean. The western Fram Strait is dominated by cold and fresh East Greenland Current coming from the Arctic Ocean and continuing southwards along the Greenland coast.

The other branch of the Atlantic Current turns eastward into the Barents Sea and contributes to the warm and salty Atlantic water mass dominating the southern parts of the sea. The Arctic water is found further north in the Barents Sea. This water mass is coming from the Arctic Ocean. The water masses meet in a frontal area called the Polar Front. The position of the Polar

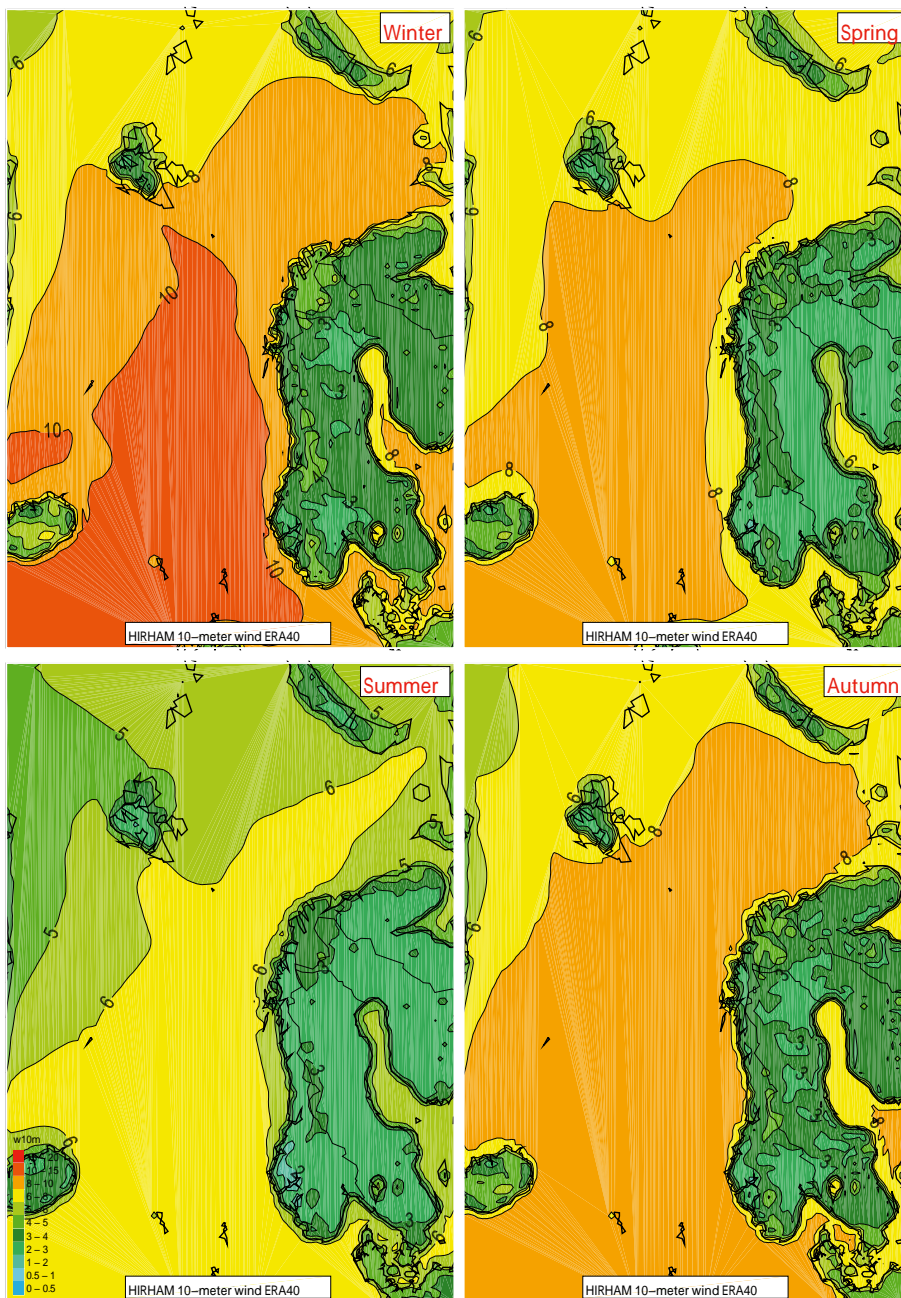


Figure 2.7b Seasonal mean 10 meter wind speed (m/s) for the period 1961-2000 based upon HIRHAM25 downscaling with forcing from ERA40 data. Upper left: Winter (DJF), upper right: Spring (MAM), lower left: Summer (JJA) and lower right: Autumn (SON).

Front is stable in the western part as it is locked to the bank topography. In the east the front is less pronounced and the position more variable.

The fresh Norwegian Coastal Current is found inshore of the Atlantic Current. It follows the Norwegian coast northwards and thereafter eastwards into the Barents Sea. The associated fresh water mass, the Coastal water, is the southernmost water mass in the Barents Sea. The currents and the water masses in the Barents Sea are shown in figure 2.8.

The Norwegian Sea is ice-free except for the northernmost part in the Greenland Sea/Fram Strait (Figure 2.2 and 2.3). The Atlantic water mass in the Barents Sea is also ice free, while most of the Arctic water has seasonal ice cover. The Barents Sea is now essentially ice free in the summer, with ice typically covering only a small area in the northeastern part. The ice coverage is, however, highly variable between years (Figure 2.9).

2.7 Available climate and scenario data from the Norwegian Arctic

eKlima

Meteorological and climatological data from The Norwegian Meteorological Institute (met.no) can be accessed free of charge via the eKlima portal (www.eklima.no). All users have full access to all digital data owned by met.no, as well as data from several other station owners. eKlima has been tested with most of the current browsers.

Examples of content in eKlima:

- Map of observation stations
- List of current weather stations
- Changes in the station network (2006 – present)
- Single observations
- Time series
- Climate products

wsKlima technology allows setting up clients that extract climate data and metadata from met.no's eKlima database (does not require any registration).

yr.no

yr.no (www.yr.no) offers weather forecasts in English for more than 700,000 places in Norway (incl. Arctic & Antarctic sites). yr.no is a joint online weather service from the Norwegian Meteorological Institute (met.no) and the Norwegian Broadcasting Corporation (NRK). yr.no is unique in Europe because of very detailed weather forecasts and free data policy. The weather forecasts on yr.no are based on data provided by Norwegian Meteorological Institute and its international partner institutions such as European Centre for Medium-Range Weather Forecasts (ECMWF) and European Organisation for the Exploitation of Meteorological Satellites (EUMETSAT)

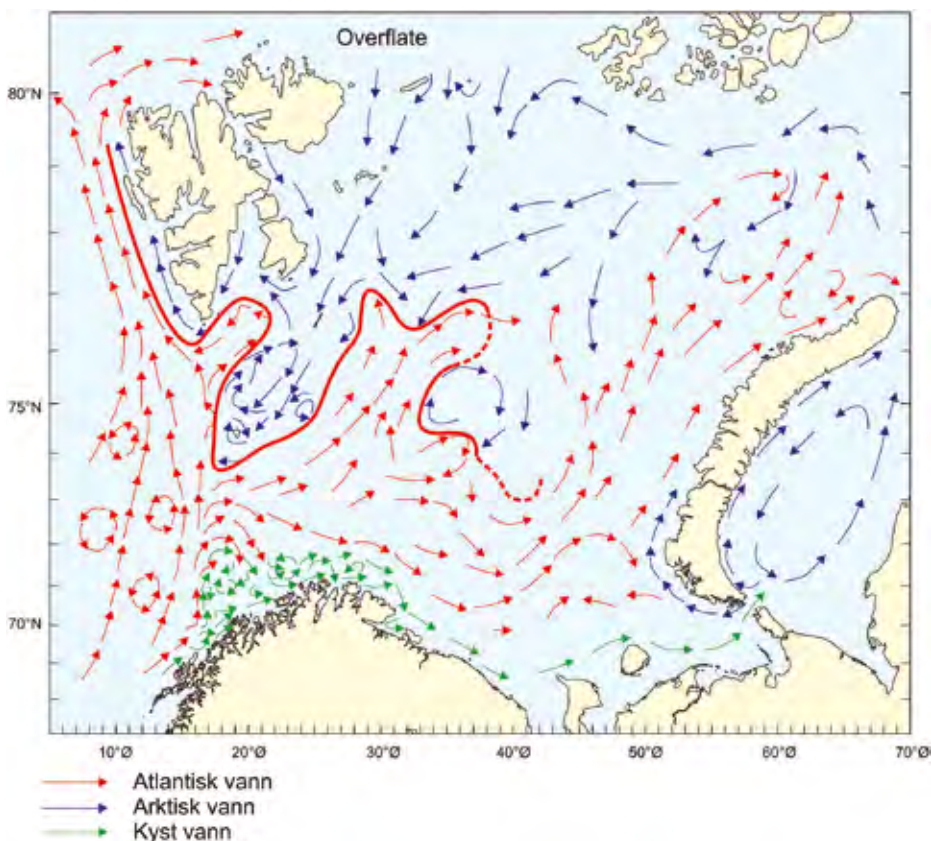


Figure 2.8 The current system and the water masses in the Barents Sea (Loeng and Sætre, 2001)

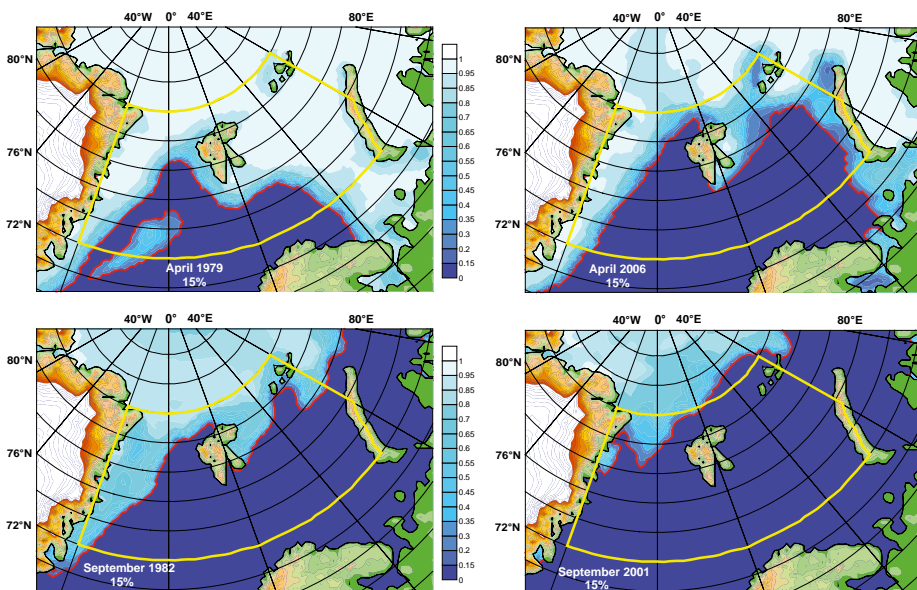


Figure 2.9 Upper panels: Maximal and minimal winter ice coverage (April mean) for the period 1979-2008, derived from passive microwave satellite data (area with ice concentration >15%). Lower panels: Maximal and minimal summer ice coverage (September mean) for the same period (From Gerland in NorACIA (2009))

Examples of detailed products and weather forecasts available from yr.no:

- Forecasts: Hour by hour, next weekend, long term
- Observations and climate statistics for selected sites
- Advanced Maps
- Radar & Satellite maps
- News and facts related to weather and climate

seNorge

seNorge.no (www.senorge.no) is a web-site developed by the Norwegian Water and Energy Directorate (NVE), the Norwegian Meteorological Institute (met.no) and the Norwegian Mapping Authority (Statens Kartverk). The seNorge web-site updates daily snow, weather, water and climate maps for Norway. Data are given as daily, monthly and annual values, as

well as for climate periods and scenarios. There are daily maps back to the 1960s and up to tomorrow. Dozens of themes are presented as several hundred thousand maps. These are useful for hazard mitigation for flood, drought, energy supply shortages, avalanches, landslides and climate change, as well as for businesses and outdoor enthusiasts.

Climate Adaptation Norway

A national web-site for planners on climate adaptation in Norway (incl. Arctic) is now established (www.klimatilpasning.no) as this is a new and unfamiliar area for decision makers.

Aims:

- Strengthen knowledge on adaptation to climate change
- Exchange of information between sectors and administrative levels

Needs:

- Relevant, correct, credible, formal, up to date
- A new and unfamiliar area for decision makers
- Information on adaptation and effects of climate change
- Good examples on adaptation
- Tools to integrate adaptation in planning

Target groups

- Local and regional planners

MOSJ

MOSJ (Environmental Monitoring System for Svalbard and Jan Mayen, <http://mosj.npolar.no/>) has the following objectives:

- Collect and process data on elements impacting the environment and on the status of the environment and cultural remains
- Interpret the data in order to assess trends and developments in the environment
- Give advice on needed actions, research or better monitoring.

MOSJ covers both the atmosphere and the terrestrial and marine environments on and surrounding Svalbard and Jan Mayen.

3. Climate variability and trends in the 20th century

3.1 Introduction

Due to the harsh environment and the sparseness of the observation network, it is difficult to monitor climate variability over the Arctic. On Svalbard the first permanent weather station was established in Green Harbour in 1911, and stations on Bjørnøya and Jan Mayen were established in 1920 and 1921. For studies of long-term climate variability and trends, it is crucial to base the analyses on homogeneous series. Real climatic trends may be masked or amplified when analyses are based upon inhomogeneous series, and it is accordingly important to adjust series for inhomogeneities before they are used in studies of long-term climate variations. Earlier studies have revealed that inhomogeneities in meteorological elements in the Nordic region often are of the same magnitude as typical long-term trends (Hanssen-Bauer & Førland, 1994, Nordli et al., 1996). Inhomogeneities in Arctic series may be caused by relocations of sensors, changed environment (buildings etc.) and instrumental improvements. Because of the harsh weather conditions, even small changes at Arctic measuring sites may cause substantial changes in measuring conditions for wind and precipitation. Identification of inhomogeneities in Arctic series is also complicated by the sparse station network. A survey of inhomogeneities and adjustment factors for the Norwegian Arctic temperature and precipitation series are given by Nordli et al. (1996).

3.2 Land surface air temperature

Global and Pan-Arctic

The global mean surface temperature (IPCC, 2007) has increased with a linear trend of ca. 0.074°C per decade over the last 100 years (1906–2005). The warming is widespread over the globe, with a maximum at higher northern latitudes. In average, the land temperatures over the Arctic north of 65°N increased almost twice the global average rate over the past 100 years and also from the late 1960s to the present. It should be stressed that in the Arctic, a warm period, almost as warm as the present, was observed from the late 1920s to the early 1950s. Although data coverage was limited in the first half of the 20th century, the spatial pattern of the earlier warm period appears to have been different from that of the current warmth. In particular, the current warmth is partly linked to the Northern Annual Mode and affects a broader region (Polyakov et al., 2003).

The average surface temperature in the Arctic (ACIA, 2005) increased by approximately 0.09°C per decade over the past century, and the pattern of change is similar to the global trend (i.e. an increase up to the mid-1940s, a decrease from then until the mid-1960s and a steep increase thereafter with a warming rate of 0.4°C per decade). Because of the scarcity of observations across the Arctic before about 1950,

it is not possible to be certain of the variation in mean land-station temperature over the first half of the 20th century. However, it is probable that the past decade was warmer than any other period of the instrumental record. The observed warming in the Arctic in the latter half of the 20th century appears to be without precedence since the early Holocene. Concerning the warming in the early 20th century, it should be noted that between 400 and 100 years BP, the climate in the Arctic was exceptionally cold (ACIA, 2005).

Norwegian mainland - North Norway

The annual mean temperature in different parts of Norway has during the latest 130 years increased by between 0.04 and 0.12°C per decade (Hanssen-Bauer, 2005). The increase in annual mean temperature is statistically significant at the 1% level everywhere, except in the interior parts of Finnmark. For the winter temperature there are no statistically significant trends for any of the six Norwegian temperature regions. Spring temperatures have increased significantly everywhere. Summer temperatures have increased significantly in northern regions, and autumn temperatures have increased significantly everywhere except in mid-Norway and the inland of Finnmark. In spite of the linear trends: There have been substantial decadal and multi-decadal temperature variations during the last 130 years. After a rather cold period around 1900 followed the “early 20th century warming”, which culminated in the 1930s. A period of cooling followed, before the recent warming which has dominated the whole country since the 1960s. In southern Norway, the warmest decade of the last 130 years occurred near the end of the series. In most parts of North Norway, the warmest decade occurred around the 1930s.

The long-term temperature development in North Norway is outlined in Figure 3.1 and Table 3.1. The annual temperature has increased significantly with a linear trend of ca. 0.1°C per decade – i.e. the annual temperature is more than 1°C higher than around year 1900. The warm period in the 1930s is very evident in the figure, and still the year 1938 ranks as the warmest year recorded in the instrumental era. On the other hand, Figure 3.1 clearly demonstrates an overwhelming majority of years since 1989 with annual temperatures above the 1961-90 average. The only year with a negative anomaly is 1998. For all parts of North Norway except for Finnmarksvidda, there are significant positive trends for the spring, summer and autumn seasons (Table 3.1). The largest temperature increase (–0.15°C/decade) has been recorded for the spring season (Figure 3.1). Thus the spring temperature is approximately 1.5°C higher than around year 1900. For Finnmarksvidda, none of the linear trends for annual and seasonal temperature development are statistically significant. For the winter season there is even a small (insignificant) negative trend. The main reason is that the warm period in the 1930s still has strong influence on the temperature development in this region.

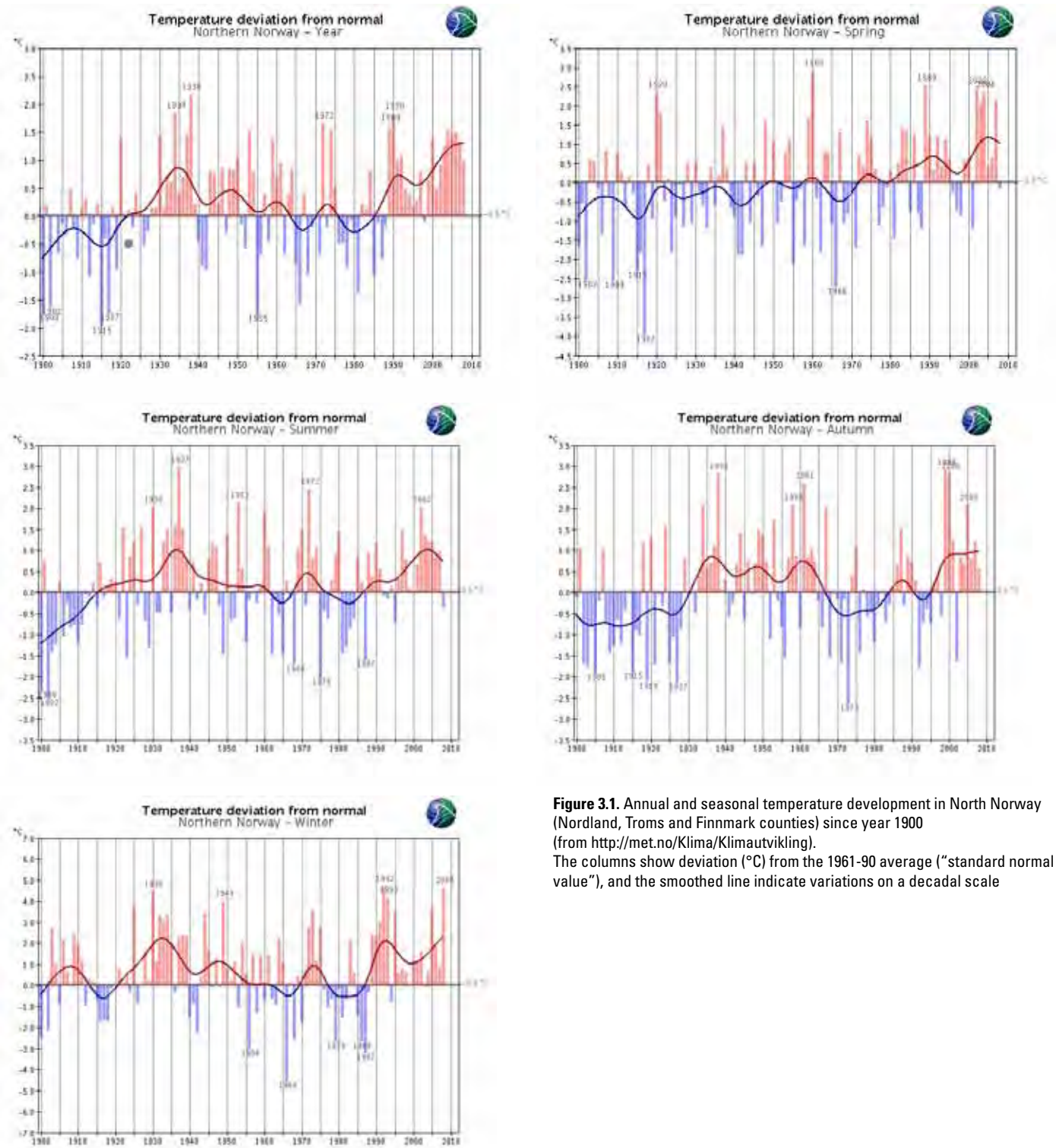


Figure 3.1. Annual and seasonal temperature development in North Norway (Nordland, Troms and Finnmark counties) since year 1900 (from <http://met.no/Klima/Klimautvikling>). The columns show deviation (°C) from the 1961-90 average ("standard normal value"), and the smoothed line indicate variations on a decadal scale

Svalbard and Jan Mayen

Hanssen-Bauer et al (2009) studied variability and trends in the Norwegian Arctic temperature and precipitation time series. Linear trends were calculated, even though there is certain scepticism against using linear trends as a measure for climate change, because such changes not necessarily occur linearly (Benestad, 2003). However, the statistical significance of the trends was tested by the Mann-Kendall non-parametric test (Sneyers, 1995), in which the sequence numbers of the values are tested rather than the actual values. For Longyearbyen an updated version of a composite Green Harbour – Longyearbyen

– Svalbard Airport series starting in the autumn 1911 was used.

The correlation coefficients between the annual mean temperature at the stations on Spitsbergen and Hopen are very high (Hanssen-Bauer et al., 2009). Also the correlation between the Spitsbergen and Hopen series and the series from Bjørnøya tend to be >0.90. The correlation with Jan Mayen is smaller, but still significant. Similar analyses on seasonal basis show that the correlation is best during winter and poorest during summer. Between the Spitsbergen stations, the correlation coefficients are still around 0.9 during summer.

The time series of annual and seasonal mean temperature (Figure 3.2) for Svalbard Airport/ Longyearbyen show large inter-annual variability, especially during winter. There also seems to be a tendency for clustering of cold or warm years, e.g. the years before 1920, and the 1960s were mainly cold, while the 1930s, the 1950s and the latest decade were for the most part warm. This is seen both on annual and seasonal basis. The tendency for warm and cold clusters of years is clearly seen in the low-pass filtered series (Figure 3.2).

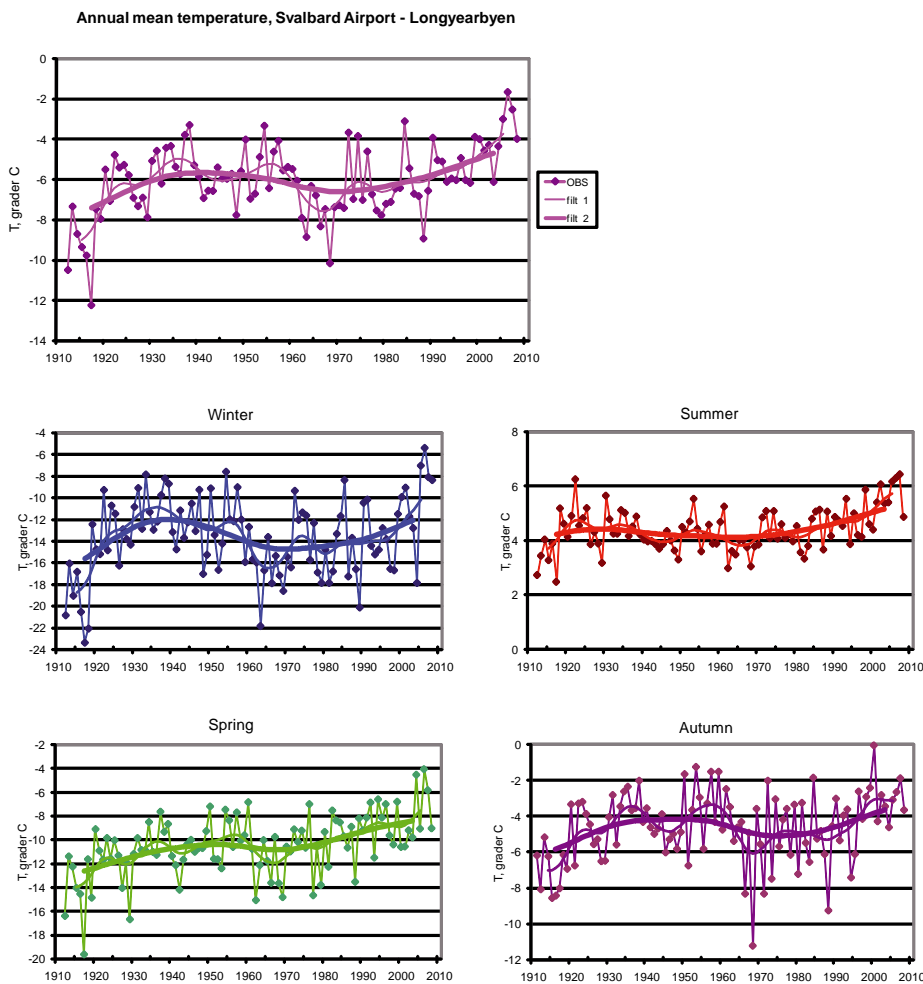


Figure 3.2 Annual and seasonal temperatures at Svalbard Airport/Longyearbyen 1911-2007. The smoothed curves (Fit. 1 and 2) show variations on a decadal resp. 30-years scale

Figures 3.2 and 3.3 also show that there is variability on a multi-decadal scale, leading to mainly positive temperature trends before the 1930s, a rather warm period the next couple of decades, a temperature fall from the 1950s to the 1960s, and thereafter a general temperature increase. These features are seen for annual mean temperature and in the seasonal temperatures for winter and autumn. In spring the period of temperature decrease is less expressed. In summer, there is in general less temperature variability,

but the latest period of temperature increase is still recognized.

Linear trends in the series obviously depend strongly of start and ending point. Earlier studies (e.g. ACIA, 2005) have shown that the longest series by optimal choice of breaking points can be divided into three periods where the first and the last show statistically significant warming, while the middle period shows statistically significant cooling. In order to make the

trends in the different periods directly comparable, Hanssen-Bauer et al (2009) chose not to use these “optimal periods”, but rather to calculate trends for three 35-year periods with 5-year overlap (1912-1946, 1942-1976 and 1972-present). In the first 35-year period, the composite Svalbard Airport series is the only one running from the start. This series shows a strong warming, significant in all seasons except for the summer. In the period 1942-1976, all stations tend to show negative trends in annual temperatures as well as for autumn and winter, but the trends are not statistically significant. During the latest 35-year period, all trends are positive in all seasons, though not all of them are statistically significant. The consistency between the trends in all seasons and at all stations is specific for this period.

The trends for the whole measurement period for all stations are given in Table 3.1. The annual mean temperature has increased significantly in the Svalbard Airport/Longyearbyen area from 1912 to present. The linear trend indicates a warming of 2°C during the 95 year period, which is about three times the estimated global warming during the same period. Statistically significant warming has occurred in spring, summer and autumn. The spring seasons towards the end of the series are typically more than 4°C higher than those in the beginning. In winter, the temperature increase is still not statistically significant. The trends in the shorter series depend on their start and end-point. Ny-Ålesund which has been running since 1969 shows a positive trend, while Isfjord Radio, which started in the warm 1930s and ended in 1976, shows a negative trend. The trends in the other series are not statistically significant for annual values.

The timeseries of annual mean temperatures at the Norwegian Arctic stations show a quite similar longterm pattern (Figure 3.3). The temperature has increased in all seasons – and with strongest increase winter and spring. Figure 3.3 also shows that while Longyearbyen/Svalbard Airport through the whole period has the lowest mean winter temperatures, this station after ca. 1945 has had the highest mean summer temperature. The figure also shows that the summer temperatures on Hopen are substantially lower than at the other Norwegian Arctic stations.

The composite Svalbard Airport series (Figure 3.2) shows periods with warming from 1912 to the 1930s and from ca. 1970 to present, but with cooling from the 1950s to 1970. For this series there is a linear trend +0.22°C per decade from 1912 to 2007. This trend is statistically significant at the 1% level. Up to year 2000 the annual trend from the beginning of the series was not statistically significant. This was due to some mild years in the 1930s and 1950s. These periods were at least as warm as the mild years in the 1990s. However, after year 2000 there have been several exceptionally warm years at

Table 3.1 Linear temperature trends for long station series, °C per decade. Trends statistically significant at the 5% level are marked in bold (* From Hanssen-Bauer et al., 2009, ** From Hanssen-Bauer, 2005)

Station	Period	Annual	Winter	Spring	Summer	Autumn
Ny-Ålesund *	1969-2006	+0.49	+0.72	+0.67	+0.22	+0.40
Svalbard Airport *	1912-2006	+0.21	+0.15	+0.44	+0.09	+0.14
Isfjord Radio *	1935-1976	-0.28	-0.84	+0.09	-0.02	-0.42
Hopen *	1946-2006	+0.19	+0.01	+0.38	+0.24	+0.10
Bjørnøya *	1920-2006	+0.05	-0.14	+0.26	+0.08	0.00
Jan Mayen *	1921-2006	-0.01	-0.12	+0.06	+0.03	0.00
Finnmarksvidda **	1875-2004	+0.05	-0.02	+0.11	+0.08	+0.05
Varangerhalvøya **	1875-2004	+0.12	+0.11	+0.15	+0.12	+0.10
Nordland, Troms, W.Finnmark **	1875-2004	+0.09	+0.04	+0.14	+0.09	+0.07

Svalbard and Jan Mayen. The year 2006 was the warmest ever recorded at Svalbard Airport/Longyearbyen, with 2007 and 2005 on second and third position. Jan Mayen had its highest annual mean temperature in 2002, followed by 2006 and 2004.

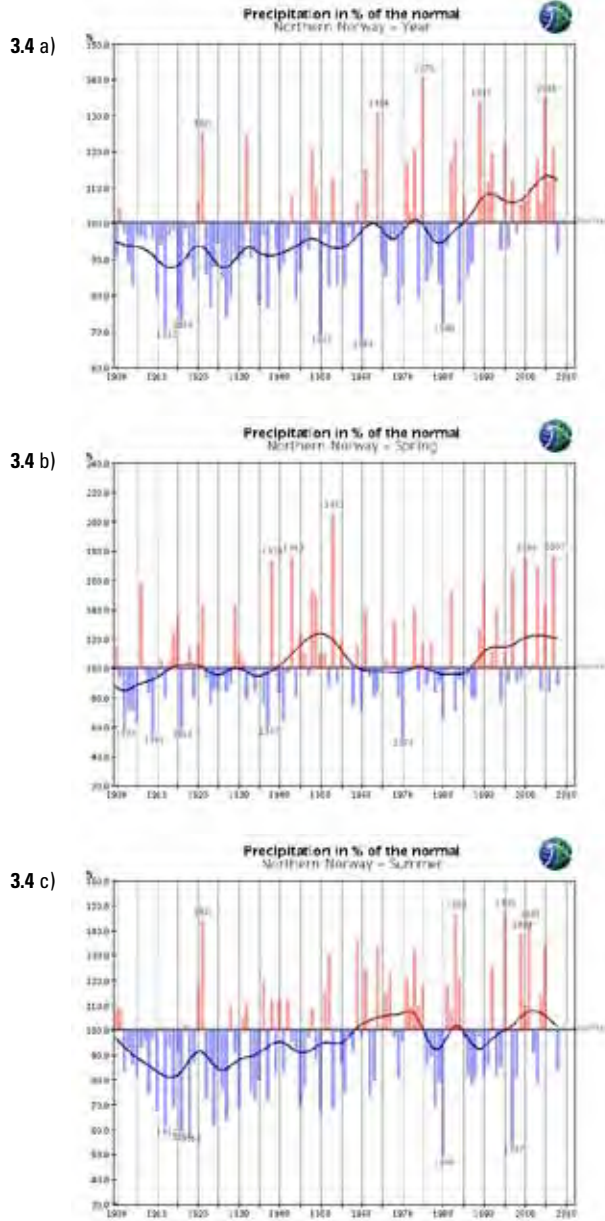
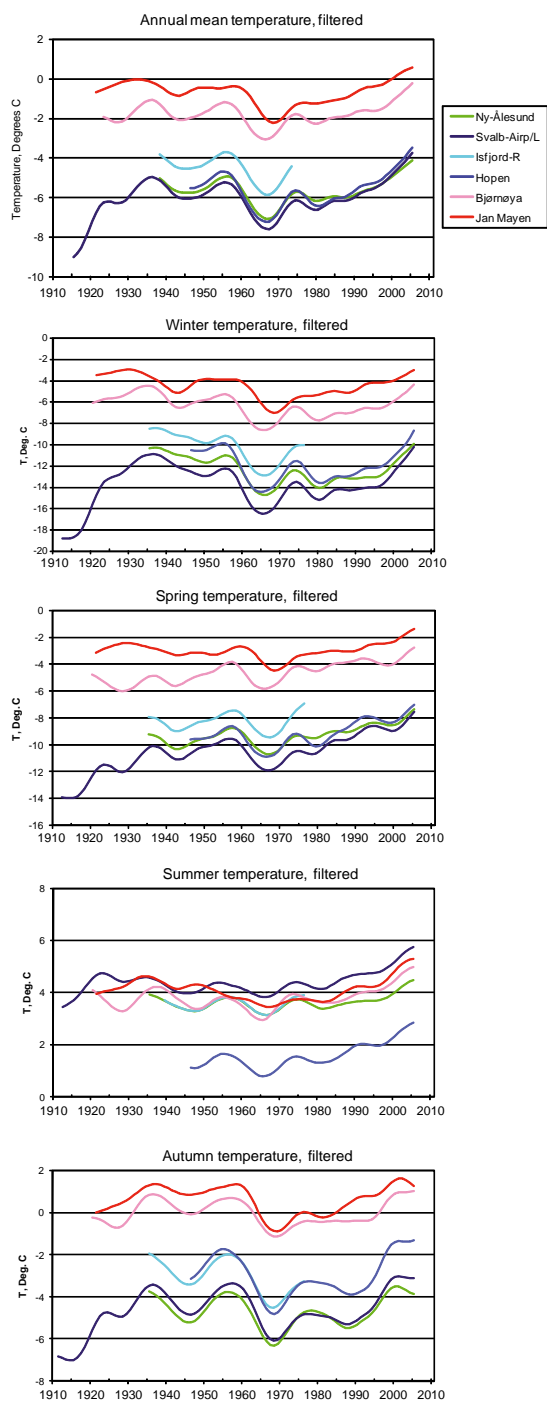
The linear seasonal temperature trends at Svalbard Airport/Longyearbyen from 1912 to 2007 are +0.21°C per decade (winter), +0.46 (spring), +0.10 (summer) and +0.16 (autum). Except for the winter season all seasonal trends are statistical significant at least at the 5%-level.

3.3 Precipitation

Pan-Arctic

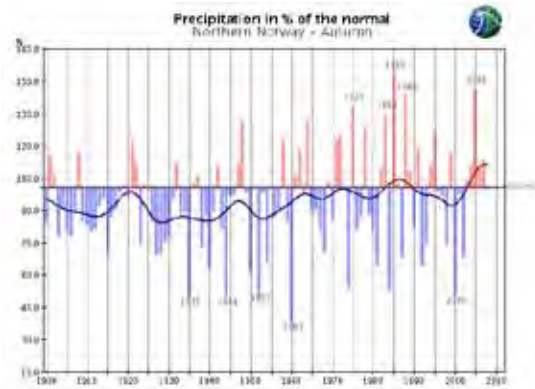
Observations suggest that it is probable that total annual precipitation has increased by roughly 14% in the Arctic north of 60°N over the past century (ACIA, 2005). The greatest increases were observed in autumn and winter. However (cf. chapter 2.3), uncertainties in measuring precipitation in the cold Arctic environment and the sparseness of data in parts of the region limit confidence in these results. There are large regional variations in precipitation across the

Arctic, and also large regional variations in the changes in precipitation. According to ACIA (2005) the precipitation increased by about 2% per decade during the Arctic warming in the first half of the 20th century (1900-1945), with significant trends in the Nordic region. During the two decades of Arctic cooling (1946-1965), the high latitude precipitation increase was roughly 1% per decade. Since 1966, annual precipitation has increased at about the same rate as during the first half of the 20th century. Also IPCC (2007) states that there has been a widespread increase in precipitation over northernmost Europe during 1900-2005.



Figur 3.3 Annual and seasonal temperature development at Norwegian high-Arctic stations. The smoothed curves show variability on a decadal scale

3.4 d)



3.4 e)

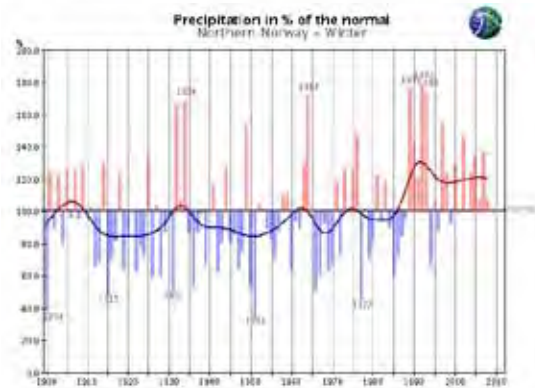


Figure 3.4 Annual and seasonal precipitation development in North Norway (Nordland, Troms and Finnmark counties since year 1900 (from <http://met.no/Klima/Klimautvikling>).

The columns show deviation (%) from the 1961-90 average ("standard normal value"), and the smoothed line indicate variations on a decadal scale

Norwegian mainland - North Norway

Annual precipitation at the Norwegian mainland has during the latest 110 years increased significantly (at the 5% level) in 9 of 13 "precipitation regions" (Hanssen-Bauer, 2005). No region shows a negative trend. The largest increase (15-20% increase) is found in the north-western regions. Autumn precipitation has increased significantly in most southern regions. Winter and spring precipitation has increased significantly in the north-west, and to some degree in inland regions. Summer precipitation has increased significantly in most of the northern regions.

The long-term precipitation development in North Norway since year 1900 is shown in Figure 3.4 and linear trends are outlined in Table 3.2. Except for the Varanger peninsula, the annual precipitation in North Norway has increased with approximately 2% per decade during the latest 100 years – i.e. the annual precipitation is ca. 20% higher than around year 1900. During the latest 20 years, just three years have annual values below the 1961-90 average (Figure 3.4). For Nordland, Troms and eastern Finnmark, there is a statistically significant increase (-2.5% per decade) in spring precipitation (Table 3.2). For the Varanger peninsula there is a (insignificant) decrease in precipitation during winter and spring.

Svalbard and Jan Mayen

The precipitation series from the Norwegian high-Arctic stations show quite different patterns both on an annual as well as a decadal timescale (Figure 3.5). This is in contrast to the quite similar development for temperature, and the main reason is that precipitation varies locally on a smaller spatial scale than air temperature. The series though have one common feature: All series show a positive trend in annual precipitation throughout the period of observations (cf. Table 3.2). The trends in annual precipitation at Svalbard Airport and Bjørnøya are statistical significant at the 1% level. At Svalbard Airport the annual precipitation has in average increased by 4 mm per decade (2% per decade), while the increase on Bjørnøya is 12 mm per decade (3% per decade). At Svalbard Airport the summer- and autumn precipitation show a statistical significant increase, while on Bjørnøya the winter, spring and autumn precipitation has a statistical significant increase.

Table 3.2 Linear precipitation trends (% per decade) for long station series. Trends significant at the 5% level are indicated in bold. "Spitsbergen" is a composite western Spitsbergen series based on data from Longyearbyen, Svalbard Airport and Ny-Ålesund. (* From Hanssen-Bauer et al., 2009, ** From Hanssen-Bauer, 2005)

Station	Period	Annual	Winter	Spring	Summer	Autumn
"Spitsbergen" *	1912-2006	+2.6	+0.3	+2.2	+5.2	+3.2
Svalbard Airport *	1912-2006	+2.1	-0.8	+1.6	+4.5	+2.9
Ny-Ålesund *	1969-2006	+3.2	+3.7	+1.0	+2.8	+5.7
Hopen *	1946-2006	+3.1	+5.8	+4.0	-0.5	+3.4
Bjørnøya *	1920-2006	+3.1	+4.1	+4.3	+1.2	+2.6
Finnmarksvidda **	1895-2004	+1.8	+3.0	+2.4	+1.4	+1.2
Varangerhalvøya **	1895-2004	+0.3	-1.3	-1.6	+3.2	+0.6
Nordland, Troms, W.Finnmark **	1895-2004	+1.9	+2.6	+2.6	+2.4	+0.5

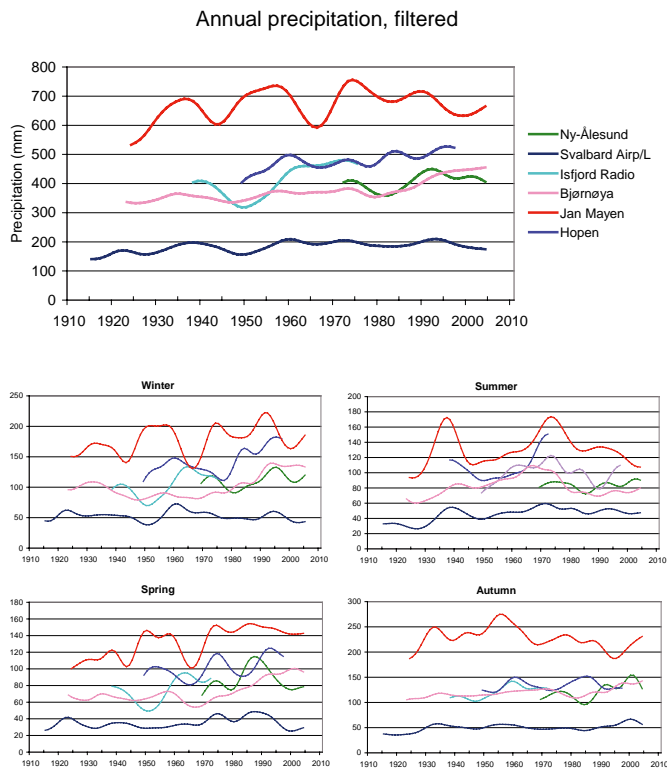


Figure 3.5 Annual and seasonal precipitation development at Norwegian high-Arctic stations. The smoothed curves show variability on a decadal scale.

on Janssonhaugen below ZAA provides evidence for secular warming, since it is nonlinear, with warm-side temperature deviation from the deeper thermal gradient (Figure 3.6.). The smooth temperature profile from Janssonhaugen supports a very low geothermal disturbance from undesirable elements and non-climate sources and contains a preserved climate signal particularly suited for reconstructing the ground surface temperature history. Using a one dimensional heat conduction inversion model a climatic reconstruction shows a warming of the permafrost surface of 1–2 °C for the period 1920–2000 (Isaksen et al. 2000).

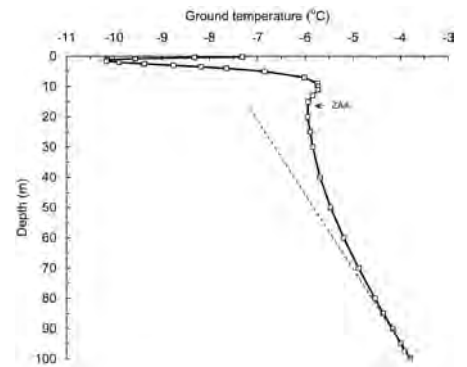


Figure 3.6: Ground temperature profile in permafrost at Janssonhaugen, recorded 22nd April 2005. The arrow indicate the approximate depth of Zero Annual Amplitude (ZAA), equivalent to the depth where seasonal amplitudes are diminished to 0.1 °C. The dotted line is an extrapolation of the thermal gradient measured in the lowermost part of the borehole (85–100 m), which is assumed to be unaffected by recent warming trends (modified after Isaksen et al. 2007a).

3.4 Snow

Analyses of long-term development of snow conditions are emphasized in international climate research, e.g. in connection with the International Polar Year (IPY). The reason is partly that snow is an important indicator of climate changes, but also because the snow cover has substantial feed-back effects in the climate system. For Norway changes and variability in snow accumulation are of great importance for the hydro-power production, as well as for agriculture, forestry, reindeer husbandry, transportation etc. Improved knowledge of long-term variability of snow cover and snow depth is thus of great importance.

Snow cover extent over higher northern latitudes has declined by about 10% over the past 30 years, and model projections suggest that it will decrease an additional 10–20% before the end of this century (ACIA, 2005). Also the latest IPCC-report (IPCC, 2007) concluded that the snow cover has decreased in most regions, especially in spring. The Northern Hemisphere snow cover observed by satellite over the 1966–2005 period decreased in every month except November and December, with a stepwise drop of 5% in the annual mean in the late 1980s (IPCC, 2007).

For Norway, Dyrddal & Vikhamar-Schuler (2009) found that the snow season has decreased during the latest hundred years at most of the 41 long-term snow series they analysed. At most stations there was a clear tendency to a later start and an earlier end of the snow season. Also for maximum annual snow depth they found a majority of negative trends. However, for maximum

daily increase in snow depth (i.e. an indicator for heavy snowfalls) they found a tendency to increasing values in North Norway.

3.5 Permafrost

Measuring sites for permafrost

In North Norway, there are few quantitative studies on permafrost and no long-term monitoring of permafrost. However, in Svalbard a permafrost site was established in 1998 at Janssonhaugen in Adventdalen, 270 m a.s.l. (Isaksen et al., 2000). The depth of the hole is 102 m and the site is equipped for long-term monitoring for future climate studies. The observations at Janssonhaugen are representative for bedrock with relatively low ice content, typical for the mountain areas in central and western Spitsbergen. In permafrost areas with debris and unconsolidated rock that have higher ice content, the temperature response in the ground will be weaker and the temperature increase less.

Major ground temperature increase

A geothermal profile from Janssonhaugen is presented in Figure 3.6. Ground temperatures vary seasonally down to a depth of 18 m (amplitude of temperature wave less than 0.1°C), equivalent to the depth of “Zero Annual Amplitude”, (ZAA). The analysis of the geothermal profile

Isaksen et al. (2007a) found that the permafrost at Janssonhaugen presently is warming up rapidly. The annual temperature signal below 20 m depth is free of any response to annual or shorter-term temperature variations. At these depths any recorded systematic temperature time variations must correspond to a longer period of several years and decades. Figure 3.7 shows the observed temperature increases at depths of 25, 30 and 40 m. At 30 m depth, the temperature increased by 0.28 °C in the period 1999–2008. At a depth of 40 m, the ground temperature increased by 0.15 °C during the same period. The observed warming is statistically significant down to a depth of 60 m.

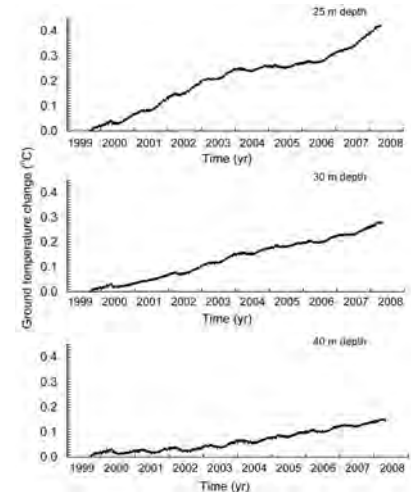


Figure 3.7: Observed relative ground temperature change for three selected depths (25 m, 30 m and 40 m) at Janssonhaugen

Since the temperature is observed continuously over several years, it is possible to calculate the temperature trends at different depths (Figure 3.8). The average temperature increase at 30 m depth is about 0.35 °C per decade and at 60 m 0.05 °C per decade. These values are used to estimate the temperature changes on the surface of the permafrost (~2 m). Findings show that the temperature at the top of the permafrost is now increasing by an average of 0.7 °C per decade. This value is representative for the last two to three decades. The analyses also show that the temperature increase in the permafrost is accelerating, particularly in the last decade. The ground temperature shows a strong correlation with the air temperature, and is therefore a valuable supplement to more traditional temperature data presented in chapter 3.2.

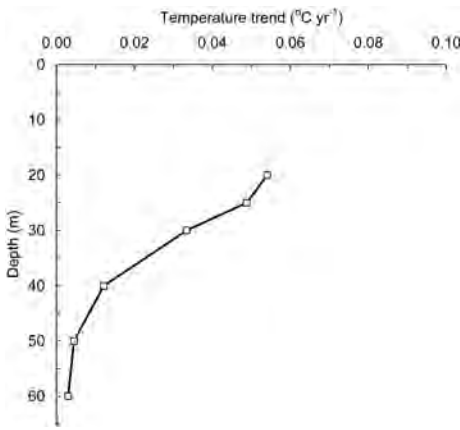


Figure 3.8: Observed linear trends in ground temperature as a function of depth. Statistically significant positive trends are found to 60 m depth. Time series at Janssonhaugen start in 1999, and last for six years (modified after Isaksen et al. 2007a)

Extreme permafrost warming in 2006

The mean temperature for winter and spring 2005–2006 on Svalbard was extremely high (Figure 3.2). The weather stations recorded one of the largest temperature anomalies over a six-month period ever observed at any location in recent times (Isaksen et al. 2007b). The effect of this extreme situation on temperature conditions in the permafrost on Svalbard was studied by Isaksen et al. (2007b) in the context of results from climate models.

The mean temperature in 2006 on the upper layer of the permafrost at about 2 m depth on Janssonhaugen was as much as 1.8 °C higher than the mean for the previous six years (Figure 3.9). Seen in isolation, this is a substantial anomaly for this kind of annual mean temperature. Moreover, the minimum temperature at 15 m depth was 0.3 °C higher than the mean for 1999–2005. Knowing that this episode follows a long period of dramatic and accelerating temperature increase in the permafrost makes the results all the more alarming. In 2006, the thickness of the active layer, that is the layer above the permafrost that thaws each summer, was greater than ever before recorded at Janssonhaugen (Figure 3.10). The thickness increased by about 11 percent in relation to the average for the period 1999–2005.

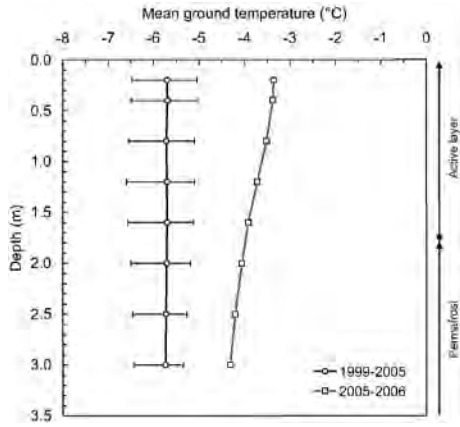


Figure 3.9: Mean annual ground temperature profile in the active layer and uppermost permafrost for 2005–2006 (squares) compared with the mean (circles) for 1999–2005. Horizontal bars show the absolute variations of the previous years (after Isaksen et al. 2007b)

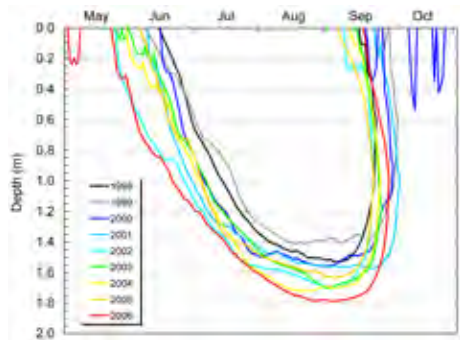


Figure 3.10: Active layer evolution (24 h resolution) and depth (0°C) on Janssonhaugen summer and autumn 1998–2006

In general, it can be assumed that the warming of the permafrost will occur gradually, which is also supported by models. With an Arctic undergoing rapid change, including an increased frequency of temperature extremes, the future warming of the permafrost, however, can to a greater degree be more irregular than regular.

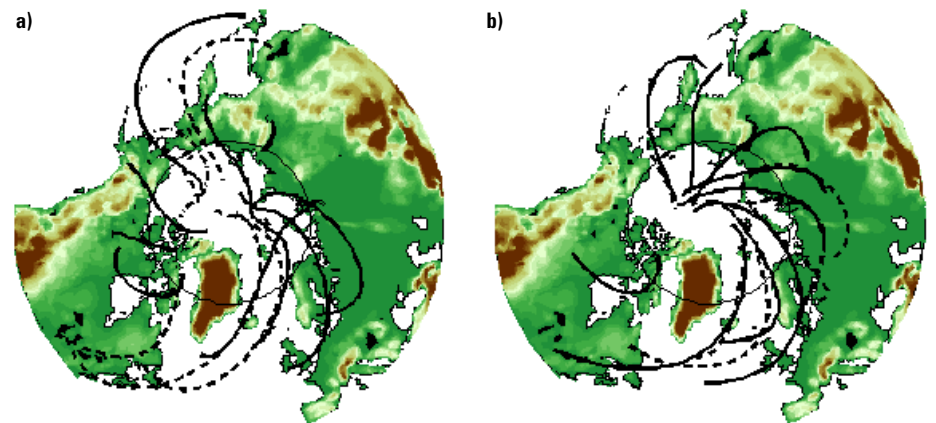


Figure 3.11: Main winter (a) and summer (b) cyclone tracks for cyclones entering the Arctic (taken from Sorteberg and Walsh, 2008)

3.6 Cyclones entering the Arctic

With around 140 individual cyclones and a mean residence time of 2.6 days, cyclones entering the Arctic are a common feature (Figure 3.11). In terms of number of cyclones the Greenland/Norwegian Seas (30°W–30°E) are the main pathways for cyclones entering the Arctic (Sorteberg and Walsh, 2008) and being the main heat and moisture transporter into the Arctic, variability in numbers and/or intensity of cyclones will influence the Arctic climate strongly.

Although regional differences still remain between the different analyses due to their choice of threshold values for identifying the cyclones etc., several authors have reported long term trends in the Arctic cyclone activity (Sorteberg and Walsh, 2008; Zhang et al. (2004), Serreze et al. (1993); McCabe et al. (2001). Focusing only on cyclones entering the Arctic from the Greenland/Norwegian Seas (30°W–30°E), trends are seen in both the mean intensity of the cyclones and in the intensity of the most intense cyclones (around 12% increase over the 1950–2006 period). Heat and moisture transport is linked to both the number and intensity of cyclones. Thus a cyclone activity index (CAI) which takes into account variability or systematic changes in both parameters has been shown to give a good overall indication of the cyclone effect on moisture and heat transport (Sorteberg and Walsh, 2008).

Table 3.3 shows that CAI has increased in all seasons, but strong interannual variability makes the trend only significant during wintertime and on annual basis. Annually there has been a 27% change in the cyclone activity (CAI) over the 1950–2006 period. If this was the only source of atmospheric variability this indicates an increased heat and moisture transport into the European Arctic over the period.

It should be noted that the tracking methodology, changing data availability and the assimilation procedure in the reanalysis may influence the trend estimates (Bengtsson et al., 2004) and that the attribution of the apparent trends to any external forcing is even more difficult due to strong decadal variability in the Arctic climate (Sorteberg et al., 2005, Sorteberg and Kvamstø, 2006).

Table 3.3. Linear trends in cyclone parameters for cyclones crossing 70°N in the Greenland/Norwegian Seas (30°W–30°E) region, over the 1950–2007 period. Intense cyclones are defined as the 10% strongest cyclones. Unit: % per decade, sign. 10% level: bold. Cyclones are detected using relative vorticity. CAI: Cyclone Activity Index, measured as the accumulated relative vorticity at 70°N. Thus, this indicates changes both in number and intensity of the cyclones. For details on cyclone identification and CAI see Sorteberg and Walsh (2008).

Cyclone parameter	Annual	Winter	Spring	Summer	Autumn
Number of individual cyclone tracks	2.4	5.7	2.3	3.1	0.3
Average Intensity at 70°N	2.0	0.2	1.2	1.0	2.8
Intensity of intense cyclones at 70°N	2.2	-0.9	0.8	1.8	2.9
Cyclone Activity Index (CAI)	4.8	6.6	4.0	3.9	3.1

3.7 Marine indices

The temperatures in the Norwegian and Barents Seas show large interannual variability. The ocean temperature in the area is determined by the strength and the temperature of the Atlantic inflow and the heat exchange with the atmosphere.

The Norwegian Institute of Marine Research monitors the temperature development in the area by a set of fixed coastal stations and repeated hydrographic sections crossing the Atlantic Current. Some of the coastal stations provide time series back to the 1930s. The longest time series in the area is the Russian Kola series covering the whole century. This series is monitored by the PINRO institute in Murmansk.

On the longest time scale, as seen from the Kola series (figure 3.12), the temperature is dominated by the multidecadal oscillation, cold at the beginning of the century, warm in the 1930–50s, then cold again in the 1970–80s before the present warm period. Both 2005 and 2006 gave new record high temperatures, thereafter the conditions have become slightly colder.

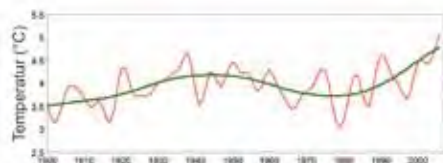


Figure 3.12 Temperature development in the Barents Sea. The temperature development in the Kola section is based on data from PINRO (Murmansk). The data are filtered using Butterworth Lowpass Filter over 5 years (red) and 30 years (green). From Loeng (2008).

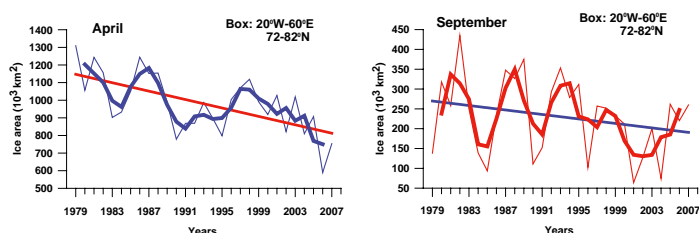


Figure 3.13 Trends for sea ice extent in the Barents Sea for April and August. Thin curve shows annual mean values, thick curve shows the 3-year annual mean, while the straight line shows the trend for the period 1997–2008. (From Gerland in NorACIA (2009)).

The sea ice coverage can be reliably estimated by satellites. This gives data back to the 1970s. The data show a decline in sea ice coverage, for the whole Arctic and for the Barents Sea in particular. ACIA (2005) stated that it is very probable that there have been decreases in average Arctic sea-ice extent over at least the past 40 years, and that there will be a decrease in multi-year sea-ice extent in the central Arctic. It is however worth mentioning that the time series started when the ocean temperature was lower than average and the ice cover perhaps larger than average.

The time series of ice coverage for April and August (maximum and month before minimum ice coverage) are shown in Figure 3.13. The April series shows a strong reduction. For the summer ice, the reduction is even more pronounced. After year 2000 there have been four years with essentially no summer ice. Less data is available on ice thickness, but a time series from Hopen shows a reduction in ice thickness over a 40 year period.

4 Climate projections for the 21st century

4.1 Climate modelling and downscaling

Global climate models (AOGCM)

The comprehensive Atmosphere Ocean General Circulation Models (AOGCMs) include dynamical descriptions of atmospheric, oceanic, sea ice processes and often land surface processes and are the most sophisticated tools available for projecting global warming. The resolution in the AOGCMs is presently probably sufficient for modelling most of the large-scale features, but

in general still too coarse to enable these models to reproduce the climate on regional or local scale. During the six years from the IPCC Third Assessment Report (TAR, IPCC 2001) to the Fourth Assessment Report of the IPCC (AR4, IPCC 2007) much progress has been made. Transport schemes and resolutions have been increased, more processes have been included and parametrizations improved. The most important is probably that most of the models no longer use flux adjustments to reduce climate drift. Over 20 models from different centers were available to produce the climate projections analyzed in the AR4. The descriptions of the large-scale dynamical systems are quite comprehensive in these models, but there are still many unresolved physical processes such as cloud formation and precipitation mechanisms in the atmosphere, wave induced mixing and formation of water masses in the ocean and sea ice processes. These processes are therefore represented by parametrizations. Uncertainties and differences in parametrizations is the major reason behind the differences in the climate projections between different AOGCMs (IPCC 2007).

At higher latitudes the natural variability is larger and can also explain much of the differences (Sorteberg et al. 2005). The resolution of AOGCMs is continually improving, but still insufficient to capture the fine-scale climatic structure in many areas such as in the NorACIA region. When more detailed climate data are needed, output from AOGCMs can be used to drive regional climate models that have even more detailed process representations comparable to AOGCMs in addition to a much higher spatial resolution. One reason for the high climate variability in the Arctic is feed-back mechanisms connected to snow and ice. An important (though it is not the only) condition for making realistic climate projections, is thus that the AOGCM that is used for driving the regional model, gives a reasonably good description of the present climate in the Arctic. Though no single AOGCM can be said to be “best” to use in an assessment of the Arctic, Walsh et al. (2008) have evaluated and ranked 15 of the IPCC AR4 models according to their ability to reproduce the observed sea level pressure, temperature and precipitation.

The trend in the elaborations of AOGCMs is to make them more general by adding modules for important climate processes. This next generation is called an Earth System Model (ESM) and employs a carbon cycle model including atmosphere, ocean, vegetation changes and other terrestrial processes. Other important modules included in some ESMs are land use changes, ocean biology, prognostic ice sheet and additional atmospheric aerosol and chemistry models. A new Norwegian ESM is now being developed as a joint effort between the climate research centers in Norway. The aim is that the model should be ready to contribute to the next IPCC report, meaning that it must be operational by the end of 2009.

AOGCM simulations in Norway

The Bergen Climate Model (BCM) is developed at the Bjerknes Centre for Climate Research. It consists of an atmospheric model (ARPEGE/IFS) together with a global version of the ocean model MICOM (including a dynamic – thermodynamic sea-ice model). The coupling between the two models is done with the software package OASIS. The atmosphere model has a linear T63 (2.8°) resolution with 31 vertical levels. Key quantities regarding climatic means and variability of the control integration have been evaluated against available observations, most of the model design and characteristics are documented in Furevik et al. (2003). The BCM system has been documented by several authors (see http://bcmwiki.nersc.no/index.php/Main_Page#Publications).

Compared to Furevik et al. (2003) several changes were introduced in BCM for the IPCC (2007) runs. Flux adjustment is no longer used and additional important modifications include an increase in the horizontal resolution along the equator from 2.4 to 1.5 degrees and increasing the number of levels from 24 to 35 in the ocean model. The updated BCM also includes the horizontal velocity of the ocean when atmospheric turbulent surface fluxes are computed which was important near the equator. In combination with the resolution enhancements this was necessary for reducing a strong cold bias in the upwelling areas there. Several minor improvements in conservation of mass, heat and salt and a new routine for vertical mixing was also included in the ocean model.

The BCM was one of five European GCMs that delivered results to the IPCC AR4. An extensive set of simulations was made and generally the results agreed reasonable with the multitude of other models participating. In the Arctic region the general feature seen in the results from all IPCC models is that the changes get stronger (polar amplification) but the spread also increases (Figure 4.1). In this case, part of the larger spread at high latitudes may be due to increased sampling fluctuations associated with lower real number of independent data points (real degree of freedom), which is a consequence of the planetary geometrical shape (Benestad, 2005). Thus, the figure exaggerates the inter-model differences at high latitudes. However, increased spread due to larger sampling fluctuations is expected to take place in the southern hemisphere on equal terms to that in the northern hemisphere, and the greater scatter in the north (Figure 4.1) also reveals real model differences associated with different descriptions of the sea-ice extent.

The BCM was one of the colder models with too much sea ice in the Arctic. The most likely explanation was a generally too low surface temperature and too zonal storm tracks in the northern Atlantic region with insufficient heat transport to the Arctic giving a cold bias in all runs. The relative changes between present climate control run and the future scenarios are reasonable in many regions. In the Arctic, however, too much ice in the initial climate lead to unrealistic regional dis-

tribution of the projected warming. Experiences with NorACIA-RCM (see chapter 4.2) clearly showed that results from the individual runs unfortunately were not suited for input to regional climate runs due to the unrealistic cold bias.

Sensitivity tests performed later showed that this was mainly caused by the atmosphere model employed in the BCM. An error in the parametrization of vertical turbulent fluxes used with a stable boundary layer was then discovered. When this was corrected the surface energy balance was considerably improved. The present version of BCM includes a new sea ice model that further improves the sea ice distribution.

Regional climate models (dynamical downscaling)

Since AOGCMs only support large-scale and synoptic scale atmospheric features, regional climate models (RCMs) have been developed during the last decades for dynamical downscaling of AOGCMs at regional and local scales. The hypothesis behind the use of high-resolution RCMs is that they can provide meaningful small-scale features over a limited area at affordable computational cost compared to high-resolution GCM simulations. The Regional Climate Model HIRHAM with 25 km resolution has earlier been applied in a transient climate simulation over Greenland and adjacent seas (Stendel et al. 2008). The HIRHAM RCM used in NorACIA was run with 25 km grid distance nested within the global data available every 12 hours with a 250 km grid. The same physical parameterisations are used in the RCM as in the global model, except for tuning to account for the finer

grid in HIRHAM. The integration area is shown in Figure 4.2.

Successful implementation of a RCM depends on a number of conditions, e.g. nesting strategy, domain size, difference in resolution between the AOGCM and RCM, the physical parameterisations, quality of the driving data and spin-up time. Generally the RCM cannot be expected to improve errors in the AOGCM results on a large scale, but should be able to develop small-scale features, at least due to more realistic surface forcing. As for its global counterpart, it is certainly necessary to realistically simulate present climate. Observed data can then be used for validation, as a first attempt to trust the output from climate change experiments.

The HIRHAM RCM (Christensen et al. 1998) was imported from Max Planck Institute (MPI), Hamburg, in 1997 and a similar version has been used at the Danish Climate Centre, Copenhagen. The main components of HIRHAM are described in Bjørge et al. (2000). The physical parameterisations in HIRHAM include radiation, cumulus convection utilizing a mass flux scheme, stratiform clouds, planetary boundary layer, gravity wave drag, sea surface and ice processes, and land processes including surface hydrology. In the land surface scheme temperature is calculated as prognostic variable for five soil layers and one moisture layer. A simple one-layer snow model is coupled to the land surface scheme. The albedo of snow (and ice) is parameterized to be temperature dependent near melting (decreasing albedo with increasing temperature). The effect of vegetation on albedo during snow-covered periods is parameterized

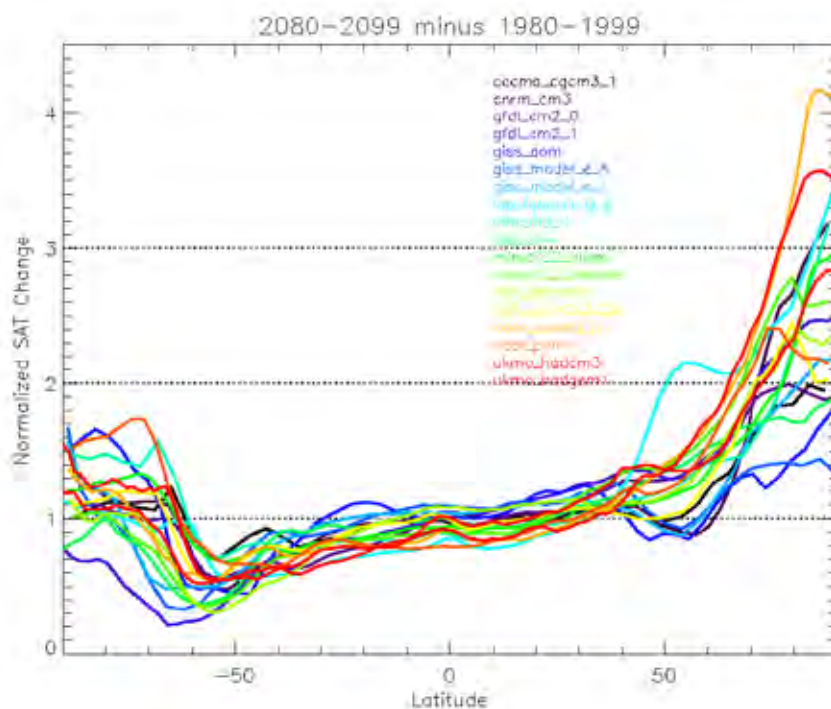


Figure 4.1 Zonal mean surface temperature change at 2080–2099 relative to 1980–1999 for models archived at PCMDI for the IPCC AR4. The temperatures are normalized by the global mean to emphasize the relative polar amplification across models. Confidence limits and error bars are shown. Note, the estimated zonal means represent varying degrees of freedom depending on the latitude (Benestad, 2005), and thus the spread at low latitudes are not comparable with the high-latitude spread. Figure from: <http://www.realclimate.org/index.php/archives/2006/01/polar-amplification/>

over fractional forested area, effectively reducing the albedo with increasing forest coverage.

In the RegClim project simulations with a regional climate model were run for several global models and emission scenarios (Haugen & Iversen, 2008). These simulations demonstrated large differences in the projections of regional temperature and particularly precipitation for Norway. To achieve more robust climate projections, Haugen & Iversen (2008) combined eight RCM-simulations in a multi-model ensemble. The projections were adjusted to be valid for a time horizon of 70 years. Some main results for temperature and precipitation projections from these analyses are summarized in Table 7.1, and an example of maps based on these multi-model runs is shown in Figure 4.22.

Empirical / statistical downscaling

Empirical downscaling (also called statistical downscaling) consists of revealing empirical links between large-scale patterns of climate elements (predictors) and local climate (predictands), and applying them to the output from global or regional climate models. Successful downscaling depends on the following conditions (1) the climate model should reproduce the large-scale predictor fields realistically (2) the predictors should account for a major part of the variance in the predictands, (3) the links between predictors and predictands should be stationary, and (4) when applied in a changing climate, predictors that “carry the climate signal” should be included (Giorgi et al., 2001).

The philosophy behind empirical downscaling is that the local climate partly is a result of local conditions that are quite constant (e.g. topography and vegetation), and partly of large scale weather patterns. In a comparison of results from empirical downscaling and regional climate modelling for Scandinavia, Hanssen-Bauer et al. (2005) concluded that there were few statistically significant differences between the results. Empirical downscaling may catch several local features that are not “resolved” in the present regional climate models. On the other hand the regional climate models provide better temporal resolution as well as a number of climate variables which the empirical downscaling is not able to reproduce. Another limitation is that basically the empirical downscaling may just be used for localities with observational time series long enough to develop robust relationships between local climate and large scale patterns.

Empirical downscaling is far less resource demanding than regional modelling, and is therefore a well suited tool to illustrate the spread in climate projections from different climate models for key variables and for selected localities. In NorACIA it was decided to use empirical downscaling to deduce projections for a number of locations in the Svalbard region and North Norway. The downscaling was performed by the free-software programme clim.pact (Benestad 2004), and was mainly based upon the global climate simulations with the emission scenario A1B (SRES, 2000) produced for the IPCC (2007) report. Description of methodology

and results for the NorACIA downscalings are published in Benestad et al. (2005) and Benestad (2008).

4.2 The NorACIA Regional Climate Model

Model description

In the Norwegian RegClim project (www.reg-clim.met.no) the regional climate model (RCM) HIRHAM was used for dynamical downscaling with a spatial resolution (grid size) of 55 km over northern Europe. The integrations in RegClim mainly focused on the time slices 1961-90 and 2071-2100 (Haugen and Iversen, 2008). Norway is contributing to the EU project ENSEMBLES (<http://ensembles-eu.metoffice.com>), in which several European countries are performing RCM-simulations for a common model domain. Unfortunately this model domain does not cover the Norwegian Arctic; the northern limit for the ENSEMBLES domain is around the latitude of Bjørnøya. Thus the Svalbard region is outside the domain of the Norwegian RCM simulations within ENSEMBLES, and border effects in the regional modelling may even influence the simulations for North Norway. Within NorACIA it was therefore decided to establish a regional climate model focussing on the Norwegian Arctic. By using the same model setup as in the ENSEMBLES simulations, it is possible to compare climate projections in a profile from the Mediterranean to north of Svalbard.

The development of the new NorACIA-RCM was based on an improved version (HIRHAM-II) of the regional model (HIRHAM-I) used in the RegClim project. The model domain for the NorACIA-RCM covers the Norwegian Arctic (see Figure 4.2). The NorACIA RCM has a spatial resolution at the surface of ca. 25x25 km (HIRHAM-I: 55x55 km), and has a vertical resolution of 31 levels (HIRHAM-I: 19 levels). Other improvements compared to HIRHAM-I are:

- A new time-integration scheme
- A new scheme for lateral forcing of global boundary data
- Improved simulations of precipitation in mountainous area
- Improved snowmodel (better description of albedo over snowcovered ice)

A detailed description of the HIRHAM-II model used in the NorACIA RCM simulations

is found in Haugen & Haakenstad (2006). Table 4.1 shows examples of climate elements mapped by output from the NorACIA-RCM simulations.

Present climate modelled by the NorACIA Regional Climate Model

To evaluate whether the NorACIA RCM gives a realistic description of the climate within the model domain, the RCM was run with input from the ECMWF gridded ERA40 dataset. This dataset is a high-quality analysis of the weather development during the period 1958-2002, and is performed at the European Centre for Medium-Range Weather Forecast (ECMWF) in UK (ERA40 = ECMWF Re-Analysis for 40 years). To validate the results of the NorACIA present-day simulations, two datasets were used: 1) Monthly ERA40 surface analysis for several climate elements, but with a better spatial resolution than the dataset used for the NorACIA RCM simulation. 2) Monthly gridded data based on surface observations. This latter dataset (CRU TS 2.1) is developed by the Climate Research Unit at the University of East Anglia, UK, and contains several climate elements which are directly comparable to the output from the NorACIA-RCM. The NorACIA simulations and the two validation datasets were compared in a common validation grid. In addition the 2 m temperature was adjusted for difference in elevation between ERA40, CRU TS 2.1 and HIRHAM-II model topography by anticipating a vertical temperature gradient of -0.65°C per 100 m. The validation was performed for the period 1961–2000.

Examples of the validation of NorACIA-RCM results against CRU TS 2.1 are shown in Figure 4.3. For temperature (Figure 4.3.a) the simulations show lower temperature than CRU in western mountainous regions in southern Norway, and lower temperatures over large parts of Svalbard. For precipitation (Figure 4.3b) the RCM-simulations give higher values both in mountain areas on the Norwegian mainland and over large parts of Svalbard. Compared to ERA40 the NorACIA-RCM shows somewhat lower air temperature at the 2m level above ice covered surface and a little higher temperature over ocean; also there are some minor differences over mountain regions. As both the ERA40 and CRU-datasets have a poorer spatial resolution than HIRHAM-II, it is reasonable to conclude that the novel NorACIA RCM results are more realistic than the two other datasets.

Table 4.1 Examples of available maps of climate elements based on simulations by NorACIA-RCM

CLIMATE ELEMENT	SEASONAL / ANNUAL
AVERAGE AIR TEMPERATURE (2 m level):	DJF, MAM, JJA, SON
PRECIPITATION SUM	DJF, MAM, JJA, SON
EXTREME 1-DAY PRECIPITATION (1 occurrence per year)	ANNUAL
EXTREME 1-DAY PRECIPITATION (5 year return period)	ANNUAL
1-DAY PRECIPITATION > 20 MM	ANNUAL
DAILY SNOW FALL > 10 CM/DAY	ANNUAL
EXTREME WIND SPEED (1 occurrence per year)	ANNUAL
EXTREME WIND SPEED (5 year return period)	ANNUAL



Figure 4.2: Domains for different Norwegian Regional Climate Model simulations: RegClim-project (northern black frame), EU-project ENSEMBLES (southern black frame), NorACIA (red frame).

The NorACIA-RCM is also used to simulate daily series of temperature and precipitation for a number of locations in North Norway and the Svalbard region. Figure 4.4 shows examples of distribution of daily temperature and precipitation at Svalbard Airport/Longyearbyen throughout the year. The frequencies are based on observations, direct interpolation from ERA40, and use of ERA40 as input to the NorACIA-RCM. Figure 4.4a shows that the novel RCM simulations for Svalbard give a realistic description of the temperature conditions at Svalbard Airport. For precipitation (Figure 4.4b) the simulations show too few days with no precipitation, and a tendency to over-estimation of the frequencies of days with precipitation above 0.2 mm/day. The observed values are not corrected for undercatch, and on Svalbard this implies that a large portion of the daily precipitation values give a substantial under-estimate of the “true precipitation” (cf. chapter 2.1).

The conclusion of comprehensive validations within NorACIA was that the present-day simulations by NorACIA-RCM give a reasonable description of the observed climate in the region. The main features are that compared to the ERA40 and CRU-datasets as well as observations, the novel simulations give an improved description of the physical weather parameters and reduced discrepancies compared to observed values than earlier simulations.

4.3 Mean temperature

Earlier temperature projections for the Arctic

Global climate model simulations (ACIA, 2005) indicate that by the end of the 21st century, Arctic temperature increases are projected to be 7°C

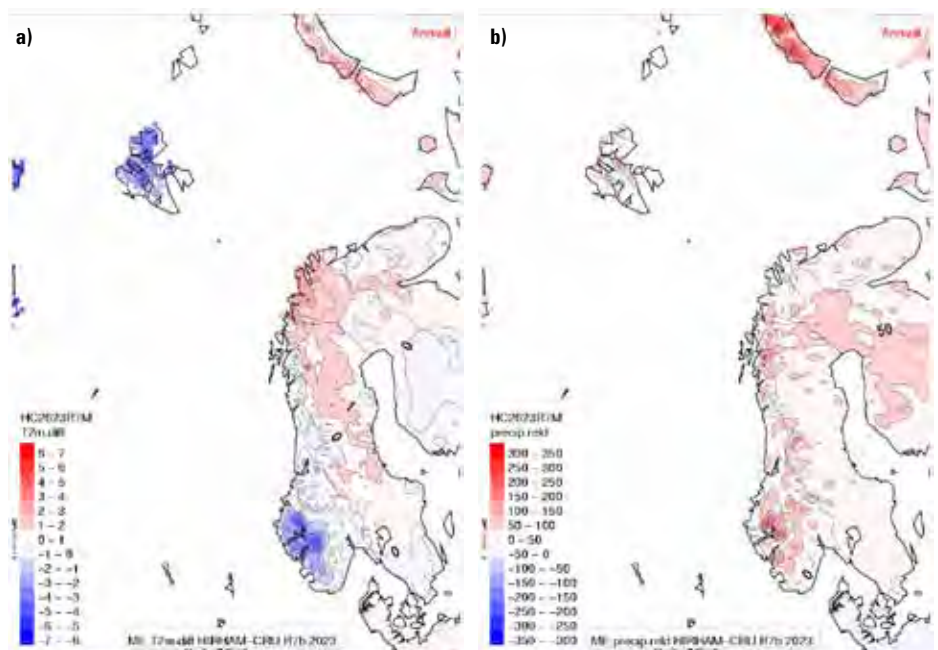


Figure 4.3 Differences in annual means for a) Temperature (2m level) and b) Precipitation between NorACIA RCM simulations and gridded datasets based on observations (CRU TS2.1)

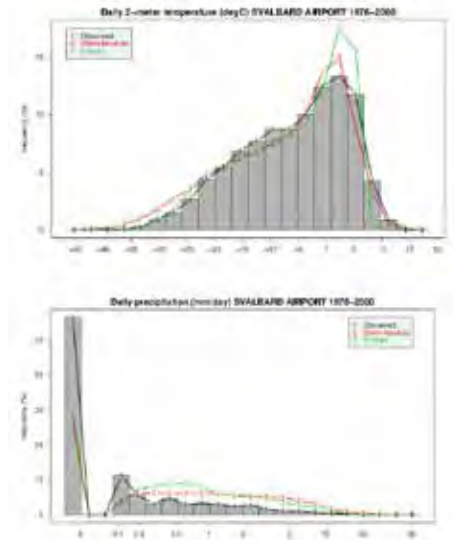


Figure 4.4 Frequencies of daily values of a) Temperature and b) Precipitation for Svalbard airport for the period 1976-2000. Observed values are indicated in black, ERA40-values by green and values deduced from the NorACIA RCM are indicated in red

and 5°C for the A2 and B2 scenarios, respectively, compared to the present climate. For the five ACIA-designated model projections the global mean temperature increase (from 1981–2000 to 2071–2090) under the B2 emission scenario has an average of 1.9°C. In the Arctic, the increase in mean annual temperature projected by the five ACIA-models is significantly larger, reaching 3.7°C – i.e. north of 60°N the increase is twice the increase in the global mean. The strongest warming will occur during autumn and winter, where the average temperatures are projected to increase by 3 to 5°C over most Arctic land areas.

The Multi-Model Dataset (MMD) used in the regional climate projections for IPCC (2007) projected an annual warming of the Arctic of

5°C at the end of the 21st century. There is a considerable across-model range of 2.8°C to 7.8°C. Over both ocean and land, the largest (smallest) warming is projected in winter (summer). By the end of the century, the mean warming ranges from 4.3°C to 11.4°C in winter and from 1.2°C to 5.3°C in summer under the A1B emission scenario.

NorACIA-RCM simulations for the period 1980-2050

The NorACIA-RCM was run with input data from MPI's global climate model ECHAM4 T42, and with the emission scenario IS92a (SRES, 2000) which was a basis in the IPCC TAR report (IPCC, 2001). Choice of emission scenario is not essential for projections up to year 2050 because for this period there are relatively small discrepancies in global warming (expressed as increase from 1990) between the various SRES emission scenarios (IS92a: +1.1°C, B2: +1.4°C and A1B: +1.5°C (from IPCC, 2001)). The simulation was performed for the period 1981 – 2050, and to study the changes throughout this period, two time slices 1981–2010 (“MPI P2”) and 2021–2050 (“MPI S2”) were compared. The same global model, emission scenario and period were also used in the RegClim project, but with a poorer (55x55 km²) spatial resolution. The simulations are performed with a time-step of a few minutes, but results are just stored for intervals of 1, 3, 6 or 24 h.

Figure 4.5a indicates an increase in annual temperature of approximately 1°C in the coastal areas in Nordland and Troms, and between 1.5–2.0°C in eastern parts of Finnmark and southwest of Spitsbergen. The largest increase is projected for the eastern parts of Svalbard, and between Spitsbergen and Novaja Zemlja. The smallest seasonal changes (Figure 4.6) are projected for the mean summer temperature. For autumn, winter and spring a large increase is projected east and northeast of Svalbard. A large gradient in the magnitude of the increase is present from south-western to north-eastern parts of the Svalbard region. This pattern is found in many scenarios (e.g. Haugen and Iversen, 2008). The projected decrease in sea-ice coverage will largely influence the temperature in the lower atmosphere. In connection with this pattern, the largest increase on the Norwegian mainland is found in northern areas (Finnmark).

NorACIA-RCM simulations for the time slices 1961–90 and 2071–2100

The NorACIA-RCM was forced by MPI's global climate model ECHAM4 T106, and with emission scenario B2 (SRES, 2000). The simulations were performed for the time slices 1961–1990 (“MPI CN”) and 2071–2100 (“MPI B2”). The same global model, emission scenario and time period were also used in the RCM-simulations in the RegClim project but with coarser (55x55 km) spatial resolution and with an earlier version

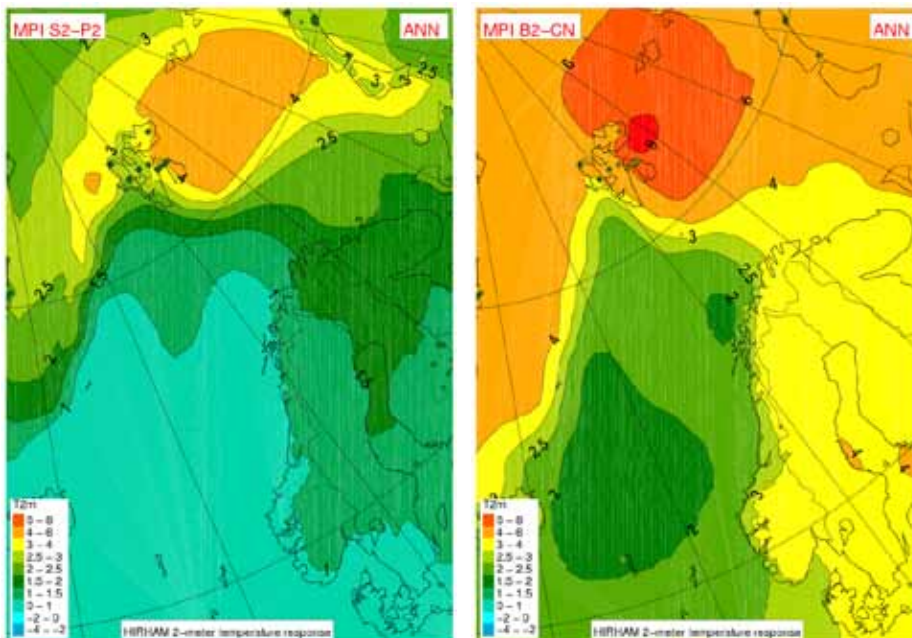


Figure 4.5 Projected change (°C) in average annual temperatures from a) 1981–2010 to 2021–2050 b) 1961–90 to 2071–2100

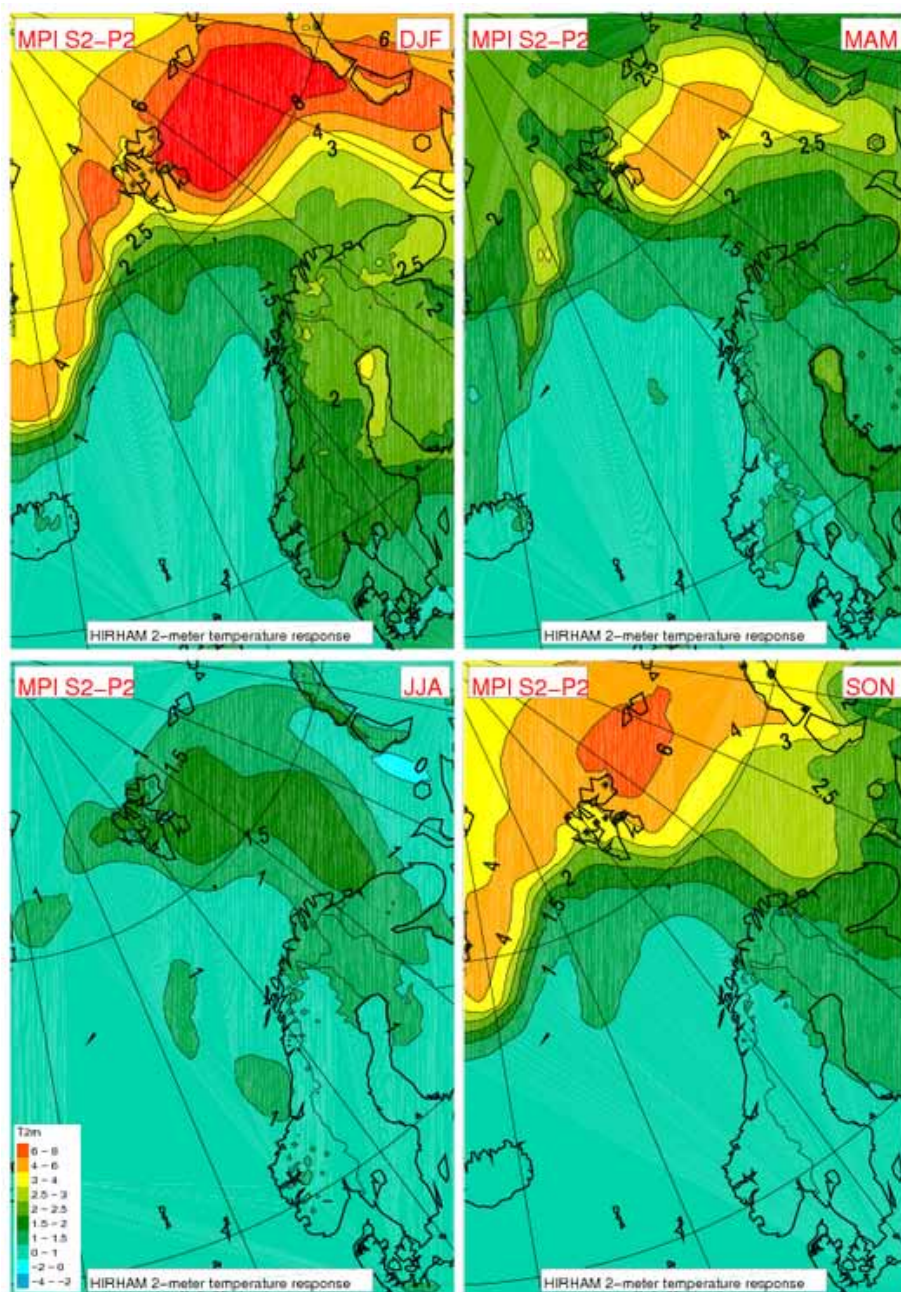


Figure 4.6 Projected change (°C) in average seasonal temperatures from 1981–2010 to 2021–2050

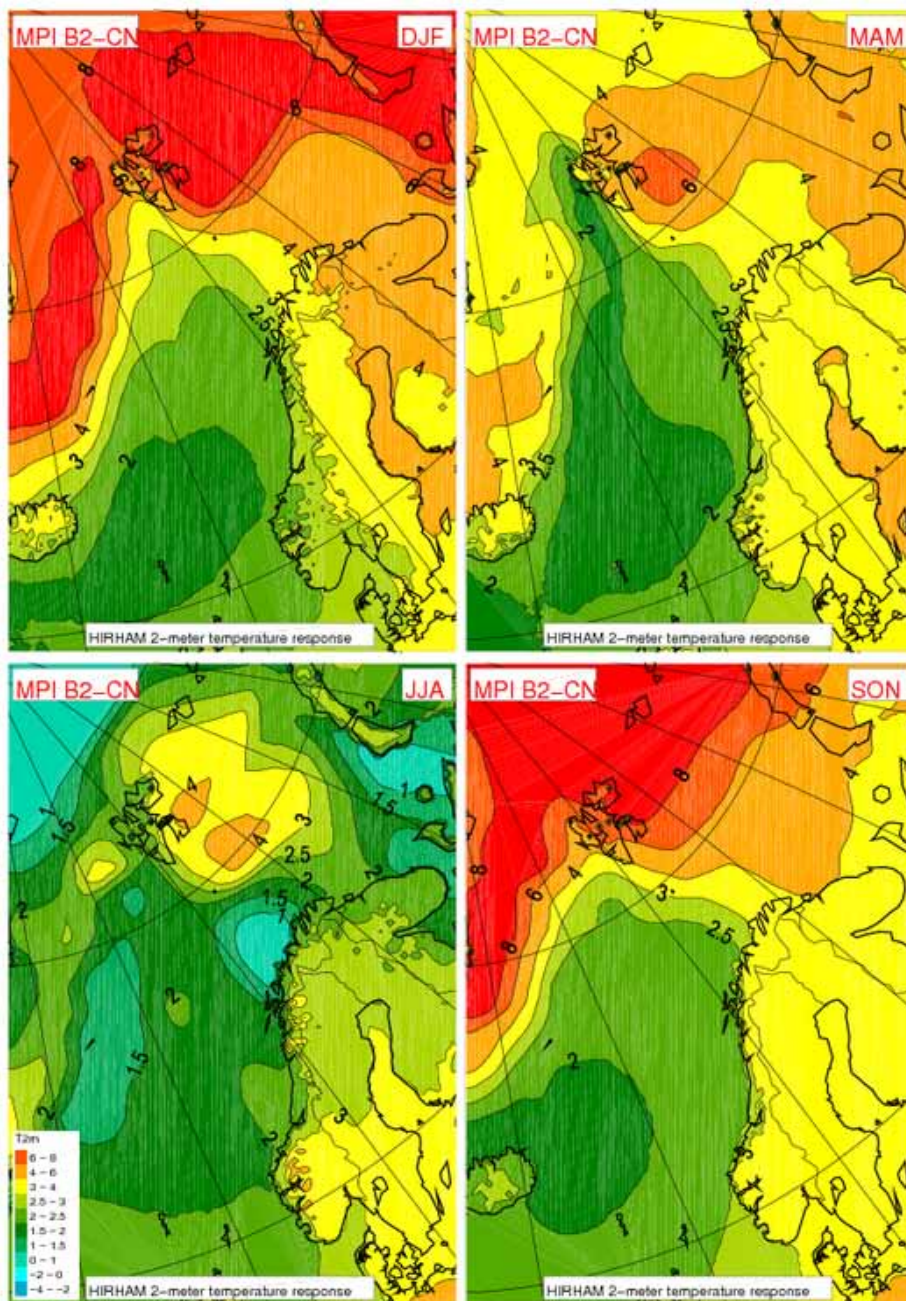


Figure 4.7 Projected changes (°C) in seasonal temperatures from 1961–1990 to 2071–2100

of HIRHAM. Up to 2100 the emission scenario SRES B2 implies a global warming (expressed as change from 1990) of 2.4 °C while A1B gives 2.8 °C (IPCC, 2007). The data from the simulations were stored in intervals of 1–24 hours.

Figure 4.5b demonstrates a stronger annual warming than up to year 2050 (Figure 4.5a). In large parts of North Norway the temperature is projected to increase by 2.5–3.5 °C, and in the Svalbard area between 3–8°C. The strongest increase in annual mean temperature is found east of Nordaustlandet. The seasonal increase in temperature for North Norway is 1–4 °C in the different seasons – with largest increase in winter temperature and larger increase at Finnmarksvidda and Varanger than at the coast in southwest. Because of the reduced extension of sea-ice, a substantial temperature increase (larger than 8°C) during autumn, winter and spring is projected for the ocean areas east of Svalbard. Over the Svalbard land areas there are large spatial

gradients in projected warming – autumn and winter about 4°C at the south-western coast to more than 8°C in the eastern parts of Nordaustlandet and Edgeøya.

Comparison of temperature simulations for 2021–2050 and 2071–2100

By comparison of the projections up to 2021–2050 vs. 2071–2100 one should note that they are based on different SRES emission scenarios and that they indicate changes from different control periods (1981–2010 vs. 1961–90), i.e. changes during 40 resp. 110 years. For temperature the projections for both scenario periods show substantial larger increase in north-eastern than south-western parts of the Svalbard region. A common feature for both periods is that the temperature increases over the whole region and for all seasons. Rough estimates of the magnitude of the temperature increase over North Norway and the Svalbard region from

1981–2010 to 2021–2050 and from 1961–90 to 2071–2100 are summarized in Table 7.1.

Empirically downscaled temperatures

Benestad (2008) carried out Empirical-Statistical Downscaling (ESD) for monthly mean temperature for a selection of Norwegian Arctic sites, based on the most recent global climate model simulations described in IPCC (2007). The downscaling analysis incorporated Multi-Model Dataset (MMD) ensembles based on 50 integrations for temperature and 43 for precipitation. This model ensemble includes both simulations for the 20th century (20C3M) and scenario runs for the 21st century following the emission scenarios A1b (SRES, 2000).

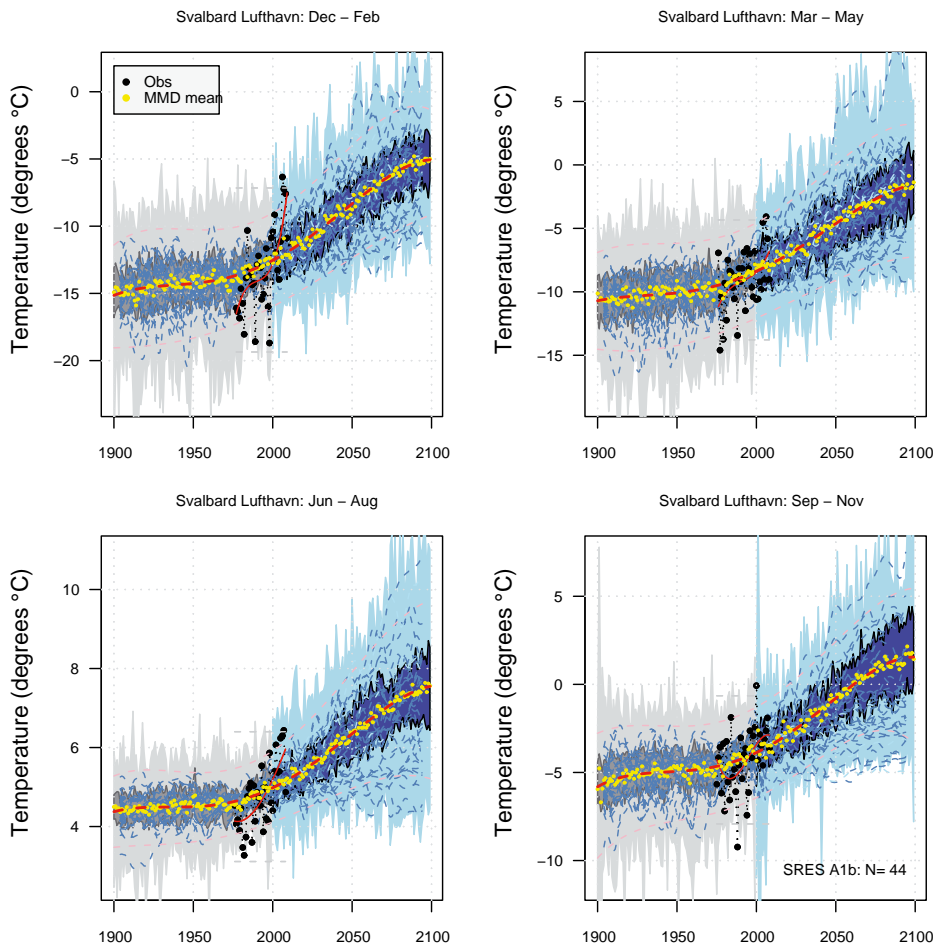
The analysis performed by Benestad (2008) involved new ways of combining results from the 20th century (CTL) with results from the 21st century (SCE), and a quality control was used to ‘weed out’ global climate models with a poor reproduction of present climate. The results were found to be sensitive to the choice of predictor domain, but smaller domains were taken to be more reliable. Some of the GCMs have been used to make several parallel runs, differing only by using different initial conditions (starting point). The ESD was applied to the MMD ensemble for both the 20th century and the 21st century simulations separately.

The point values shown in Figure 4.8 demonstrate that the empirically downscaled annual temperatures have quite similar variability as the observation-based values, and that the model based long-term temperature development is in good accordance with the observation based curve. Observation-based annual temperatures which in present day climate would have been characterised as “extremely high values”, will in the end of this century be found in the lower part of the future temperature distribution. Figure 4.9 showing so-called box-plots, demonstrates median, 25 and 75 percentiles, as well as extreme values for the distribution of seasonal and annual temperatures on Bjørnøya. Figure 4.8 and 4.9 also illustrate the large uncertainty in the downscalings. Climatological values for present (1961–90) and future (2070–2099) climate are summarised in Table 4.2, and a comparison with RCM results is given in Table 7.1.

4.4 Precipitation

Earlier precipitation projections for the Arctic

The ACIA (2005) climate scenarios projected that over the Arctic (60–90°N), annual total precipitation will increase by roughly 12% from 1981–2000 to 2071–2090. IPCC (2007) states that there has been an improved understanding of projected pattern of precipitation since the IPCC (2001) report, and that increases in the amount of precipitation are very likely at high latitudes. The spatial pattern of the projected precipitation change (IPCC, 2007) shows the greatest percentage increase over the Arctic Ocean (30 to 40%) and smallest (and even slight decrease) over the northern North Atlantic (< 5%). By the end of the 21st century, the



projected change in the annual mean Arctic precipitation for the A1B emission scenario varies from 10 to 28%, with an ensemble median of 18%. The percentage precipitation increase is largest in winter and smallest in summer, consistent with the projected warming.

NorACIA-RCM simulations for the period 1980–2050

The mean annual precipitation is projected to increase by approximately 10% over large parts of North Norway and Svalbard (Figure 4.10a). For the summer season there are small changes (Figure 4.11), while an increase is projected for autumn, winter and spring. For the winter season Figure 4.11 indicates an increase of ca 60% in an area between Svalbard and Novaya Zemlya. It must however be stressed that during the winter season the precipitation amounts in this area are usually very small, and thus that just a small change in mm precipitation may lead to large changes in the percentages.

Figure 4.8 Plume plot for temperature at Svalbard Airport (99840), showing the time evolution of the observed values (black), the 20th century simulations (grey), and the future scenarios (blue)

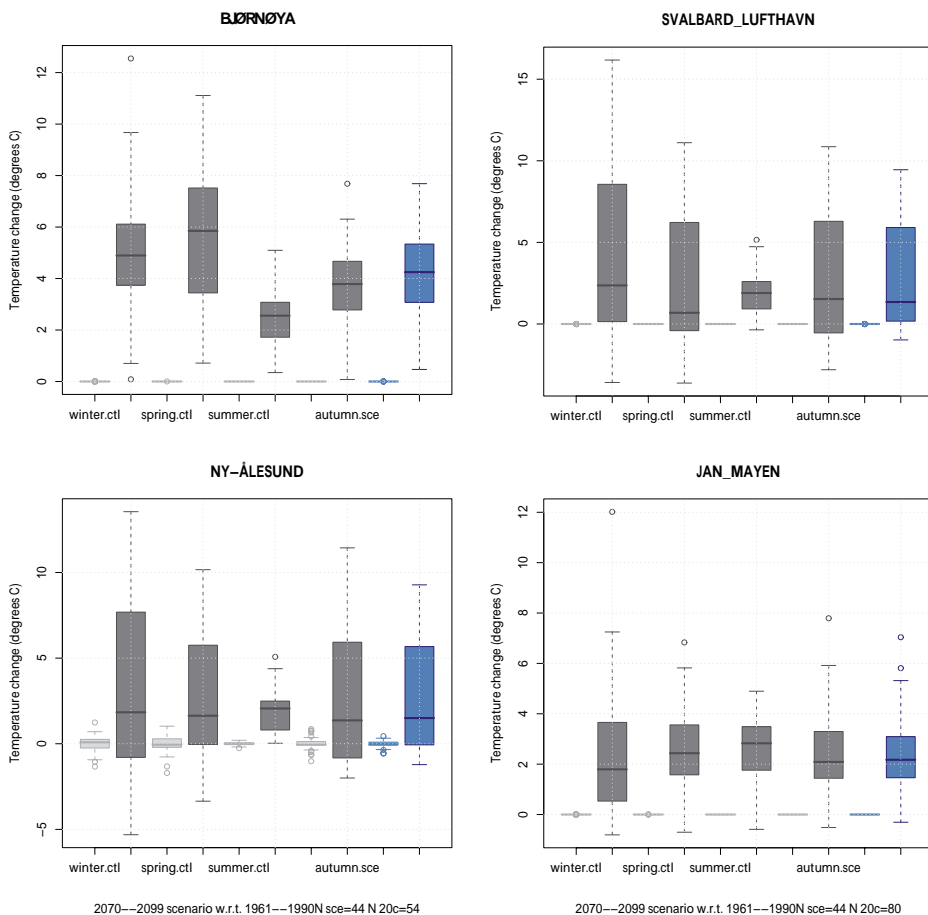


Figure 4.9 Box-plot spread in estimates of changes from 1961-90 to 2071-2100 in seasonal and annual mean temperatures for Bjørnøya, Svalbard Airport, Ny-Ålesund and Jan Mayen based on empirical downscaling from 16 global models under emission scenario A1B. The hatched “boxes” indicate interval for 25 and 75 percentiles; median and extreme values are marked by short horizontal lines

Table 4.2 Seasonal mean temperature (unit: °C) from empirical-statistical downscaling. TAM (1961–1990) are mean values for the reference period 1961–90 and ΔTAM are projected changes from 1961-90 to 2070-2099. “±” indicate the 90-percentile interval for the projections. Location of stations is shown in Figure 2.1

TAM					ΔTAM				
Station	Winter	Spring	Summer	Autumn	Station	Winter	Spring	Summer	Autumn
Tromsø	-4.0	0.8	10.5	2.7	Tromsø	4.0 ± 3.1	4.2 ± 3.0	3.3 ± 2.5	4.0 ± 2.4
Kautokeino	-16.0	-5.2	10.7	-1.0	Kautokeino	11.4 ± 7.9	7.0 ± 4.4	3.9 ± 2.6	4.7 ± 3.3
Hammerfest	-4.8	-0.7	9.9	2.2	Hammerfest	4.2 ± 3.3	5.0 ± 3.3	3.9 ± 2.6	3.8 ± 2.3
Karasjok	-15.9	-3.2	11.3	-1.8	Karasjok	11.0 ± 8.0	6.2 ± 4.3	3.7 ± 2.7	7.3 ± 4.2
Vardø	-4.7	-0.7	8.2	2.6	Vardø	3.6 ± 2.3	3.5 ± 2.5	2.6 ± 2.0	3.3 ± 1.9
Kirkenes	-11.0	-2.3	10.4	0.2	Kirkenes	7.3 ± 4.5	4.9 ± 3.3	3.3 ± 2.7	4.3 ± 2.7
Bjørnøya	-7.6	-4.8	3.6	-0.5	Bjørnøya	5.6 ± 4.4	6.5 ± 4.7	2.8 ± 2.0	4.3 ± 2.7
Hopen	-13.3	-9.9	1.3	-3.7	Hopen	10.1 ± 6.8	6.0 ± 3.9	2.2 ± 1.4	7.6 ± 4.4
Svalbard Airport	-14.8	-10.1	4.3	-5.0	Svalbard Airport	8.9 ± 5.0	7.4 ± 5.3	2.4 ± 2.1	4.1 ± 4.7
Ny-Ålesund	-13.5	-9.3	3.5	-4.9	Ny-Ålesund	10.0 ± 5.6	6.9 ± 5.1	2.9 ± 2.2	7.7 ± 4.8
Jan Mayen	-5.7	-3.5	3.7	-0.2	Jan Mayen	4.8 ± 4.3	3.2 ± 3.7	1.8 ± 2.2	2.8 ± 3.0

NorACIA-RCM simulations for the time slices 1961–90 and 2071–2100

The projected increase in mean annual precipitation up to year 2100 (Figure 4.10b) is larger than up to year 2050 (Figure 4.10a). For large parts of North Norway the increase is 20-30%, while for northeastern parts of Spitsbergen the projected increase is up to 40%. The seasonal precipitation (figure 4.12) is projected to increase over the whole region during all seasons – with the largest increase (30-40%) during winter and spring. It should also be stressed here that precipitation is quite scarce in this region during the winter season – implying that despite the large percentage increase the absolute increase in precipitation just is a few millimetres.

Comparison of precipitation simulations for 2021–2050 and 2071–2100

By comparing the projections up to 2021–2050 vs. 2071–2100 one should note that they are based on different SRES emission scenarios and that they indicate changes from different control periods (1981–2010 vs. 1961–90), i.e. changes during 40 resp. 110 years. The main pattern for the precipitation projections is an increase during all seasons over most of the region; but generally largest increase north and east of Spitsbergen. Rough estimates of increase in precipitation over North Norway and the Svalbard region from 1981–2010 to 2021–2050 and from 1961–90 to 2071–2100 are summarized in Table 7.1.

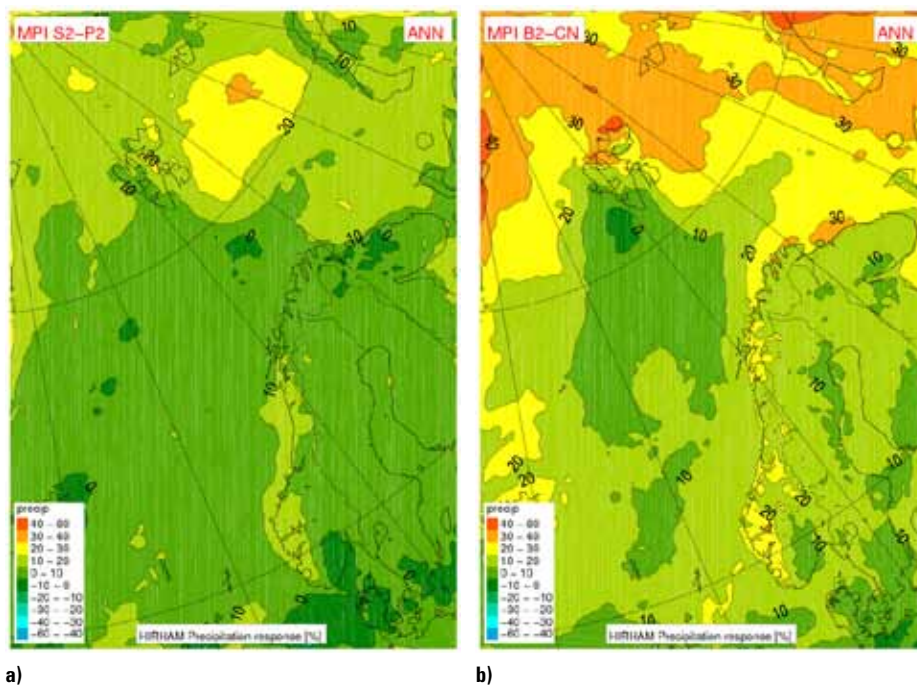


Figure 4.10 Projected change (%) in mean annual precipitation a). From 1981-2010 to 2021-2050, and b). From 1961-90 to 2071-2100

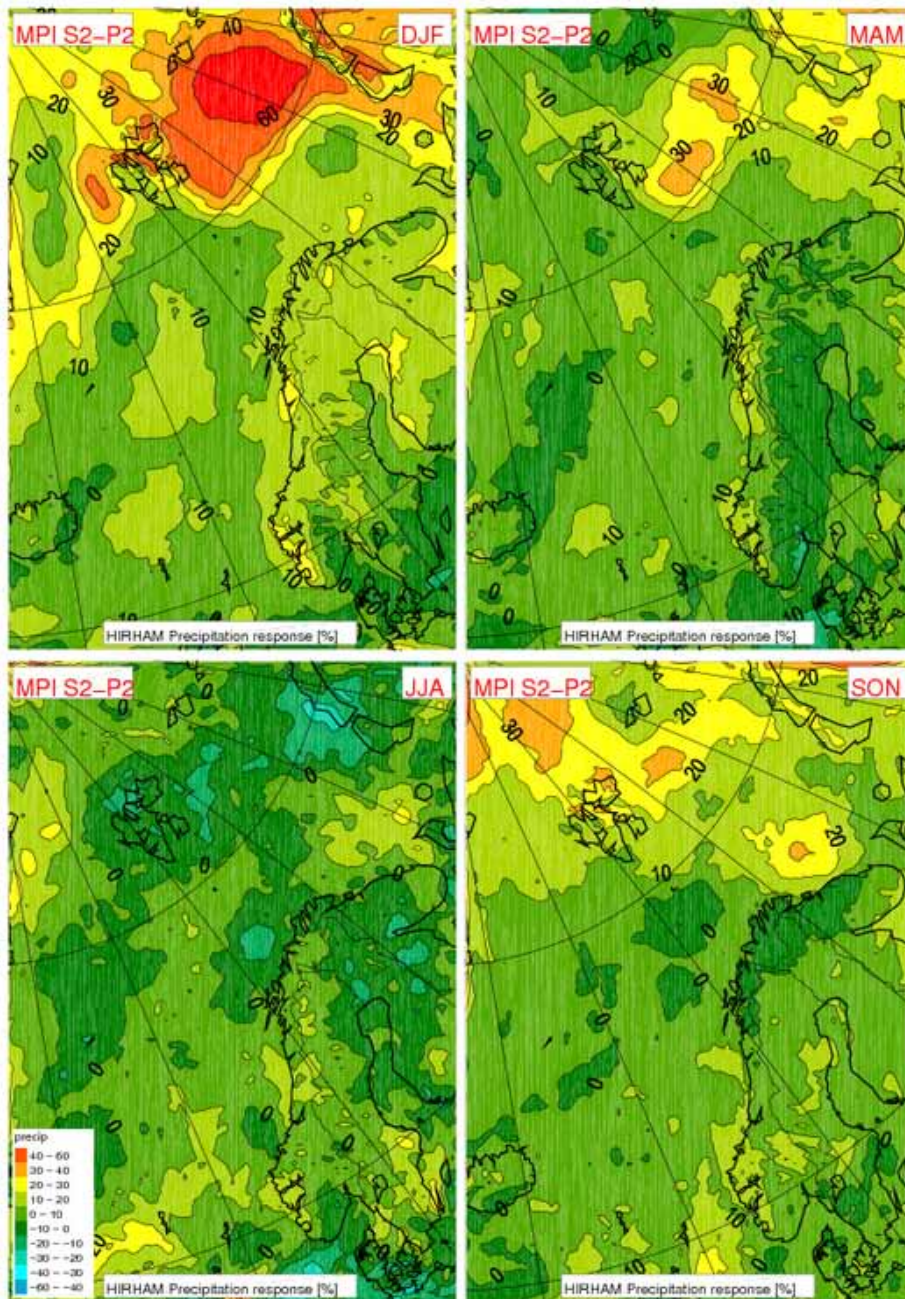


Figure 4.11 Projected change (%) in mean seasonal precipitation from 1981–2010 to 2021–2050

Empirically downscaled precipitation

Benestad (2008) carried out Empirical-Statistical Downscaling (ESD) for monthly precipitation totals for a selection of Norwegian Arctic sites, based on the most recent global climate model simulations described in IPCC (2007). The downscaling analysis incorporated multi-model ensembles based on 50 integrations for temperature and 43 for precipitation. This model ensemble includes both simulations for the 20th century (20C3M) and scenario runs for the 21st century following the emission scenarios A1b (SRES, 2000).

The results for the empirically downscaled precipitation (see e.g. Figure 4.13) suggest that the downscaled (shaded areas) year-to-year variability (variance) is underestimated, but that there are also stronger secular variations in the actual observations (black symbols) than seen in the ESD results for the past (grey). A summary of climatology for the period 1961–90 and ESD-projections for 2070–2099 is provided in Table 4.3. A comparison between ESD and RCM results is given in Table 7.1.

Table 4.3: Seasonal precipitation from Empirical-Statistical Downscaling. RR(1961-90) are mean seasonal precipitation (mm) for the reference period 1961-1990 and Δ RR are projected changes up to 2070-2099 expressed as fractions (%) of the 1961-90 values. “ \pm ” indicate the 90-percentile interval, while “x” indicate that the results are unreliable. Location of stations is shown in Figure 2.1

a) RR (1961-90)

Station	Winter	Spring	Summer	Autumn
Tromsø	288	185	218	340
Kautokeino	30	32	194	92
Hammerfest	215	169	176	253
Karasjok	47	52	171	96
Vardø	149	98	146	171
Kirkenes	89	65	162	116
Bjørnøya	93	67	89	121
Hopen	119	84	102	134
Svalbard Airport	45	42	49	48
Ny-Ålesund	94	94	80	114
Jan Mayen	174	135	145	229

b) Δ RR

Station	Winter	Spring	Summer	Autumn
Tromsø	107 \pm 31	105 \pm 41	109 \pm 36	103 \pm 32
Kautokeino	118 \pm 51	114 \pm 86	115 \pm 28	121 \pm 55
Hammerfest	x	105 \pm 29	110 \pm 31	x
Karasjok	128 \pm 39	120 \pm 46	115 \pm 37	118 \pm 34
Vardø	108 \pm 30	113 \pm 32	114 \pm 37	105 \pm 20
Kirkenes	115 \pm 35	105 \pm 41	113 \pm 35	110 \pm 30
Bjørnøya	151 \pm 50	128 \pm 32	108 \pm 36	113 \pm 29
Hopen	125 \pm 36	128 \pm 47	114 \pm 38	105 \pm 20
Svalbard Airport	144 \pm 60	106 \pm 50	115 \pm 51	117 \pm 31
Ny-Ålesund	116 \pm 63	94 \pm 50	113 \pm 56	118 \pm 66
Jan Mayen	115 \pm 29	115 \pm 37	109 \pm 37	108 \pm 35

The ESD results for some stations (e.g. Hammerfest) were dubious. The reason may be short observational series and an improper model calibration. Another reason may be that the statistical link between the local (rain gauges) and the large-scale (ERA40) precipitation is weak in general and of a very local nature (Benestad et al., 2007). The precipitation from ERA40 is also model-derived and may contain biases and systematic errors. In addition, some of the models may not reproduce the regional precipitation characteristics very well, thus introducing further errors and uncertainties in trying to identify the important spatial rainfall patterns in the AOGCMs.

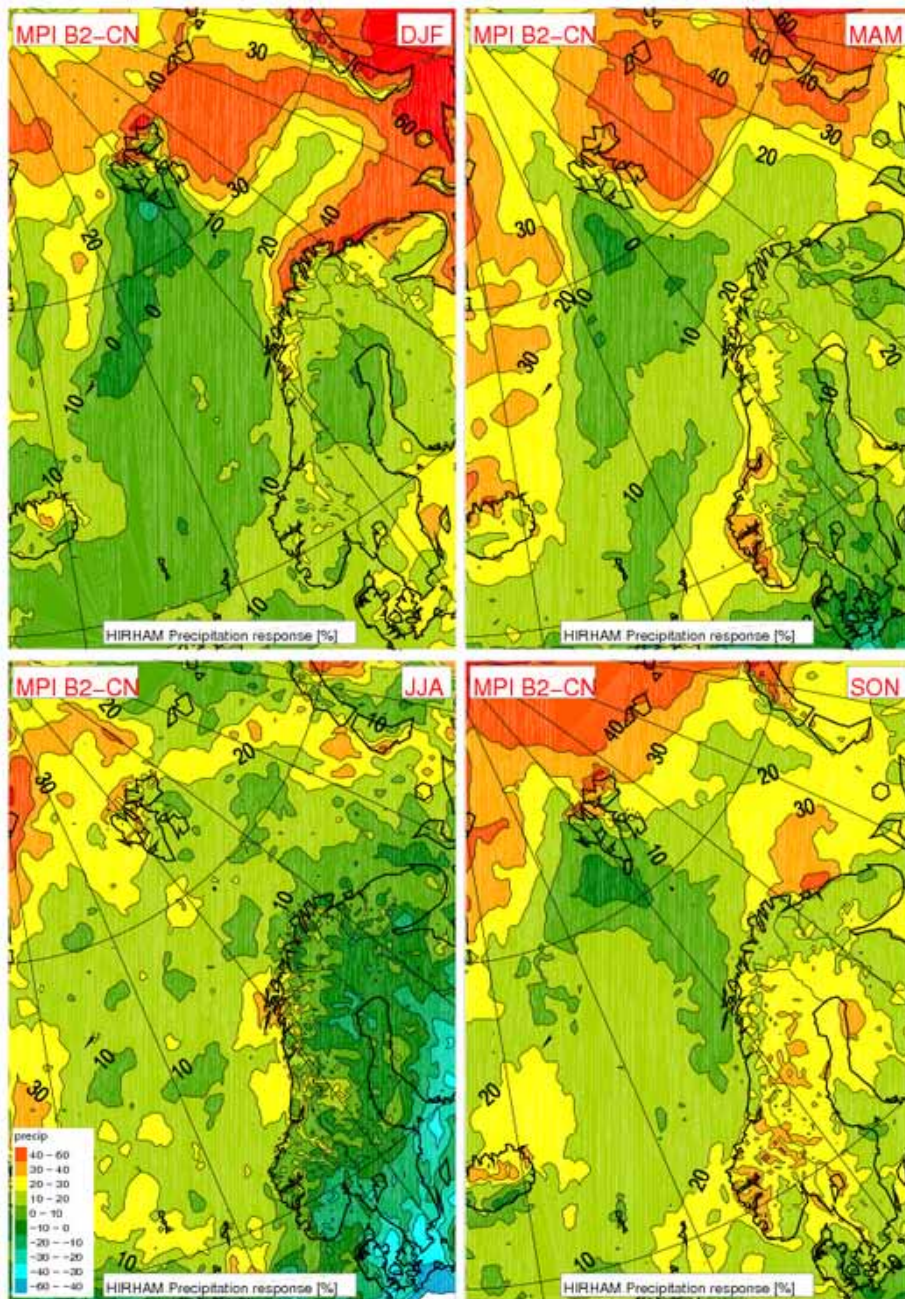


Figure 4.12 Projected changes (%) in seasonal precipitation from 1961–1990 to 2071–2100 (Global model: MPI ECHAM4, SRES: B2; RCM: NorACIA 25 km)

4.5 Snow

The ACIA climate scenarios project that the Arctic snow cover will continue to decrease (ACIA, 2005) with the greatest decreases projected for spring and autumn. Snow cover extent over higher northern latitudes has declined by about 10% over the past 30 years, and model projections suggest that it will decrease an additional 10–20% before the end of this century (ACIA, 2005). Figure 4.14 indicates that for North Norway the season with snow cover will be reduced substantially up to the end of the 21st century. The strongest decrease (more than two months) is projected for the coastal areas in North Norway, while in interior part of Finnmarksvidda the decrease is less than one month.

The NorACIA-RCM simulations also provide information on whether the precipitation falling is snow or rain. For the Svalbard region these simulations are not validated. The direct Nor-ACIA-RCM results for total precipitation amount in the period December – February are shown in Figure 4.15. The maps indicate reduced amounts falling as snow in low-altitude areas in North Norway and in south-western parts of Spitsbergen. Increasing values (up to 40 %) are found in northern and north-eastern parts of the Svalbard region.

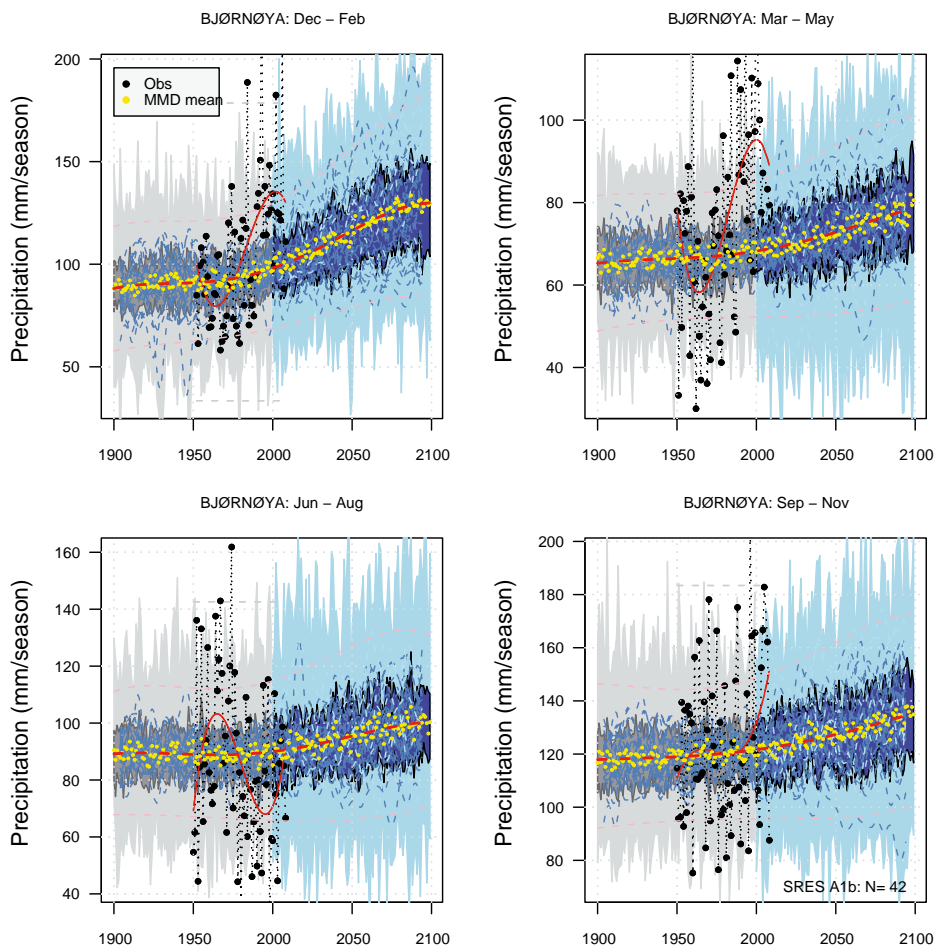


Figure 4.13: Plume plot for Bjørnøya, showing the time evolution of the observed values (black), the 20th century simulations (grey), and the future scenarios (blue)

Other examples of snow simulations by NorACIA-RCM are shown in Figures 4.16 and 4.17. Neither the results from the simulations of number of days with snowfall >10 cm nor change in snow depth are validated against surface observations, but are included as examples of results available from the NorACIA-RCM simulations.

4.6 Wind

The downscaled projections of changes in wind conditions are not giving robust signals. The NorACIA-RCM simulations of average daily maximum wind speed for the period 1980-2050 (Førland et al., 2008) indicate small changes during summer, but an increase north and east of Svalbard during the other seasons.

Also up to the end of the 21st century rather small changes are projected over North Norway. However, Figure 4.18 indicates a larger than 10% increase in average maximum daily wind speed during winter north and east of Svalbard. This feature is linked to the extensive shrinking of sea ice modelled for this area.

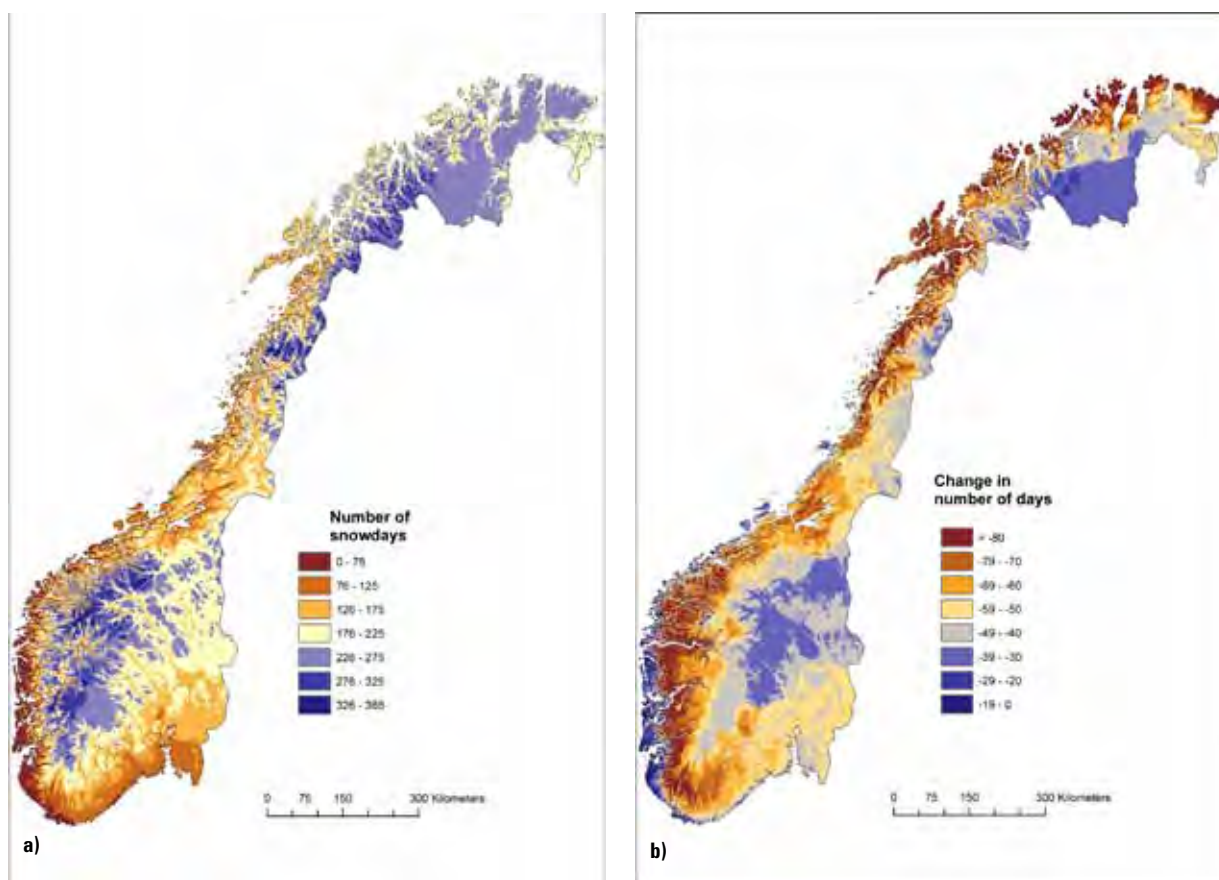
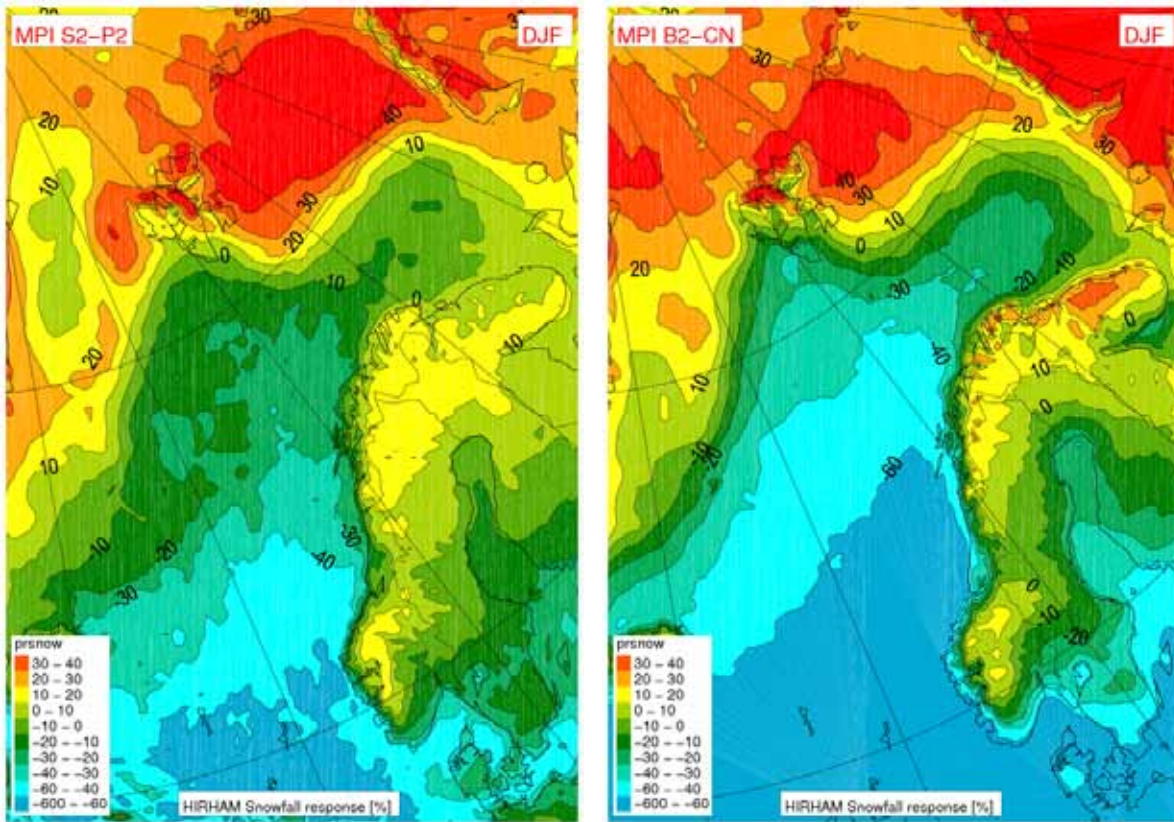
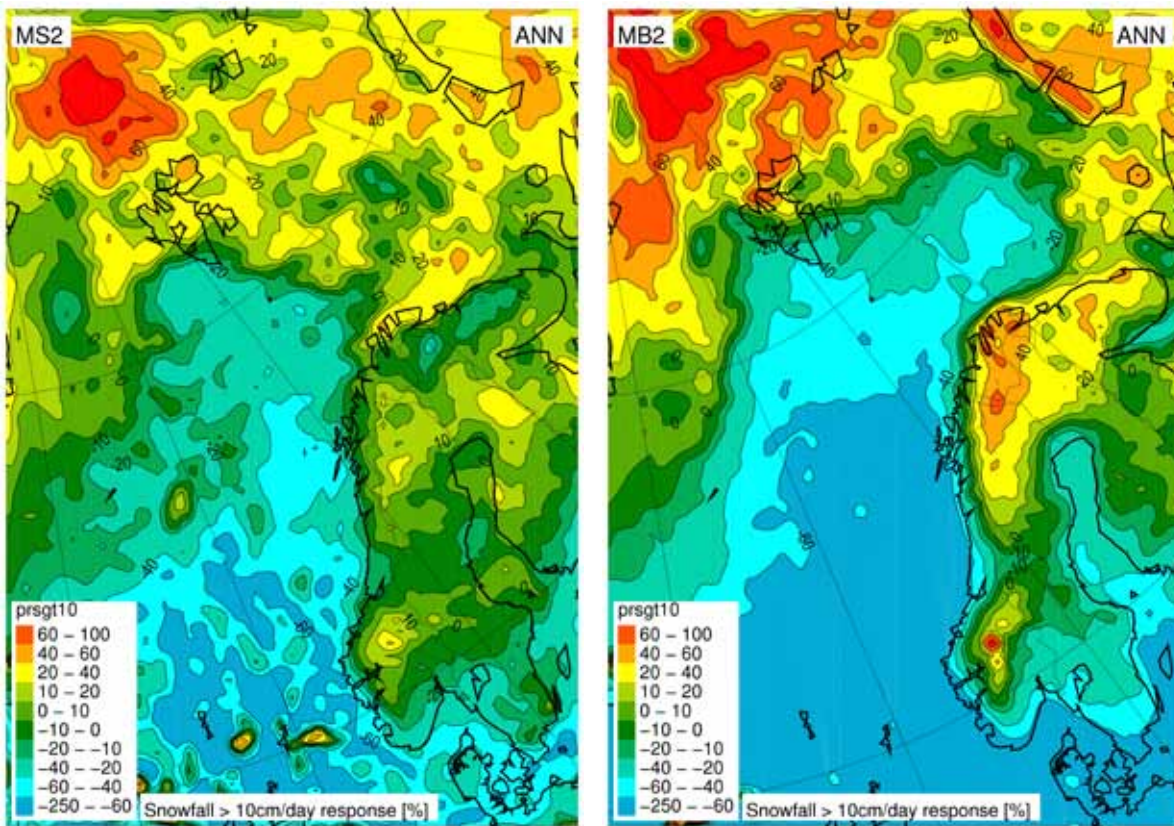


Figure 4.14. Number of days with snow cover (>50% of the ground snowcovered) a). Values for the period 1961-90, b). Projected changes from 1961-90 to 2071-2100. (Global model MPI ECHAM4, SRES: B2, RCM: RegClim). From Vikhamar-Schuler et al. (2006)



a) b)
Figure 4.15: Projected change (%) in precipitation amount falling as snow during December – February.
 a). From 1981–2010 to 2021–2050, b). From 1961–1990 to 2071–2100



a) b)
Figure 4.16: Projected change (%) in number of days with snowfall >10 cm/day
 a). From 1981–2010 to 2021–2050, b). From 1961–1990 to 2071–2100

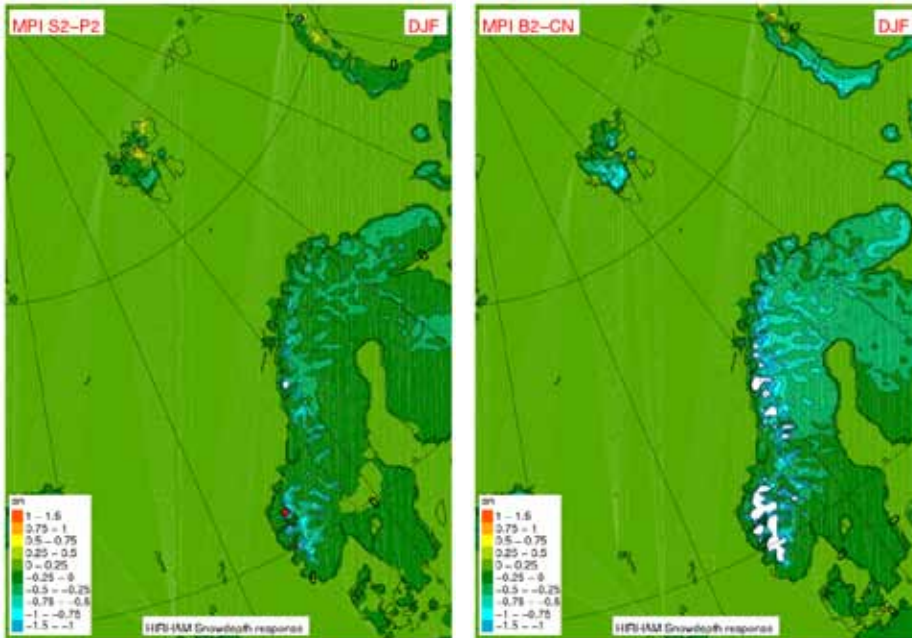


Figure 4.17: Projected change (m) in average snow depth in the period December – February. Left: From 1981–2010 to 2021–2050, Right: From 1961–1990 to 2071–2100

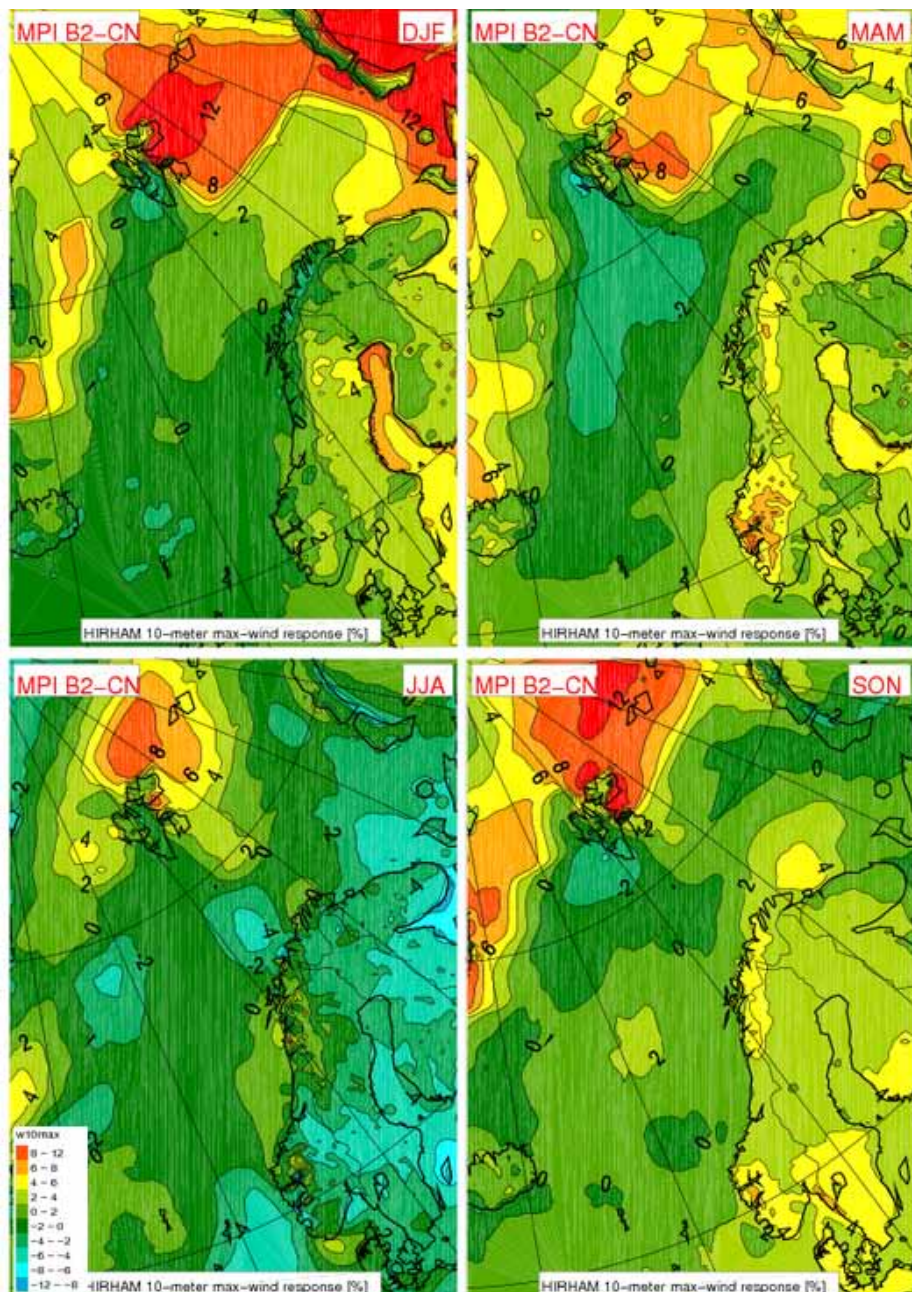


Figure 4.18: Projected seasonal change (%) in average daily maximum wind speed from 1961–1990 to 2071–2100. (Global model: MPI ECHAM4, SRES: B2; RCM: NorACIA 25 km)

4.7 Climatic extremes

Heavy 1-day precipitation

To illustrate changes in extremes, the 5-percent exceedance value (“95-percentile”) was used by Førland et al. (2008). Figure 4.19 indicates that for 1-day rainfall, this 95%-value at the end of this century over most of the area will be exceeded 1-1.5 times more frequently than in present day climate.

Figure 4.20a shows number of days with “heavy rainfall” (i.e. daily precipitation larger than 20 mm) based on the control run with the NorACIA-RCM for the period 1961-1990. The figure illustrates the large gradients in the area: In parts of Nordland there is in average more than 30 days/year with precipitation amounts exceeding 20 mm, while in the Svalbard region and eastern and interior parts of North Norway there may pass many years between each event of “heavy rainfall”. The projected changes up to year 2100 (figure 4.20b) are based on NorACIA-RCM downscaling of MPI B2, and shows an increase in number of days with heavy rainfall over the whole region. However, except for parts of Nordland County, the number of days with heavy rainfall will still be quite modest over large parts of region.

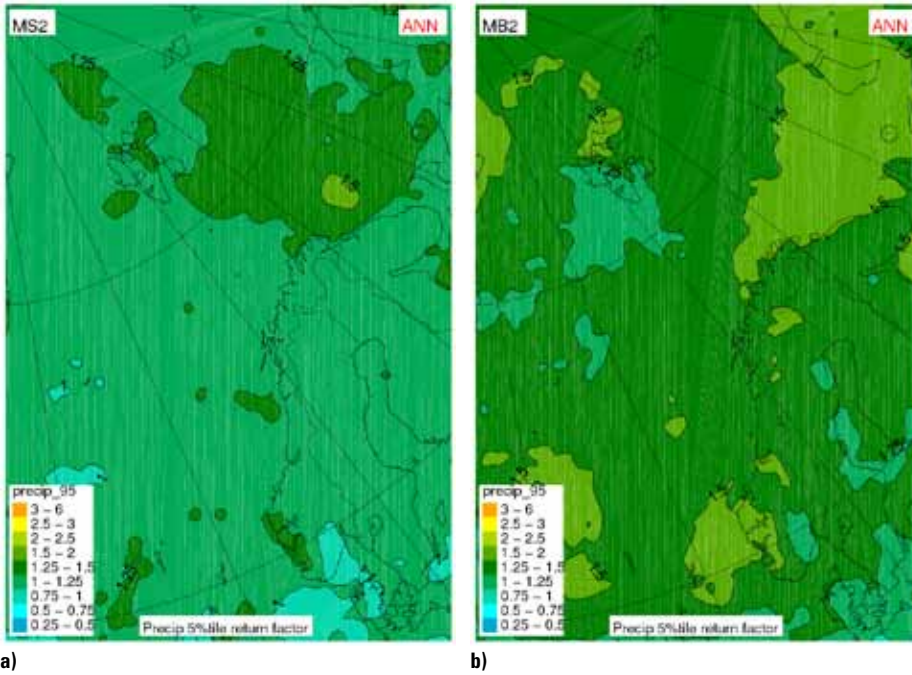


Figure 4.19: Projected change in occurrence of the 95 percentile for 1-day precipitation a). From 1981-2010 to 2021-2050, b) From 1961-90 to 2071-2100.

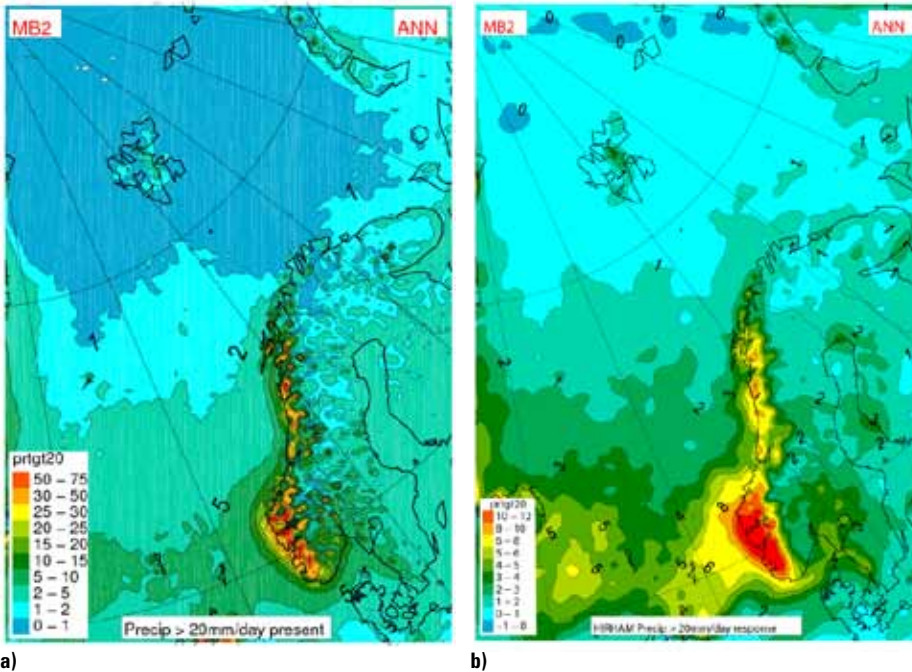


Figure 4.20. Number of days with "heavy rainfall", i.e. >20 mm/day a). Present level, b). Changes from 1961-90 to 2071-2100

High wind speeds

The NorACIA-RCM simulations for changes in maximum wind speed are shown in Figure 4.21. The projections for the period 2021-2050 indicate that the values exceeding the 95 percentile will occur more frequent in the future. The largest increase (1.5-2 times more frequent than present level) is indicated in an area between Spitsbergen and Novaja Zemlja. However, the projections for the end of this century shows a moderate decrease in frequencies of high wind speed in western parts of Spitsbergen and over large parts of the Norwegian Sea. As mentioned in chapter 4.6, the downscaled projections of changes in wind conditions are not giving robust signals, and large uncertainties are connected to the patterns shown in Figure 4.21.

Heavy snowfall

Figure 4.22 shows simulations of changes in number of days with snowfall >10 cm per day from the RegClim multi-model analyses (Haugen & Iversen, 2008). Similar results from the NorACIA-simulations are shown in Figure 4.16. Qualitatively the patterns are quite similar, but it is evident that topographical features are better resolved by the improved spatial resolution in the NorACIA-RCM simulations.

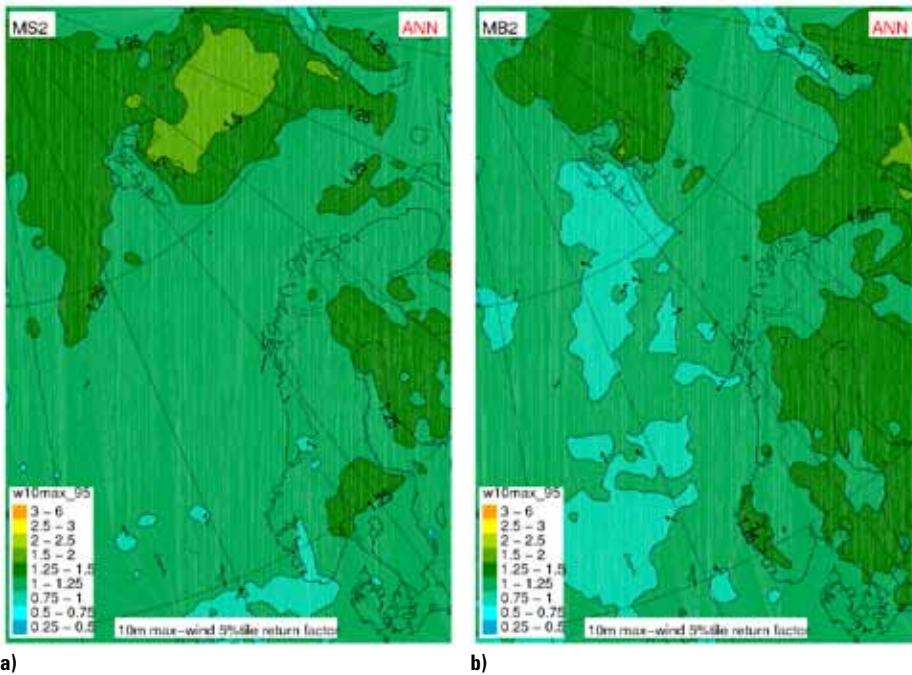


Figure 4.21: Projected change in occurrence of the 95 percentile for maximum wind speed (Values >1 indicate more frequent occurrence in the future climate).
 a) From 1981-2010 to 2021-2050, b) From 1961-90 to 2071-2100.

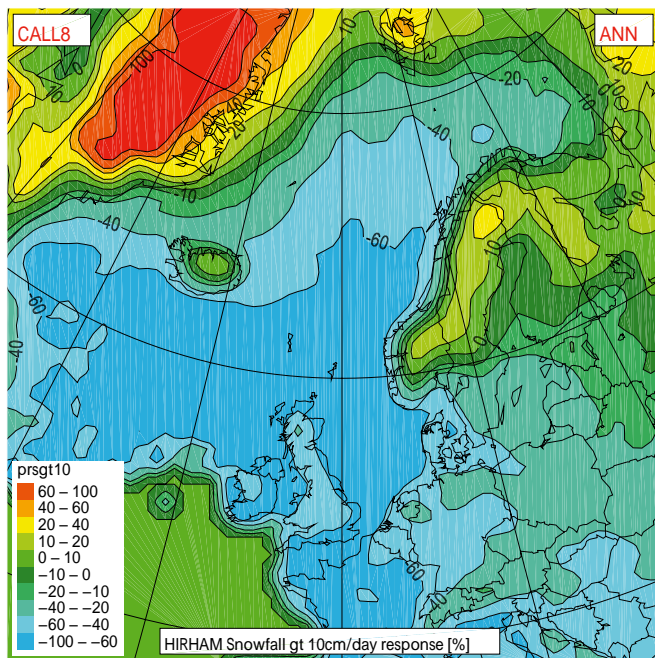


Figure 4.22. Projected change (%) in number of days with snowfall >10 cm/day during 70 years (from RegClim combination of 8 models, 55x55 km). Similar NorACIA-simulations with 25x25 km resolution are shown in Figure 4.16.

4.8 Polar Lows

Introduction

The Norwegian Sea and Barents Sea are areas where dangerous weather situations caused by cold air outbreaks over relatively warm ocean may occur. Such outbreaks are often observed in the cold air on the west-side (“backside”) of a regular low over northern Europe. The polar lows are generated by a combination of strong horizontal and vertical temperature gradients. Heat flux from the surface is an extra source of energy. In a typical cold air outbreak, a polar low may be generated close to the sea-ice border when a small vortex passes from the sea-ice to

open waters. The polar low then may be intensified by large heat fluxes from the ocean. Some polar lows develop a structure similar to tropical hurricanes, with spiral shaped clouds around an “eye”, and are connected to very strong winds and heavy precipitation. To provide realistic simulations of polar lows, an atmospheric model with higher resolution than the global models is needed. The NorACIA-RCM has a spatial resolution of 25 km, and it was evaluated whether this model was able to describe changes in polar lows in a future climate.

Method

In a diagnostic study of marine cold air outbreaks (MCAO), Kolstad and Bracegirdle (2008) take into account both global reanalyses of present climate and the results from climate change scenarios collected from IPCC. The analysis is based on the following indicator for MCAO

$$\Delta\theta/\Delta p = (\theta_s - \theta_{700}) / (SLP - p_{700})$$

where SLP is surface pressure, p_{700} is pressure at 700 hPa, θ_s and θ_{700} are potential temperatures at the surface (e.g. sea and sea-ice temperature) and at 700 hPa, respectively. The unit is K/bar (1 bar = 1000 hPa). In the same way, the analysis here is based on daily values for the months November – March (extended winter season), and the 95 percentile is used as a threshold for rare MCAO events. Assuming that a typical MCAO duration is three days, this corresponds in average to one episode pr month during the extended six winter months.

Results

Figure 4.23 displays the spatial distribution of the MCAO index from one of the NorACIA 25km simulations, forced by the ECHAM4 B2 scenario. As expected, the area with high values is extended northward in accordance with decreased ice coverage. The figure shows lower maximum value in the area outside the coast of Norway. In conclusion, it seems that the potential for polar lows outside the coast of Norway will decrease. This is in agreement with the analysis of 13 A1B scenarios for 2081-2100 performed by Kolstad and Bracegirdle (2008). They concluded that there is a relatively large negative trend due to heating of the atmosphere combined with minor changes in the sea surface temperature in that area (when looking at areas free of ice in present climate).

4.9 Oceanic simulations

The IPCC AR4 report (IPCC, 2007) considers the ocean and sea ice component of the AOGCM runs. On large scale, most models show a gradual decrease in the Atlantic Meridional Overturning Circulation. This signal is however dominated by the general warming.

For regional assessment of ocean climate, the AOGCMs have too coarse resolution. This gives too broad and smooth features. Topographic features and mesoscale eddies are not resolved. Important processes on shelf seas, like tides and the associated mixing are not implemented in these coupled models. A solution is therefore to dynamically downscale the results from the AOGCMs. This is done by using the results from the AOGCM as surface and lateral boundary conditions for a regional ocean model. For the North Sea the Regional Ocean Model System (ROMS) has been used to downscale the results from the Bergen Climate Model (BCM) (Ådlandsvik and Bentsen, 2007; Ådlandsvik, 2008).

The same procedure has been more difficult in the Barents Sea. Most IPCC models, including

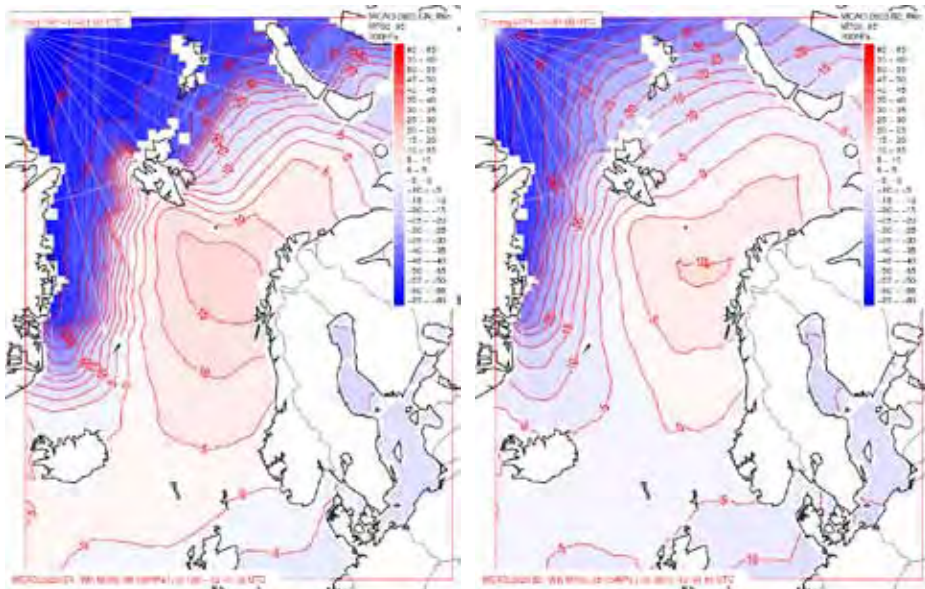


Figure 4.23. Indice for Marine Cold Air Outbreak (MCAO), $\Delta / \Delta p$ in K/bar. The indice is estimated from the NorACIA 25km simulation forced by the ECHAM4 B2 scenario

BCM, have too much sea-ice in the simulation of last century climate (20C3M). In the future scenarios the Barents Sea ice melts. As an ice cover severely limits the heat exchange with the atmosphere, the ocean behaves very differently if it is covered by ice or not. With too cold conditions and too much ice in the control run, the difference between scenario and control shows an unrealistic warming.

One marine downscaling of the Barents Sea is reported in the literature. This work (Ellingsen et al., 2008) is based on an older SRES B2 simulation with the ECHAM4 model from Max-Planck Institut. This model had quite realistic ice coverage for the Barents Sea. The regional ocean model SINMOD has been used to downscale these results for the period 1995-2059. The ocean boundary forcing is taken from climatology based on the present climate. This may give a bias towards the present climate and underestimate the climate change. Their results can be summarized with a temperature increase of 1°C during this 65 year period. The scenario has a clear reduction in sea ice, in particular the summer ice disappears. The Polar Front is displaced slightly towards east and north. The simulation shows no significant change in the amount of inflowing Atlantic water.

A new downscaling has been performed at IMR with the regional ocean model system (ROMS). This is based on the NASA GISS AOM model, one of the three IPCC models giving best results for sea ice in the Arctic Ocean and the Barents Sea in the comparison by Overland and Wang (2007). The control run for the present climate covers the period 1986-2000 from the 20C3M simulation, while the scenario is taken from the period 2051-2065 from the A1B simulation. This downscaling has been done on a rather large area, covering the North Atlantic and the Arctic Ocean. It uses stretched coordinates with a resolution of 10 km in our areas. The control run (Figure 4.24) shows good results in the western Barents Sea. In the east, however, the model suffers extensive heat loss to the GISS AOM atmosphere which has surface conditions with ice. Figure 4.25 shows the similar figure for the future scenario. Due to ice melting in the AOM model, the conditions in the east look more realistic. The mean temperatures at 50 m depth in September increased by 0.9°C in the area covered by the figures. The spatial pattern of this warming is presented in Figure 4.26. The ice problem in the control run shows up as an unrealistic warming in the eastern part of the Barents Sea. In the western part the warming is less than one degree. The cooling between Sentralbanken and Storbanken is due to a shift in the polar front, while the cooling west of Svalbard is caused by a weakening of the Spitsbergen Current. The position of the polar front is more or less fixed along Svalbardbanken. The front at the south flank of Sentralbanken has dissappeared, opening this area for Atlantic water. The downscaling shows a slight weakening of the Atlantic inflow to the Barents Sea with approximately the same heat transport.

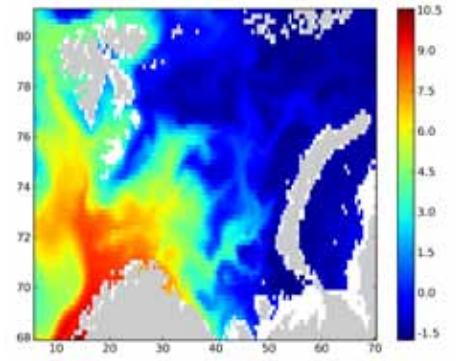


Figure 4.24 Mean September temperature at 50 m depth from the period 1986–2000, downscaled from the GISS ADM 20C3M simulation

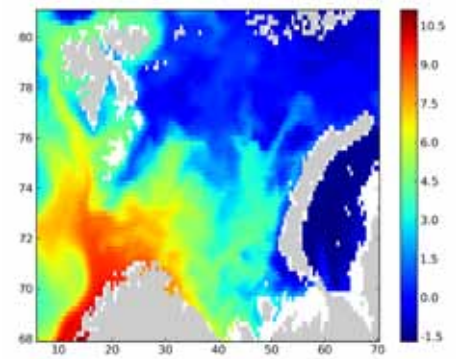


Figure 4.25 Mean September temperature at 50 m depth from the period 2051–2065 downscaled from the GISS AOM A1B simulation

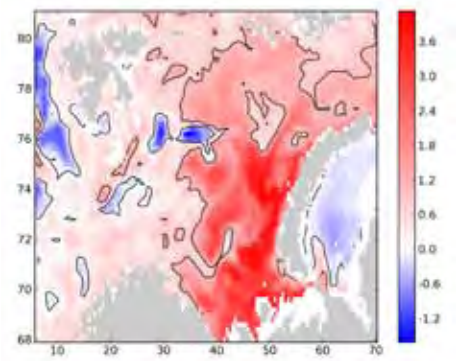


Figure 4.26 Mean September temperature change at 50 meter depth from the period 1986–2000 to the period 2051–2065. The contour lines are isobaths at 50, 100, 200, 300, and 500 m

4.10 Sea level and storm surges

The sea level is expected to increase during the 21st century. The main causes are melting of glaciers and thermic expansion of sea water. Changes in circulation in atmosphere and ocean influence the mean sea level regionally. New estimates (Drange et al., 2007) indicate a sea level increase along the coast of Troms and Finnmark of 18-20 cm towards 2050 and 45-65 cm towards 2100. These numbers are corrected for land rise. These numbers are quite uncertain because of diverging estimates of projected melting of glaciers in Greenland and Antarctica.

Downscalings have been performed to assess changes in future wave and storm surge climate (Debernard and Røed, 2008). These simulations are performed by met.no's operational models forced with downscaled wind scenarios. Areas that are presently ice-covered in winter and ice-free in the future will experience a rougher wave climate. Otherwise the changes are not significant. The estimated changes in significant wave height are shown in Figure 4.27.

The storm surge climate does not show a significant change on a yearly basis, but there is a significant increase in the autumn surge activity. However, combined with the mean sea level increase, the impact of the surges may become more severe.

5. Uncertainties and shortcomings in climate projections

Projections of local climate changes are affected by a range of uncertainties and shortcomings:

- **Unpredictable internal natural variability** (particularly large in the Nordic Arctic region, cf. Figure 4.1)
 - Influence on representation of present climate and past climate variability
 - Dependency of initial state
- **Uncertainty in climate forcings**
 - Natural forcings: Variability in solar input, volcano eruptions
 - Human emissions of gases and aerosols (as specified in the SRES (2000) report)
- **Imperfect climate models**
 - Imperfect knowledge about forcings and processes
 - Imperfect physical and numerical treatment of processes
 - Poor resolution in the global models (processes, topography)
- **Weaknesses in downscaling techniques**
 - Dynamical downscaling/Regional Climate Models:
 - Still too poor spatial resolution for most impact studies (real topography is still not taken proper care of)
 - Systematic bias: Cannot be directly compared to observations
 - Choice of model domain
 - Empirical/Statistical downscaling:
 - Most appropriate for monthly/seasonal/annual values
 - Presently just methods for a few climate elements
 - Not necessarily spatial or temporal consistent
 - Best suited for sites with long series of observations
 - Choice of model domain

6. Knowledge gaps and suggested scientific actions

6.1. Long-term monitoring

Monitoring long-term climate variability in the Arctic is crucial – both for assessing observed trends and for climate model evaluation. Consequently continuation of long-term records is essential, as well as implementing an observation strategy that integrates remote sensing, in situ observations data, and climate modelling, and enables feedback among them. Enhanced use of past and present in situ observations from different parts of the Arctic should be encouraged in initializing, validating and improving climate models. As stated by ICARP II (2005): “The overarching challenge is integrating the strengths of remote sensing with complementary observations and models to describe how the Arctic system works, how it is changing and what those changes mean for the future”.

The Norwegian weather stations in the Arctic form a good platform for monitoring climate development both on Spitsbergen, Bjørnøya, Hopen and Jan Mayen. It is however crucial to continue these basic Arctic series and to avoid inhomogeneities caused by relocations, changes in instrumentation, measuring procedures etc. Particular problems are connected to measuring snow and precipitation in the harsh Arctic climate. As pointed out in chapter 2.3 the present precipitation gauges in the Arctic do not give proper measure of neither “true precipitation” nor “real precipitation trends”. Consequently a comprehensive Reference Precipitation Gauge as recommended by WMO (Goodison et al., 1998) should be established at a site on Spitsbergen.

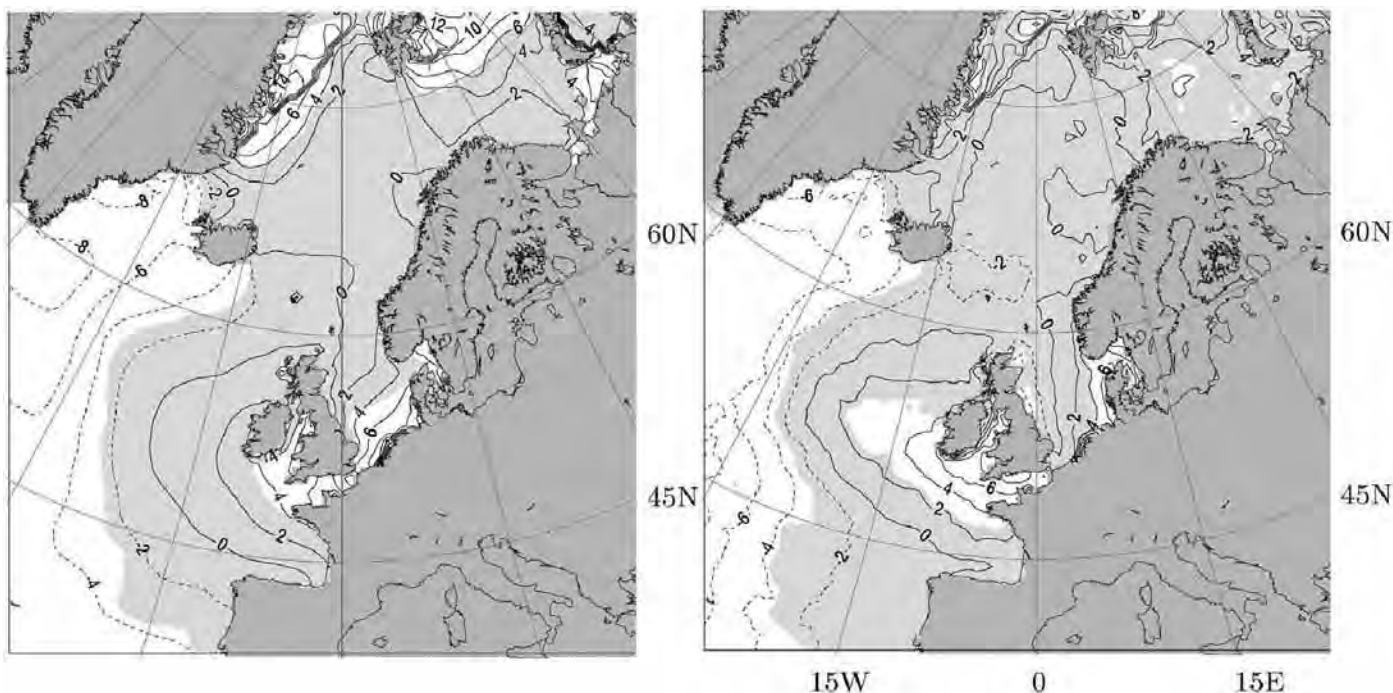


Figure 4.27 Estimated change (%) in average significant wave height from present climate (DJF, left panel) and in extreme wave heights (99 percentile, right panel)

Suggested actions

- Secure continuation of long-term atmospheric and oceanic series
- Establish a “Super site” to get a measure of “true precipitation” and to be able to monitor “real precipitation trends”
- Integrate remote sensing data with complementary observations and models

6.2. Global and regional climate models

Global and Regional Climate Models have traditionally only considered the physical components of the climate system. A new generation of models referred to as Earth System Models (ESM) are now under development (cf. chapter 4.1). These models include a more complete representation of the range of feedbacks between the anthropogenic, physical, chemical and biological components of the climate system, as well as to directly simulate the response of key environmental systems to climate change. Special attention for the Arctic regions should be given to regional atmospheric – ocean – sea-ice feedbacks, essential cryospheric feedbacks, a predictive carbon cycle, and biogeochemical feedbacks in the ocean.

Suggested action

- A particular focus in the development of ESMs should be on the representation of important Arctic earth system processes

6.3. Spatial and temporal resolution of Arctic climate projections

The present spatial resolution (25 kmx25km) in regional climate models (e.g. NorACIA RCM) is still not sufficient for most impact and adaptation studies in the Spitsbergen region. This hampers descriptions of local climate, and impedes the analyses of extreme weather conditions for e.g. wind speed, minimum temperatures and rainfall intensity. Consequently fine-scale modelling should be performed based on the output from regional climate models (“double nesting”). The model estimates for present climate should be validated against optimal datasets of surface observations, remote sensing data and weather models.

Suggested action

- Perform fine-scale modelling with high spatial and temporal resolution for the Spitsbergen region for both present and future climate

6.4. Marine downscaling

Methods for downscaling of ocean temperature, currents, waves and storm surges are established. However, the present methods are not able to correct erroneous ice cover in the driving AOGCMs. As most AOGCMs have problems with the ice coverage, this is a serious shortcoming for the use of marine downscaling in the Norwegian and Barents Seas. The problem is caused by the lack of feedback between the atmosphere and ocean – the forcing from an AOGCM with too much sea-ice can not sustain an ice-free regional ocean model.

Suggested action

- Develop a method for consistent modification of atmospheric forcing depending on the sea-ice conditions in the regional ocean model

6.5. Uncertainties

Improvements of some of the sources of uncertainty are being performed e.g. in the Norwegian Research Council project NorClim (Climate of Norway and the Arctic in the 21st century). As mentioned in ch. 6.2 enhanced efforts should be made in developing an Earth System Model with elaborated representation of important Arctic earth system processes. Such a model would significantly reduce the uncertainties in projections of future climate development in the Arctic. On the other hand it is crucial to realize that a robust description of future climate development in the Arctic should be based on ensemble simulations (statistical and dynamical) from several climate models with different (but realistic) input premises.

Suggested action

- Perform ensemble simulations from multiple climate models

6.6. Dissemination and tailoring of climate projections for impact and adaptation studies

Developing and applying high-resolution coupled regional models (ch. 6.2), double-nesting into fine-scale models (ch. 6.3), validating against observations (ch. 6.1) and estimates of uncertainties would substantially improve the projections of local climate changes. However, to provide more useful information to local decision makers, research scientist and other users of climate data, there is in most cases a need to “tailor” the results for the specific applications. Methods for such tailoring of climate data should be elaborated in close contact with different user groups. To serve the users with updated and tailored climate data, a “Service office” should be established. The dissemination of climate projections also for the Arctic could be through the planned Norwegian governmental web-site “Climate Adaptation Norway” (www.klimatilpasning.no). This web-site is aiming to provide good examples on adaptation and tools to integrate adaptation in planning, and may be a useful platform for access to relevant climate adaptation also for the Norwegian Arctic.

Suggested actions

- Establish a “Service office” for serving users with updated and tailored climate data for various impact and adaptation activities
- Provide updated climate projections and information from the Norwegian Arctic to the “Climate Adaptation Norway” web-site

Table 7.1 Projections of changes in annual and seasonal temperature and precipitation The figure indicates intervals for geographic gradients, and does not give an estimate of the uncertainty

		Svalbard		Northern-Norway					
		A*	B*	ESD**	A*	B*	RegClim***	Comb****	ESD**
Temp (degC)	Annual	1.5 - 4	3 - 8	-	1 - 2	2.5 - 3.5	2.8	2 - 3	-
	Spring	1.5 - 4	2 - 6	6 - 7	1 - 1.5	2.5 - 3.5	2.9	2 - 3	4 - 7
	Summer	1 - 1.5	2 - 4	2 - 3	1	1 - 2	2.4	1.5 - 2.5	3 - 4
	Autumn	2 - 6	4 - 8	4 - 6	1 - 2	2.5 - 4	3.3	2.5 - 4	3 - 7
	Winter	2.5 - 8	4 - 8	6 - 10	1 - 2.5	2.5 - 4.5	2.8	2.5 - 4	4 - 11
Precip (%)	Annual	10 - 20	10 - 40	-	0 - 10	20 - 30	13	10 - 20	-
	Spring	5 - 20	10 - 40	0 - 30	0 - 10	20 - 30	11	5 - 20	5 - 20
	Summer	0	10 - 30	10 - 15	0	10	12	10 - 20	10 - 15
	Autumn	10 - 20	10 - 40	5 - 20	0	10 - 20	23	10 - 20	5 - 20
	Winter	10 - 40	0 - 40	20 - 50	10 - 20	20 - 40	7	10 - 20	10 - 30

* NorACIA-RCM: Change (A) from 1981-2010 to 2021-2050 and (B) from 1961-1990 to 2071-2100

** ESD: Empirical-Statistical Downscaling (from Table 4.2 and 4.3)

*** RegClim (2005): Change from 1961-1990 to 2071-2100 from combined analysis of RCM simulations for two global climate models

**** From Haugen & Iversen (2008): Change during 70 years from combined analysis of RCM simulations for eight global climate models

7. Summary

The latest IPCC report (IPCC, 2007) and the ACIA-report (ACIA, 2005) state that the warming in the last 30 years is widespread over the globe, but is greatest at higher northern latitudes. The greatest warming has occurred during winter (DJF) and spring (MAM). Average Arctic land temperatures have been increasing at almost twice the rate of the rest of the world in the past 100 years. The Arctic climate conditions show large variability, both from year-to-year, but also on a decadal scale. This is valid for e.g. temperature, precipitation, wind and ice conditions. A slightly longer Arctic warm period, almost as warm as the present, was observed from 1925 to 1945, but its geographical distribution appears to have been different from the recent warming since the extent was not global (IPCC, 2007).

There are large discrepancies in how different climate models describe both present and future ice conditions in the Norwegian Arctic, and the uncertainties in the Arctic climate projections are thus considerable. Most European regional climate models do not cover areas as far north as Svalbard, and North Norway is usually quite close to the northern border of the model domains. To get more focussed downscalings for the Norwegian Arctic, a novel regional climate model was established within NorACIA. This model ("NorACIA-RCM") seems to give a realistic description of the present climate conditions in North Norway and on Svalbard. Assuming that the input data are reasonable, the model is probably also giving an adequate description of future climate conditions. Just a few global climate models are currently downscaled by the NorACIA-RCM. To provide a more robust description of future climate in the Norwegian

Arctic, a summary of projections of temperature and precipitation from various analyses are presented in Table 7.1.

Robust findings for climate development in the Norwegian Arctic from 1961–90 to 2071–2100

Temperature: For North Norway the projections indicate an increase in annual temperature of 2.5–3.5 °C, with smallest increase in western coastal areas and greatest in the Varanger area and interior parts of Finnmark. For Svalbard the increase in annual temperature is ca 3°C in the southwest and ca. 8°C in the northeast. The projected warming is smallest for the summer season and greatest for autumn and winter. This is particularly valid for inland areas. For the autumn and winter seasons an increase of more than 3 °C is projected for large parts of North Norway, and more than 8°C in north eastern parts of the Svalbard archipelago. For the summer season a temperature increase of ca. 2°C is projected for North Norway, while the warming in the Svalbard region generally is in the interval 2 – 4°C. A substantial increase in air temperature is also projected for the ocean areas between Svalbard and Novaja Zemlja – particularly in the period September – May. The increase is greatest in areas where sea-ice is replaced by open waters.

Precipitation: The projections indicate an increase in precipitation during all seasons in both North Norway and in the Svalbard region. The increase in annual precipitation is generally in the interval 10–30% in North Norway and between 10–40% on Svalbard. In North Norway the increase is greatest during autumn and winter, with the strongest increase in coastal regions in Finnmark. For Svalbard the models

mainly project smallest increase in the south and southwest, and greatest increase in the north and northeast. The projections also indicate a substantial percentage increase in number of events with heavy rainfall (>20 mm/day). One should however keep in mind that in North Norway and especially in the Svalbard region there are relatively few days with rainfall exceeding 20 mm. Consequently a large percentage increase does not necessarily imply a dramatic increase in number of days with heavy rainfall. The analyses demonstrate that daily rainfall values that presently in average occur once during a five-year period, in a future climate will occur 2 – 3 times more often than in the present climate. Also the precipitation amount of the extreme rainfall event will increase.

Wind: The estimates for changes in wind conditions are uncertain, and substantial deviations exist between projections based on different models. The projections indicate small changes over North Norway, while the ocean areas between Svalbard and Novaja Zemlja may experience an increase in maximum wind speed by more than 10%.

Snow: For the coastal areas in North Norway, the projections indicate shorter a season with snow on the ground and reduced precipitation amounts falling as snow. On the other hand, over interior parts of Finnmark and in mountainous regions as well as for large parts of the Svalbard region, the amounts of snow may increase. The reason is that although the snow season will be shorter in a warmer climate, in these areas this will be compensated by the strong increase in winter precipitation as snow.

References

- ACIA, 2005: Arctic Climate Impact Assessment, Cambridge University Press, 1042 p (www.acia.uaf.edu)
- Benestad, R.E., Kirkevåg, A. and Førland, E.J. 2005: Climate scenarios for the Nordic region: Regional effects of aerosols and empirical downscaling of scenarios, met.no Report 19/2005, 50pp.
- Benestad, R.E. (2005) On Latitudinal Profiles of Zonal Means GRL 32 L19713, doi:10.1029/2005GL023652
- Benestad, R.E., 2008: Empirical-Statistical downscaled Arctic Temperature and Precipitation Series. Met.no Report 12/2008 Climate.
- Bengtsson, L., Hageman, S. and Hodges, K. I. 2004: Can climate trend be calculated from reanalysis data? J. of Geophys. Res.-Atmospheres. 109, D11111, doi:10.1029/2004JD004536.
- Bjorge, D., Haugen, J.E. and Nordeng, T.E. 2000: Future climate in Norway. DNMI Research Rep. 103, 41 pp. Norwegian Meteorological Institute, P. O. Box 43 Blindern, N-0313 Oslo, Norway, ISSN 0332-9879.
- Christensen, O.B. and Christensen, J.H. 1998: Very high-resolution climate simulations over Scandinavia. Present Climate. J. Climate, 11 (12), 3204-3229.
- Christiansen H et al. 2007: Permafrost Observatory Project: A Contribution to the Thermal State of Permafrost in Norway and Svalbard, TSP NORWAY. Eos Trans. AGU 88(52), Fall Meet. Suppl., Abstract C21A-005.
- Debernard, J & L.P.Røed, 2008: Future wind, wave and storm surge climate in the northern Seas: A revisit. Tellus, 60A, 427-438
- Dyrddal, A.V. and D.Vikhamar-Schuler, 2009: Analysis of long-term snow series at selected stations in Norway. met.no Report 05/09 Climate, Norwegian Meteorological Institute, 82pp.
- Drange, H., B.Marzeion, A.Nesje & A.Sorteberg, 2007: Up to one meter sea level rise along the Norwegian coast within year 2100 (In Norwegian). Cicerone 2, p.29-31
- Ellingsen, I., Dalpadado, P., Slagstad, D. og Loeng, H., 2008: Impact of climatic change on the biological production in the Barents Sea, Climatic Change, 87, 155-175.
- Furevik, T., Bentsen, M., Drange, H., Kindem, I.K.T., Kvamstø, N.G., and Sorteberg, A. 2003: Description and Validation of the Bergen Climate Model: ARPEGE coupled with MICOM, Clim. Dyn., Vol. 21, p.27-51 (pdf)
- Førland, E.J., Allerup, P., Dahlström, B., Elo-maa, E., Jónsson, T., Madsen, H., Perälä, J., Rissanen, P., Vedin, H. and Vejen, F. 1996: Manual for operational correction of Nordic precipitation data. DNMI Report 24/96 KLIMA, 66 pp
- Førland, E.J., 1993: Precipitation normals, Normal period 1961-1990 DNMI-Report 39/93 KLIMA, 63pp.
- Førland, E.J., Hansen-Bauer, I. and Nordli, P.Ø. 1997a: Orographic precipitation at the glacier Austre Brøggerbreen. DNMI-Report 2/97 KLIMA
- Førland E.J., I. Hanssen-Bauer and P.Ø. Nordli, 1997b: Climate statistics & longterm series of temperature and precipitation at Svalbard and Jan Mayen. DNMI-Klima 21/97.

- Førland, E.J. & I. Hanssen-Bauer, 2000: Increased precipitation in the Norwegian Arctic: True or false? *Climatic Change* 46, 485-509.
- Førland, E.J., R.E. Benestad, F. Flatøy, I. Hanssen-Bauer, J.E. Haugen, A. Sorteberg & B. Ådlandsvik, 2008: NorACIA klimascenarier for norsk Arktis. Report no. 09/08 Climate, The Norwegian Meteorological Institute, 40pp (In Norwegian)
- Giorgi F, B Hewitson, JH Christensen, M Hulme, H von Storch, P Whetton, R Jones, L Mearns, C Fu (2001) Regional Climate Information – Evaluation and Projections. In: *Climate Change 2001: The Scientific Basis. Contribution of Working Group I to the Third Assessment Report of the Intergovernmental Panel on Climate Change* [Houghton J.T., Y. Ding, D.J. Griggs, M. Noguer, P.J. van der Linden, X. Dai, K. Maskell and C.A. Johnson (eds.)] Cambridge University Press, Cambridge, U.K. and New York, NY, USA: 583-638
- Goodison, B.E., Louie, P.Y.T., and Yang, D., 1998: WMO Solid Precipitation Measurement Intercomparison. WMO/TD No 872, Geneva, Switzerland,
- Hagen, J.O. & O. Liestøl, 1990: Long-term glacier mass-balance investigations in Svalbard, 1950-1988. *Ann. Glaciol.*, Vol 14, pp. 102-106.
- Hagen, J.O. & B. Lefauconnier, 1995: Reconstructed Runoff from the High Arctic Basin Bayelva based on Mass-Balance Measurements. *Nordic Hydrology*, 26, p. 285-296
- Hanssen-Bauer, I., M. Kristensen Solås and E. Steffensen, 1990: The Climate of Spitsbergen. DNMI-Klima Report 39/90
- Hanssen-Bauer, I and E.J. Førland, 1994: Homogenizing long Norwegian Precipitation Series. *J. Climate*. Vol.7, No.6, p.1001-1013.
- Hanssen-Bauer, I., E.J. Førland, P.Ø. Nordli, 1996: Measured and true precipitation at Svalbard. DNMI-Report 31/96 KLIMA, 49pp
- Hanssen-Bauer, I. and P.Ø. Nordli, 1998: Annual and seasonal temperature variations in Norway 1876-1997. DNMI-Report 25/98 KLIMA, 29pp
- Hanssen-Bauer I., Achberger C., Benestad R.E., Chen D., Førland E.J, 2005: Statistical downscaling of climate scenarios over Scandinavia: A review. *Clim. Res.* 29, 255-268
- Hanssen-Bauer, I., 2005: Regional temperature and precipitation series for Norway: Analyses of time-series updated to 2004. met.no Report 15/2005 Climate.
- Hanssen-Bauer, I, 2007: Climate variation in the European sector of the Arctic: Observations and scenarios. In: J.B. Ørbæk et al. (Eds.) *Arctic-Alpine Ecosystems and People in a Changing Environment*. Springer-Verlag., ISBN: 3-540-48512-0
- Hanssen-Bauer, I. Førland, E.J., Johansen, K. and Nordli, Ø., 2009: The Climate of Svalbard and Jan Mayen. Analyses of time-series data from 1911 to 2007 (in manus)
- Haugen J. E. and H. Haakenstad (2006): Validation of HIRHAM version 2 with 50 km and 25 km resolution. RegClim General Technical Report No. 9. pp 159-173.
- Haugen, J.E. & T. Iversen, 2008: Response in extremes of daily precipitation and wind from a downscaled multi-model ensemble of anthropogenic global climate change scenarios. *Tellus A*, Vol. 60A, No. 3, May 2008, 411-426.
- Hurrell, J.W., 1995: Decadal trends in the North Atlantic Oscillation: Regional temperatures and precipitation. *Science*, 269, 676-679.
- Hygen, H.O., 2009: Sea-ice extension in the area between Greenland and Novaja Zemlja 1971-2000. met.no Note 01/2009
- ICARP-II, 2005: Arctic Research- A global responsibility. An Overview of the 2nd International Conference on Arctic research Planning (www.icarp.dk)
- IPCC, 2001: Climate Change 2001: The Scientific Basis. Contribution of Working Group I to the Third Assessment Report of the Intergovernmental Panel on Climate Change [Houghton, J.T., Y. Ding, D.J. Griggs, M. Noguer, P.J. van der Linden, X. Dai, K. Maskell and C.A. Johnson (eds). Cambridge University Press, Cambridge, UK and New York, NY, USA, 881p.
- IPCC, 2007: Climate Change 2007: The Physical Science Basis. Contribution of Working Group I to the Fourth Assessment Report of the Intergovernmental Panel on Climate Change [Solomon, S., D. Quin, M. Manning, Z. Chen, M. Marquis, K. B. Averyt, M. Tignor and H. L. Miller (eds). Cambridge University Press, United Kingdom and New York, NY, USA, 996p
- Isaksen K, Vonder Mühl D, Gubler H, Kohl T, Sollid J.L. 2000. Ground surface temperature reconstruction based on data from a deep borehole in permafrost at Janssonhaugen, Svalbard. *Annals of Glaciology* 31: 287-294.
- Isaksen, K., J. L. Sollid, P. Holmlund, and C. Harris 2007a. Recent warming of mountain permafrost in Svalbard and Scandinavia. *J. Geophys. Res.*, 112, F02S04, doi:10.1029/2006JF000522.
- Isaksen, K., R. E. Benestad, C. Harris, and J. L. Sollid 2007b. Recent extreme near-surface permafrost temperatures on Svalbard in relation to future climate scenarios. *Geophys. Res. Lett.*, 34, L17502, doi:10.1029/2007GL031002.
- Jania, J. & M. Pulina, 1994: Polish Hydrological studies in Spitsbergen, Svalbard: A review of some results. Proc. 10th Int. Northern Research Basins Symposium and Workshop, Spitsbergen, Norway, SINTEF Report STF 22 A96415, pp.47-76.
- Killingtveit, Å., L.-E. Pettersson, K. Sand, 1994: Water Balance studies at Spitsbergen, Svalbard. Proc. 10th Int. Northern Research Basins Symposium and Workshop, Spitsbergen, Norway, SINTEF Report STF 22 A96415, pp.77-94.
- Kolstad, E. W., Bracegirdle, T. J., 2008: Marine cold-air outbreaks in the future: an assessment of IPCC AR4 model results for the Northern Hemisphere. *Clim. Dyn.*, 80, 891-885. DOI 10.1007/s00382-007-0331-0
- Källberg, P., A. Simmons, S. Uppala and M. Fuentes (2004): The ERA-40 Archive. ERA-40 project report series no. 17., ECMWF, Reading, UK.
- Loeng, H. (red), 2008, Klimaendringer i Barentshavet - Konsekvenser av økte CO2-nivåer i atmosfæren og havet. Rapportserie, Rapport 126. Norsk Polarinstitutt, Tromsø, p. 32.
- McCabe, G. J., Clark, M. P. and Serreze, M. C. 2001. Trends in Northern Hemisphere surface cyclone frequency and intensity. *J. of Climate* 14(12), 2763-2768.
- NorACIA, 2009: Delrapport 2 (in prep.), Norwegian Polar Institute.
- Nordli P.Ø., I. Hanssen-Bauer and E.J. Førland, 1996: Homogeneity analyses of temperature and precipitation series from Svalbard and Jan Mayen, DNMI-Klima Report 16/96.
- Oldenborgh, G.J. van, S. Drijfhout, A. van Ulden, A. Sterl, C. Severijns, W. Hazeleger and H. Dijkstra, 2008: Eastern Europe is warming much faster than expected. *Clim. Past Discuss.*, 4, 897-928.
- Osokin, N.I., V.A. Zhidkov, V.V. Gokhman, 1994: Snowcover of Spitsbergen and the peculiarities of its distribution in some mountain basins. Proc. 10th Int. Northern Research Basins Symposium and Workshop, Spitsbergen, Norway, SINTEF Report STF 22 A96415, pp.484-48
- Overland, J.E. og Wang, M. (2007) Future regional Arctic sea ice declines. *Geophys. Res. Lett.*, 34, L17705, doi:10.1029/2007GL030808
- Pettersson, L.-E., 1994: The Hydrological Regime of Spitsbergen, Svalbard. Proc. 10th Int. Northern Research Basins Symposium and Workshop, Spitsbergen, Norway, SINTEF Report STF 22 A96415, pp.95-107.
- Polyakov, I.V., R.V. Bekryaev, G.V. Alekseev, U.S. Bhatt, R.L. Colony, M.A. Johnson, A.P. Makshtas and D. Walsh, 2003: Variability and trends of air temperature and pressure in the maritime Arctic, 1875-2000. *Journal of Climate*, 16, 2067-2077.
- Rahmstorf, S., Cazenave, A., Church, J.A., Hansen, J.E., Keeling, R.F., Parker, D.E., and Somerville, R.C.J., 2007: Recent climate observations compared to projections, *Science*, 316. p.709.
- RegClim, 2005: Norges klima om 100 år. Usikkerheter og risiko. <http://regclim.met.no>
- Serreze, M. C., Box, J. E. and Barry, R. G. 1993. Characteristics of Arctic Cyclone Activity, 1952-1989. *Met. And atm. Physics* 51(3-4), 147-164.
- Serreze et al., 1997: Icelandic low cyclone activity: climatological features, linkages with the NAO, and relationships with recent changes in the Northern Hemisphere circulation. *J. Clim.*, 10, 453-464
- Sneyers, R., 1995: Climate instability determination. Discussion of methods and examples. Proc. From 6th International Meeting on Statistical Climatology, 19-23 June, Galway, Ireland, pp. 547-550

- Sorteberg A. and Walsh J. E., 2008: Seasonal cyclone variability at 70°N and its impact on moisture transport into the Arctic. *Tellus A*, Vol. 60 Issue 3, Pages 570 – 586
- Sorteberg A., Furevik T., Drange H., Kvamstø N. G., 2005: Effects of simulated natural variability on Arctic temperature projections. *Geophysical Research Letter*, Vol. 32, L18708, doi:10.1029/2005GL023404.
- Sorteberg A. and Kvamstø N. G., 2006: The effect of internal variability on anthropogenic climate projections. *Tellus A* 58(5):565–574
- SRES, 2000: IPCC Special Report on emission Scenarios. [Nakicenovic, N., J.Alcamo, G.Davis, B. de Vries, J. Fenhann, S.Gaffin, K.Gregory, A.Grübler, T.Y.Jung, T.Kram, E.L. LaRovere, L. Michaelis, S.Mori, T.Morita, W.Pepper, H.Pitcher, L.Price, K.RAihi, A.Roehrl, H-H.Rogner, A.Sankovski, M.Schlesinger, P.Shukla, S.Smith, R.Swart, S. van Rooijen, N.Victor, Z.Dadi]. Cambridge University Press, United Kingdom and New York, NY, USA, 599p.
- Steffensen, E.L., 1982: The climate at Norwegian Arctic stations. *DNMI Klima*, No.5, pp. 3-44.
- Stendel M., Christensen, J.H. and Pedersen, D. 2008. *Advances in ecological Research*, Vol. 40
- Tveit, J. and Å.Killingtveit, 1994: Snow surveys for studies of water budget on Svalbard 1991-1994. *Proc. 10th Int.Northern Research Basins Symposium and Workshop*, Spitsbergen, Norway, SINTEF Report STF 22 A96415, pp.489-509
- Vikhamar-Schuler, D., S.Beldring, E.J.Førland, L.A.Roald and T.Engen-Skaugen, 2006: Snow cover and snow water equivalent in Norway: -current conditions (1961-1990) and scenarios for the future 2071-2100). *met.no Report 1/2006 Climate*, Norwegian Meteorological Institute, 34pp.
- Zhang, X., Walsh, J. E., Zhang, J., Bhatt, U. S. and Ikeda, M. 2004. Climatology and interannual variability of Arctic cyclone activity, 1948-2002. *J. Climate* 17, 2300–2317.
- Walsh, J.E., Chapman, W.L., Romanov, V., Christensen, J.H., and Stendel M. 2008. *Global climate Model Performance over Alaska and Greenland*, *J. Clim.* (in press)
- Ådlandsvik, B. og Bentsen, M. (2007) Downscaling a 20th century global climate simulation to the North Sea, *Ocean Dynamics*, 57, 453–466.
- Ådlandsvik, B. (2008) Marine downscaling of a future climate scenario for the North Sea, *Tellus*, 60A, 451–458.

Acronym	Explanation
ACIA	Arctic Climate Impact Assessment (www.acia.uaf.edu)
AO	Arctic Oscillation
AOGCM	Atmospheric Ocean General Circulation Model
BCM	Bergen Climate Model
CAI	Cyclone Activity Index
CRU	Climate Research Unit , University of East Anglia, UK
ECMWF	European Center for Medium range Weather Forecasting
ENSEMBLES	http://ensembles-eu.metoffice.com
ERA40	ECMWF Rea-Analysis for 40 years
ESD	Empirical-Statistical Downscaling
ESM	Earth System Modelling
EUMETSAT	European Collaboration on Meteorological Satellites
GCM	General Circulation Model
HIRHAM25	Regional Climate Model with 25km resolution
IMR	Institute for Marine Research , Bergen, Norway
IPCC	Intergovernmental Panel on Climate Change
IPY	International Polar Year
MCAO	Marine Cold Air Outbreaks
met.no	Norwegian Meteorological Institute
MICOM	Ocean model including a dynamic-thermodynamic sea-ice model
MMD	Multi-Model Dataset used in climate projections for IPCC 4AR
MPI	Max-Planck Institute , Hamburg, Germany
MPI B2	RCM based on MPI simulation for 2071-2100 with emission scenario B2
MPI CN	RCM based on MPI simulation for Control Normal periode 1961-1990
MPI P2	RCM based on MPI simulation for Present climate 1981-2010
MPI S2	RCM based on MPI simulation for Scenario period 2021-2050
MSLP	Mean Sea Level Pressure
NAO	North Atlantic Oscillation
NorACIA	Norwegian follow-up to Arctic Climate Impact Assessment (www.noracia.npolar.no)
RCM	Regional Climate Model
Regclim	Regional Climate development under global warming (http://regclim.met.no)
ROMS	Regional Ocean Model System
SRES	IPCC Special Report on Emission Scenarios (see SRES, 2000)
TAM	Mean Air temperature measured 2 m above the ground
TAR	IPCC Third Assessment Report (see IPCC, 2001)
WMO	World Meteorological Organisation
4AR	IPCC 4th Assessment Report (see IPCC, 2001)
20C3M	Model simulation for the 20th century

